Inductively Powered Implant for Monitoring and Application of Telemetric Metronomic Photodynamic Therapy
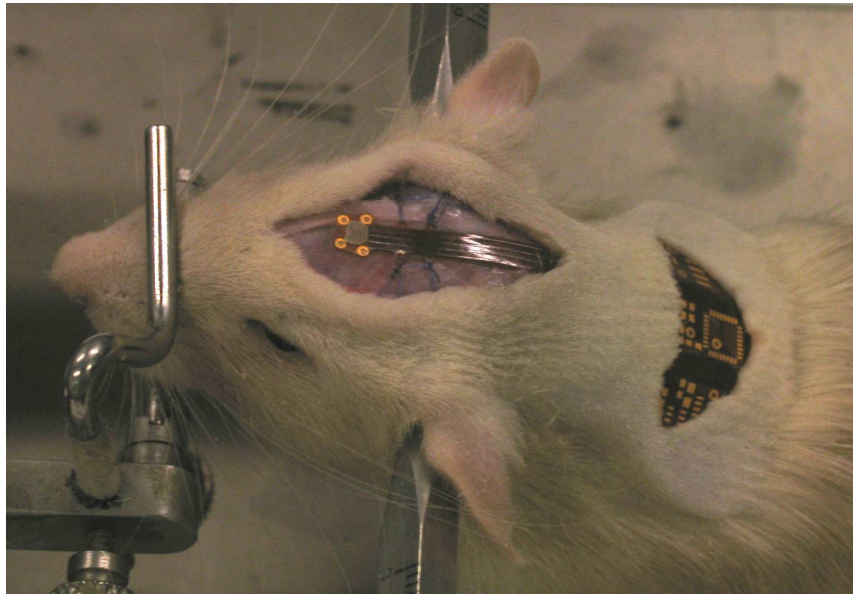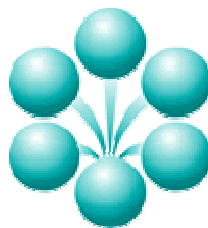
Author:	J. G. Kaptein
Student number:	1109022
Mentor and Supervisor:	Prof. Dr. P. J. French
	E. Margallo Balbás, MSc.
Date:	14 October 2008

TUDelft

Delft University of Technology

DIMES
Delft Institute of Microelectronics and Submicron Technology

Erasmus MC
University Medical Center Rotterdam

Inductively Powered Implant for Monitoring and Application of Telemetric Metronomic Photodynamic Therapy

Master of Science Thesis

J. G. Kaptein

14 October 2008

Committee Members:
Prof. dr. P. J. French
Prof. dr. H.J.C.M. Sterenborg
dr. ir. A. Bossche
dr. ir. W.A. Serdijn
dr. D. J. Robinson
E. Margallo Balbás, MSc

Abstract

Photodynamic therapy (PDT) is a promising treatment for numerous kinds of cancer. A potential advantage of PDT compared to other cancer treatments like radiotherapy and chemotherapy is its selectivity. PDT is based on a photosensitive substance that is administered to a patient. The substance has selective uptake by cancerous tissue and when illuminated with a certain wavelength it destroys the tissue in close proximity. Metronomic PDT is a new proposed technique for treating patients with cancer. For this technique a new kind of light source is needed. The purpose of this thesis is to develop the light source needed for this technique. This light source also needs to monitor the treatment and should be controlled and powered from the outside.

An optode chip has been developed which carries one or two LED's used as light source and up to four photodiodes. The photodiodes were designed after Monte Carlo simulations to get an indication of the amount of incident light. The readout of the photodiodes consists of a transimpedance amplifier and an A/D converter. The LED is driven with pulse width modulation to adjust intensity. The communication is implemented with a Radio Frequency Identification technique. The power for the implant is provided by an inductive power link that was designed for low power dissipation in the coil. The power is buffered in a capacitor in case the coupling of the two coils is lost. It also allows the field to be switched off during measurement. The whole implant is controlled with a microcontroller, which has PWM and A/D conversion on chip.

The several devices are soldered on a flexible printed circuit board. The flexible PCB was shaped in such a way that the coils for communication and power could be big enough to get a reasonable coupling and was designed for an animal model. The big part is placed on the shoulders of the rat, the optode is attached to the head of the rat. The electronic components are encapsulated with medical grade silicone. The optode chip is mounted with bond wires on the flexible circuit board and is encapsulated with a biocompatible polymer.

The main function of the implant, illuminate a specific volume with a specific wavelength, was successfully implanted. The fluence rate monitoring and temperature monitoring were also successfully implemented. The monitoring of the amount of photosensitizer and oxygen was not implemented but experiments can be done with the current optode chip.

The total system has been successfully tested outside the animal. The first animal test is planned in the near future. In the future the whole system needs to be developed further, the several discrete components on the implant need to be implemented on chip. A system with multiple optodes needs to be developed.

Table of contents

Index of figures

Index of tables

1 Introduction

1.1 Medical Background

Photodynamic Therapy (PDT) is a promising treatment for numerous kinds of cancer. An overview of the principle of the treatment is given in figure 1.1. The patient receives a dose of photosensitizer or a photosensitizer pre-cursor (A) that, to a degree, preferentially localizes in the tumour because of selective uptake in this kind of tissue (B). When the photosensitizer is illuminated (C) with light of a specific wavelength in the presence of oxygen it produces reactive oxygen species, notably singlet oxygen, which leads to the destruction of the tumour. This is achieved by direct damage to the tumour cells, by the destruction of the vasculature of the tumour, by activation of the immune system or by a combination of the three (D) [1].
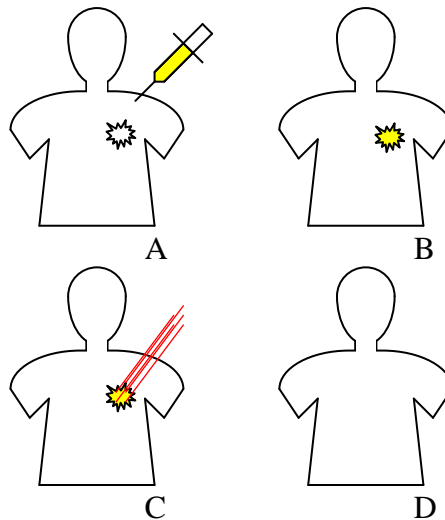
Figure 1.1 Photodynamic Therapy; A) administration of Photosensitizer, B) Selective uptake by tumour tissue, C) Illumination of tissue, D) Tumour destructed. (Adapted from [2])

A potential advantage of PDT compared to other cancer treatments like radiotherapy and chemotherapy is its selectivity. Some tumours have selective uptake for the photosensitizer and the light can be targeted to a specific volume. Another advantage is the fact that when healthy tissue is damaged it can recover from this, without scaring.

1.1.1 History
The interaction between light and tissue has been under investigation for a long time, both for diagnostic and treatment purposes. The Egyptians and Greeks already used light for treatment of several skin diseases. Light based treatment in the modern era was reported by Finsen (Nobel prize 1903) who successfully treated Tuberculosis and smallpox late in the 19th century. [3]

In the same period Raab, Jesionek and Von Tappeiner showed that the combination of a photosensitizing agent, oxygen and light could destroy cells. They called the effect the Photodynamic Effect. They were the first to use the effect to treat cancer: They

applied eosin on the surface of the skin on basal cell carcinomas (BCCs) before illuminating the surface. They defined photodynamic therapy as the dynamic interaction between light, a photosensitizing agent, and oxygen resulting in tissue destruction.[4]

The findings were recognized all over the world but the treatment did not become a standard treatment. [5]

Clinical application of photodynamic therapy had to wait for the development of light sources, for rediscovery of photosensitizers and for appreciation for the photodynamic effect.

Development in Photosensitizers

In the first experiments of the photodynamic effect eosin and dyes were used. However among the most interesting agents are porphyrins. People who suffer from porphyria also produce them. The endogenous photosensitizer accumulates in many tissues, particularly the skin. When these people are exposed to sunlight the consequence is unintentional PDT. [4]

In the 1900s Fischer (Nobel prize 1943) did a lot of work on porphyrias. During his investigations he discovered the potency of porphyrins , especially hematoporphyrin as a sensitizing agent and as a fluorescing agent. [4]

In the fifties Schwartz and Lipson created a more highly active and more refined form of hematoporphyrin, Hematoporphyrin Derivative (HpD). It was first used for diagnostic purposes, as it was used to induce fluorescence in human tumours. However it was found that it caused tissue damage during illumination and therefore substantial photosensitization of the skin. This led to treatment of recurrent breast cancer with intentional PDT with HpD. [6]

From HpD Dougherty developed the first commercially available photosensitizer: Photofrin® . The second photosensitizer to become available was another porphyrin, Verteporfin (Visudyne^{TM}), which has a higher activation wavelength and is eliminated faster from the body. The third commercially available photosensitizer was ALA (5-aminolevulinic acid), in presence of ALA, the body creates an excess of natural porphyrin, protoporphyrin IX. [4]

Several other photosensitizers have been developed and tested. They are not commercially available yet because they are going through the regulatory procedures necessary for approval. In 2002 meso-tetrahydroxyphenyl chlorin (mTHPC) or Foscan® had clinical success and was approved in Europe for the treatment of head and neck cancer. [4]

Development in Illumination sources

The first light source for unintentional PDT was the sun, but this is not useful for intentional PDT due to its high intensity (>500 W/m^2 at sea level) and broad spectrum and high intensity. It emits from 200 to 2500 nm and most intensive in the UV-blue green region of the spectrum. In that region light does not penetrate effectively in tissue and for that reason not very applicable for PDT. Red light penetrates most effective in tissue.

The requirements for a useful light source are selective activation wavelength, the ability to focus on the area of interest and availability for an indoor treatment.

In the early days of intentional PDT, around 1900, arc lamps were used for illumination. Slide projectors with filters were successfully used in later times.

The introduction of lasers made a big difference for PDT. Lasers have a precise wavelength and are easy to focus efficiently into optical fibers, thus allowing internal

organs to be illuminated. In the early 90s these lasers were very large. The Argon-dye laser was the standard and produced up to 7W of red light. With beam splitters several fibers could be used for illumination. With the introduction of the YAG/DYE laser (3.5-7 W at 630nm) PDT gained acceptance because the laser was also used for other treatments in hospitals and looked more like a medical device [4]

Diode lasers were the next development in the illumination for PDT. Diode lasers (3W) are portable and require no special cooling. Due to the user-friendly interface and relative low cost of these components PDT gained acceptance.[4]

Clinical success of PDT also depends on the use of fiber optics, they have to deliver the light from the laser to the treatment volume. The fibers have to meet very high demands, such as light distribution (shapes of the tip). Not all varieties of fibers are available, fibers are expensive and most of them are not FDA approved. But these fibers are used in experimental studies. For commercial use only diffusion fibers of 1 to 5cm are available. But the development in fibers is going on and they are getting more reliable and flexible.[4]

A major disadvantage of PDT is the fact that the activation wavelength of the photosensitizer cannot penetrate more then 1 cm into tissue. This makes the treatment selectively for superficial lesions but as a consequence PDT application is currently limited to treatment on or just beneath the skin and on the lining of internal organs like Barrets Esophagus. But the use of interstitial fibers (in large solid tumour) overcomes this problem so we can treat the liver and prostate for example.

Dosimetry
Apart from the illumination and the photosensitizer, dosimetry is a crucial part of successful PDT. Von Tappeinner already demonstrated the requirement for oxygen early in the 20th century. The complex and different mechanisms of destruction and the need for oxygen, photosensitizer and light makes the dosimetry complicated

Various clinical studies have shown that differences in optical properties and uptake/synthesis of photosensitizers can leads to wide variations of the delivered PDT dose. Differences between these parameters occur not only between individual patients but also between tumours, and change dynamically during therapy. As a consequence, monitoring of the therapy in individual patients to determine the actual PDT dose is essential.

1.1.2 PDT for Glioblastoma multiforme (GBM)
Glioblastoma multiforme is a very aggressive form of brain tumour. These tumours arise from glial cells. Symptoms are caused by the tumour invading the brain. Very often they are found in the very late stages of the disease. As a consequence the five-year survival rate is 3%; this percentage has not changed the past 30 years, despite efforts to develop treatment strategies based on radio- and chemotherapy. It is clear that a new treatment is needed and PDT has the potential to treat GBM.

The major challenge in PDT for GBM is the low selectivity of uptake and/or retention of photosensitizer in glial cells over gray matter. The consequence is damage to normal tissue and a limitation to PDT. Clinical models showed that at lower PDT dose the tumour cells are more likely to be destroyed than the normal cells. But the total amount of destroyed tumour cells is lower, thus the treatment has to be repeated everyday for a period of 2 to 3 weeks. This approach of PDT is called metronomic PDT. [7]

1.2 Problem Definition

As stated earlier the development of PDT depends among other things on the development of light sources. Challenges for this particular modality of PDT is that the light source needs to be able to deliver a well defined treatment parameters in a resection cavity inside the brain over an extended period of time. [7]

A system needs to be developed which can administer metronomic PDT: illuminate a specific volume with a specific wavelength at regular intervals over a period of several weeks and monitor the three main components of PDT, oxygen, photosensitizer and fluence rate. The goal of this project is to develop a prototype for metronomic PDT. The prototype should be applicable to laboratory rats and in the future it should be extended to a full treatment system for GBM and possibly other kinds of tumours.

1.3 Possible Solutions

1.3.1 Adapt the instrumentation the existing treatment technique

The PDT treatment for GBM could be implemented using fibers and an external light source (laser). The monitoring of the treatment would also be done using optical fibers. An impression of the treatment is given in figure 1.2.
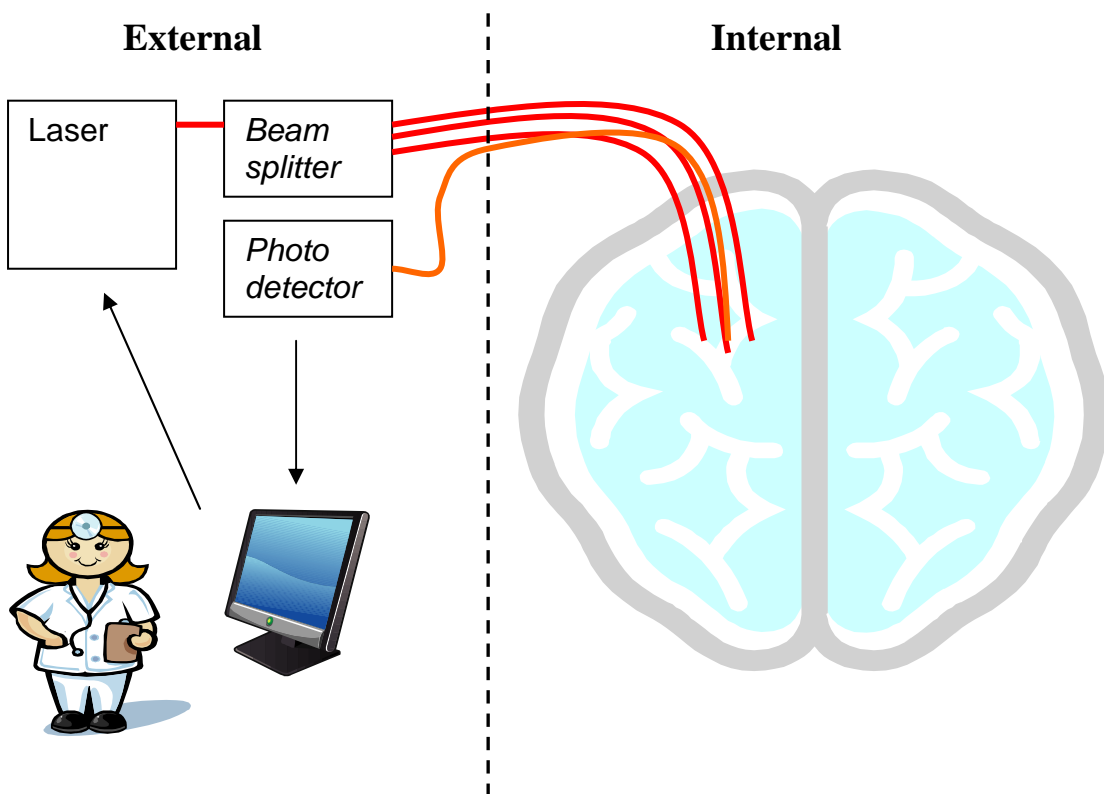
Figure 1.2 Impression of current treatment technique for photodynamic therapy

Advantage of this solution is that the technology is available and accepted. There are techniques under investigation for measuring oxygen levels and photosensitizer presence.

To adapt the current approach to PDT instrumentation for repeated treatment over extended periods of time has a number of major drawbacks.

More fibers (light sources) means that the light distribution in tissue can be tuned better to the treatment volume improving the targeting of the tumour. To measure the light distribution additional fibers are needed. However, most of the time the targeted volume is not easily accessible; due to that fact there is a maximum of fibers that can be placed.

This, combined with the fact that the activation wavelength cannot penetrate more than 1 cm into tissue makes treatment of brain tumours with metronomic PDT very challenging. Either the fibers need to be placed through the skull with a very significant risk of infection, or surgery is needed for every treatment, which is in general terms hardly acceptable. Despite these drawbacks experiments with this technique are being done.

1.3.2 Telemetric light source
Another option would be to use an implant that includes a light source. This implant needs to be able to monitor the treatment as well. The device would be implanted after resection of the tumour. It should be controlled from the outside and should be able to send measurement data to the outside. An impression is given in figure 1.3.

This solution has some challenges. The device has to be developed and needs to be accepted by the medical world. It has to stay in the body for a considerable time, which means that very strict rules on biocompatibility have to be addressed. Another consequence is that battery operation is not desired, especially because during treatment a significant amount of power is needed for a period of several weeks. It is therefore a challenge to transfer power to a device deep inside the body. The fluence rate that can be achieved cannot be as high as with an external source, it would draw to much power and probably cause too much heating. But since metronomic PDT uses low fluence rates, a different kind of light source is possible.

There are also a lot of advantages of the implant solution. In principle the device can be placed anywhere in the body. This will not cause extra inconvenience for the patient because it can be placed when the largest part of the tumour is removed during surgery.

It can stay in the body for a long time, even when treatment is over. In the case of GBM the probability that the tumour recurs at the same place is significant [8]. If the implant is still in place the treatment can be repeated easily.

The implant can potentially be very small if sensor, actuator and electronics can be combined on one chip, an optode. In this way several optodes can be connected and the target volume can be illuminated precisely. The different optodes can be constructed in such a way that they can host different sensors. For example one optode has a sensor for fluorescence and/or oxygenation, another one for temperature etc.

The different optodes can be connected to a main unit that controls the optodes, communicates with the outside world and manages the power.
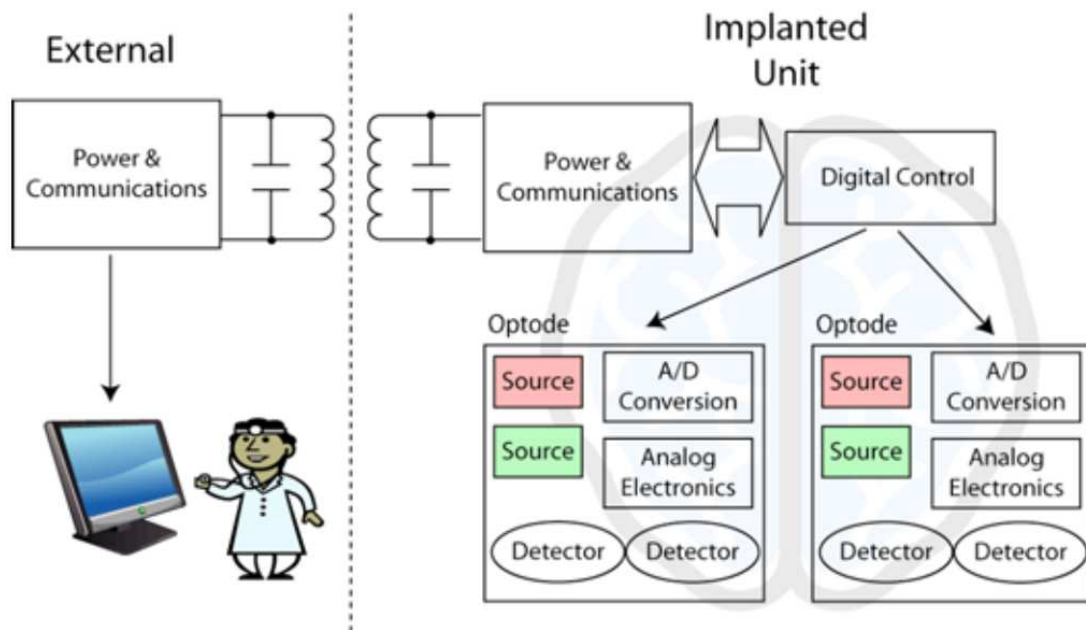
Figure 1.3 Impression of implementation of a telemetric light source system.

1.4 Goals of the project

The implementation of the telemetric light source is needed to continue research in metronomic PDT. The system that has to be developed will be used in an animal experiment, and will be designed for that purpose. In the animal experiment we aim for in this project a rat is tumours are grown within the brain of a rats GBM. After a certain time interval the device is implanted and metronomic PDT treatment is given; by repeated administration of a photosensitizer and illumination using the implant. This experiment will serves as a proof of concept to justify further development of the system. Ultimately this system will be developed for the treatment of GBM in humans.

The prototype system has the following requirements:

- The system developed in this project has to be small enough to fit in a laboratory rat
- The main function of the system is the activation of the photosensitizer by illuminating the tissue with a controllable amount of light for a specific amount of time. The system should be able to repeat this treatment for a lot of times.
- The secondary function is monitoring the treatment, ideally this consists of measuring light (reflection), oxygenation and the amount of photosensitizer present using fluorescence.
- The implant should be controlled from the outside and transmit measurement data to the outside.
- The implant should be powered from the outside.
- The implant should be biocompatible

The development of the prototype system is done in the following way. The implementation of the electronics is done with discrete devices on a flexible circuit. This way a short production time is ensured. The actual light source and detectors are

implemented/bonded on chip to ensure a small and known distance between light source and detector. Predictions on light distribution is done using Monte Carlo simulations and based on those the size of the detector is determined and designed. The electronics consist of an amplifier, micro controller, transponder IC and power management. They are implemented on a flexible substrate. The antenna and the application determine the shape of the substrate, the implantation is a rat. The communications are done with Radio Frequency Identification (RFID). This is a commonly available technology and relatively easy to adept to this application.

The inductive link is implemented with primary coil in a base plate, placed in proximity to the animal or patient, is driven by Class E circuitry, this is a highly efficient switching power amplifier. The secondary side is designed is such a way that minimal loss occurs in the antenna to prevent heating of the tissue.

2 Theoretical Introduction

2.1 Photodynamic Therapy

2.1.1 Introduction

The principle of PDT can be explained in the following way. The patient receives a dose of a photosensitizer or its precursor that localizes within the tumour because of selective uptake of this kind of tissue. When the photosensitizer is near oxygen and is irradiated with visible light it produces singlet oxygen. This leads to the destruction of the tumour tissue in the following ways: by direct damage to the tumour, by the destruction of the vasculature of the tumour, by activation of the immune system or by a combination of the three. [9]

2.1.2 Photochemistry of Photodynamic Therapy

The singlet oxygen is responsible for the destruction of the tumour cells during a PDT treatment. In figure 2.1 a Jablonski diagram is shown in which the reaction is presented. The photosensitizer is excited (A) by illumination with the appropriate wavelength. The photosensitizer can relax back to ground state under emission of a fluorescence photon (B) or can go to a triplet excited state via intersystem crossing (C). From this state it can go back to ground state under emission of a phosphorescent photon (D) or transfer energy to other molecules (E). In oxygenated environments the energy is transferred to ground state molecular oxygen $^3O_2$ that leads to production of singlet oxygen $^1O_2$. This singlet oxygen can react with organic substrates (F).
The photosensitizer can also lose its energy by internal conversion or by collisions with other molecules (G). [9]
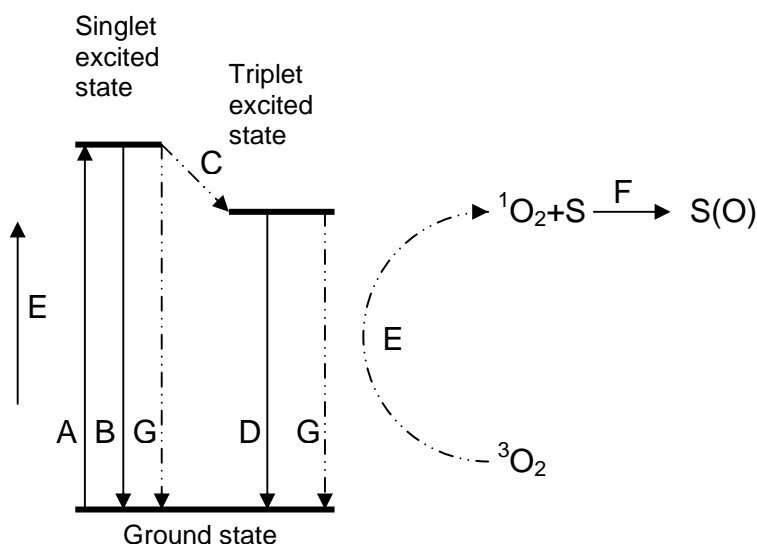
Figure 2.1 A Jablonski diagram showing the various modes of excitation and relaxation in a photosensitizer: A) excitation, B) fluorescence, C) intersystem crossing, D) phosphorescence, E) non-radiative transfer of energy to singlet oxygen, F) substrate oxidation by singlet oxygen, G) internal conversion. (Adapted from [9])

In the literature two types of photoreactions are described, type I occurs in anoxic environments, which involves the direct energy transfer from the triplet state to the surrounding environment and type II reaction which is characterized by the transfer of energy to oxygen. Type II reactions are associated with singlet oxygen production

2.1.3 Oxygen

Triplet oxygen is the normal form of oxygen, it is triplet because the electron spins in the antibonding orbital are parallel, left of figure 2.2. The state is given by the angular momentum S with the following relation: 2S+1. A parallel spin is considered to have S equal to 1 (0.5+0.5), thus state equals 3. When the spins are opposite, S = -0.5+0.5 = 0, the state is one. When they are in this state they are allowed to pair, if that happens we speak of singlet oxygen. The second state occurs when there is one unpaired electron, S = 0.5.
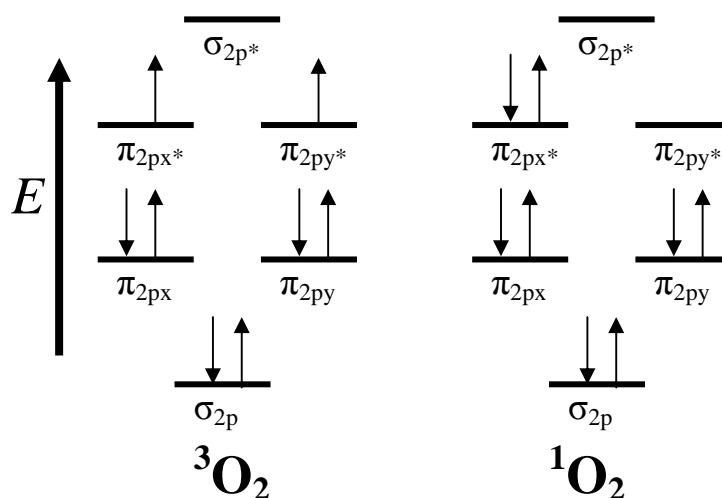
Figure 2.2 Electronspins in Oxygen, left triplet oxygen, right singlet oxygen. (Adapted from [9])

Singlet oxygen is a highly reactive form of oxygen. When triplet oxygen interacts with an excited photosensitizer the spin of the outermost electron inverts, which allows the electron to pair in the antibonding-orbital. This destabilizes the molecule and makes it highly reactive in organic substances. Singlet oxygen has a lifetime between 10 and 100 µs in organic substances, this restricts the activity to a spherical volume with a radius of 10nm. Thus the reaction is highly localized: in comparison, the cell membrane is about 10nm thick.

The oxygenation of tissue is very important for the photodynamic reaction. The oxygen consumption of the photodynamic reaction depends highly on the fluence rate of the light.

$$\frac{d[^1O_2]}{dt} = \frac{\varepsilon C \Psi}{E_\Phi}\Phi = \frac{D_{PDT}}{tE_\Phi}\Phi = k[^3O_2] \qquad (1)$$

Singlet oxygen production rate ($d[^1O_2]/dt$) is a function of fluence rate(Ψ), the total PDT dose (D_{PDT}) and the concentration of ground state oxygen [$^3O_2$]. It also depends on Concentration (C), molar extinction coefficient (ε) and the singlet oxygen quantum yield (Φ, number of singlet oxygen molecules produced per photon) of the compound.

The production rate is linear with the fluence rate when an unlimited supply of oxygen is assumed. For this reason a high fluence rate is often used in clinical situations. This reduces the treatment time. [9]

However, data from various experiments suggest that lower fluence rates expose the tumour for a longer time to singlet oxygen. During the first seconds of treatment oxygen levels drop dramatically to a fluence rate dependent level, there is no unlimited supply of oxygen. The treatment response is also dependent on the fluence rate. It has also been found that both tumour and healthy tissue is more damaged when lower fluence rates are used. [10]

2.1.4 Photosensitizer

The photosensitizer has a central role in PDT and has to fulfil a lot of demands. It has to have a high singlet oxygen quantum yield, it needs to be selectively retained in tumour tissue in high concentrations and it needs to be activated by a wavelength that penetrates tissue effectively. In addition it has to be non-toxic, water soluble and cleared in a reasonable time from the body, and rapidly from the skin to avoid photosensitivity reactions.

The most useful photosensitizers in vivo are porphyrins, chlorins, and bacteriochlorins. They have high singlet oxygen quantum yield and have absorption peaks in the red part of the spectrum. In this part of the spectrum, light penetrates relatively deep into tissue (1cm). These photosensitizers are planar-aromatic molecules, which is why they absorb light in the visible spectrum. [9] All these molecules have strong absorption around 400nm and weaker absorption peaks at 630 nm (porphyrins), 650nm (chlorins) and 710 nm (bacteriochlorins) [9]

Photofrin$^{®}$ is the first approved photosensitizer. It was developed from Hematoporphyrin Derivative (HpD) and was approved by the FDA in 1993. It is activated when illuminated with 630 nm and it has been successfully used against several kinds of cancer. At the doses used Photofrin$^{®}$ does not present systemic toxicity and appears not to be carcinogenic or mutagenic. Its damage to healthy tissue is non-cumulative like radiation and chemotherapy, which means that multiple or even chronic treatments are possible. A significant drawback of Photofrin$^{®}$ is that the skin will be photosensitized for a few weeks and severe sunburn could be a complication in these weeks after treatment.[9]

Other photosensitizers that are currently used and investigated are the prodrug 5-aminolevulinic acid (ALA, 630nm) and m-THPC (Foscan$^{®}$, 652nm). In presence of ALA the body creates an excess of natural porphyrin, protoporphyrin IX. Under normal conditions this is converted to heme, but due to the excess amount the conversion is not fast enough and the photosensitive protoporphyrin IX stays in the cells. It is used for PDT for superficial cancers up to 3 mm in depth. It is also used as photo detection agent.

Foscan$^{®}$ only needs low light and photosensitizer dose to achieve the same PDT dose as Photofrin$^{®}$. After administration it can induce photosensitivity that is usually less than 20 days. [9]

The structure, charge and hydrophobicity of the photosensitizer determine how it interacts with it surroundings and where and how it is accumulated in cells. In theory it should be possible to design a photosensitizer rationally, but this is not very realistic due to the complex processes that can influence each other in-vivo. Most photosensitizers are discovered during batch testing. When a reasonable structure is found, the chemical structure will then be fine-tuned.

2.1.5 Light

A high selectivity of PDT can be achieved if the concentration of photosensitizer in tumour tissue is higher than the one in healthy tissue. Selectivity can also be achieved by illuminating the target volume only.

PDT dose (D_{PDT}) is theoretically determined by the following formula:

$$D_{PDT} = \int\limits_{0}\int\limits_{q} \varepsilon(\lambda)C(q,t)\Psi(\lambda,q,t)dtdq \qquad (2)$$

where $\varepsilon(\lambda)$ molar extinction coefficient of the photosensitizer, $C(q,t)$ is the concentration of the photosensitizer, $\Psi(\lambda,q,t)$ the fluence rate, λ the activation wavelength, t the time and q the generalized spatial coordinate. [9] This formula assumes an infinite supply of oxygen, which is not available in tissue.

From equation 2 it follows that PDT dose ratio between healthy and tumour tissue is linear with concentration ratio between healthy and tumour tissue.

In the clinical case the concentration does not differ much, thus the light must be administered as specifically as possible.

The fluence rate depends highly on the penetration of the light into tissue. Light between 600 nm to 1300 nm penetrates relatively far into tissue. The absorption coefficients of several strong absorbers in tissue are given in figure 2.3. The penetration depth of light in tissue depends on scattering and absorption phenomena. This is further explained in subsection 2.2. The penetration depth is defined as the decrease in intensity with a factor of 1/e.
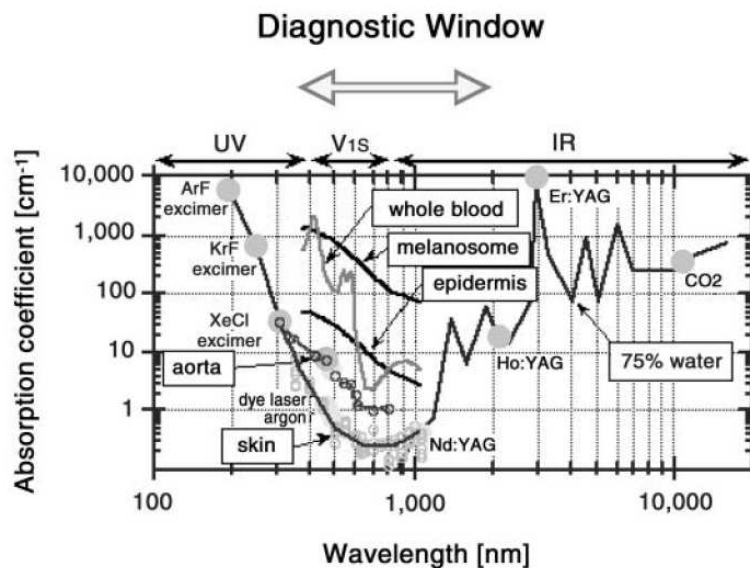
Figure 2.3 Absorption coefficient of light in tissue, dependent on wavelength and on absorbers such as water, hemoglobin, lipids and water. (Adapted from [11])

Photobleaching
Photobleaching is the term that describes the destruction of a photosensitizer under the influence of singlet oxygen that occurs when photosensitizers are illuminated light. The rate of destruction depends on the fluorophore itself, and is determined experimentally. It is generally measured by the decrease in fluorescence. In vivo changes in tissue optical properties need to be taken into account if fluorescence is to be used as a measure for the amount of photosensitizer present. PDT damage and the rate of photobleaching both increase with a decreasing fluence rate. [12]
Another application of photobleaching could be the removal of excess photofrin® from the skin with low-level illumination. [13]

Light sources
Currently lasers are mostly used as light source for PDT. This has several reasons, it is a highly coherent monochromatic light and can easily be fed into fibers that can be used as delivery devices. The fibers can be guided through an endoscope and the tip can be equipped with lenses or diffusers for optimal illumination.

2.1.6 Destructive biological reaction
In the end starvation of the tumour tissue is the goal. One way to do this is by destruction of the microvasculature and in this way starve the tumour of oxygen and nutrients. Other mechanisms that ultimately cause cell death are under investigation. Direct cell damage, damage to mitochondrion, cell membrane and lysosomes are thought to play a critical role in destruction of tumour cells.
Researchers have reported that PDT also activates or suppresses the immune system depending on certain variables. If controlled, this could also contribute to the effectiveness of PDT. [9]

2.2 Light transport in tissue

2.2.1 Optical Properties
Due to the optical properties of tissue a therapeutic window is defined as the part of the spectrum where penetrates tissue relatively deep (a few centimetres). As seen in figure 2.3 the window is in the range of wavelengths from 600 (orange/red) to 1300 nm (infrared A band).

Light simultaneously exhibits properties of both waves and particles. As a consequence light propagation can be described according to the classical theory - light is considered an oscillating magnetic field - or according to the quantum theory. Both are important for light propagation in tissue. The quantum theory is for example necessary to describe the exchange of energy or momentum between light and matter and the classical theory can be used to describe the dynamics of light transport.

The intensity of light decreases rapidly in tissue due to strong absorption, only in the therapeutic window light transport is dominated by scattering and the penetration depth can be up to 5 cm. At all wavelengths light is strongly scattered in tissue. Due to this multiple scattering effect the wave nature of light is suppressed (coherence is lost) and light intensity is the only observable parameter. This makes analysing the light transport in tissue using EM theory complicated. Instead of using the wave behaviour of light, the light energy can be used to model light transport in tissue, in what is called the radiation transport model. This model ignores interference and polarization and uses wave and quantum properties implicitly in the fundamental equations. The validity of this model for strongly scattering media has been established empirically.[11]

The propagation of light in tissue is influenced by the refractive index, absorption coefficient, scattering coefficient and the anisotropy factor. The refractive index (n) is the fundamental property of a homogeneous media and is defined as:

$$n = \frac{c}{v} \tag{3}$$

where c is the speed of light in vacuum, and v the speed of light in the medium. Of course the energy of the wave (E = h v) and the frequency are the same as in vacuum (v = c/n). [11]

Scattering
At a boundary between two media with different refractive indices light is redirected. When the boundary is large compared to the beam or wavelength, the light is partly reflected and a part is refractive transmitted. The ratio depends on the refractive indices of the media and the incident angle.

When the dimensions of the heterogeneity in refractive indices are small compared to the incident wavefront, light propagation is better described in terms of the scattering theory. This is the case when light is incident on an organelle in a cell. The light in a scattering event is redirected over a range of angles as shown in figure 2.4
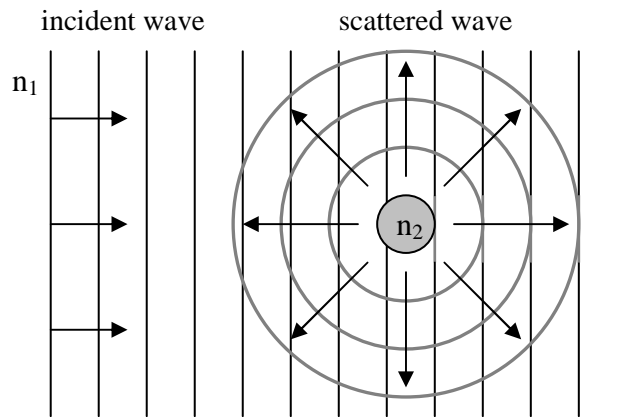
Figure 2.4 Partially scattering of an incident wave. (Adapted from [11])

$$P_{in} = I_0 A \qquad P_{scatt} = I_0 \sigma_s \qquad P_{out} = I_0 \left(A - \sigma_s \right)$$
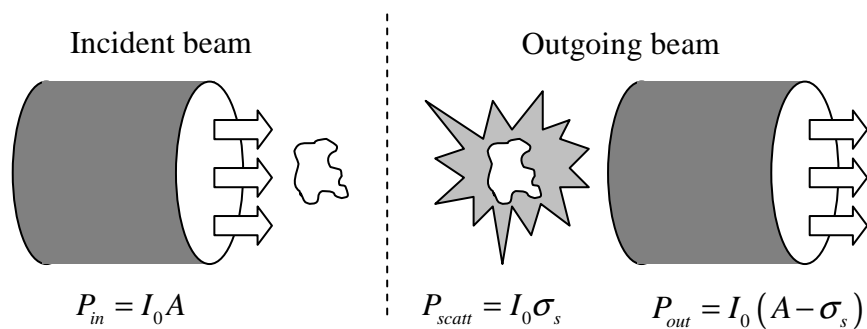
Figure 2.5 Left: Incident beam before scattering event, right: Beam after scattering event. (Adapted from [11])

Scattering is quantified using the scattering cross section. If a light beam of intensity I_0 is incident on a scattering object and P_{scatt} energy is scattered out of the incident plane wave. This is shown in figure 2.5. The scattering cross section is then:

$$\sigma_s \left(\hat{s} \right) = \frac{P_{scatt}}{I_0} \tag{4}$$

Scattering within a medium is usually characterized with the scattering coefficient σ_s. The differential cross section gives the angular distribution of the scattered radiation.

$$\frac{d\sigma_s}{d\Omega} \left(\hat{s}, \hat{s}' \right) \tag{5}$$

A scattering event and all variables involved are shown in figure 2.6.
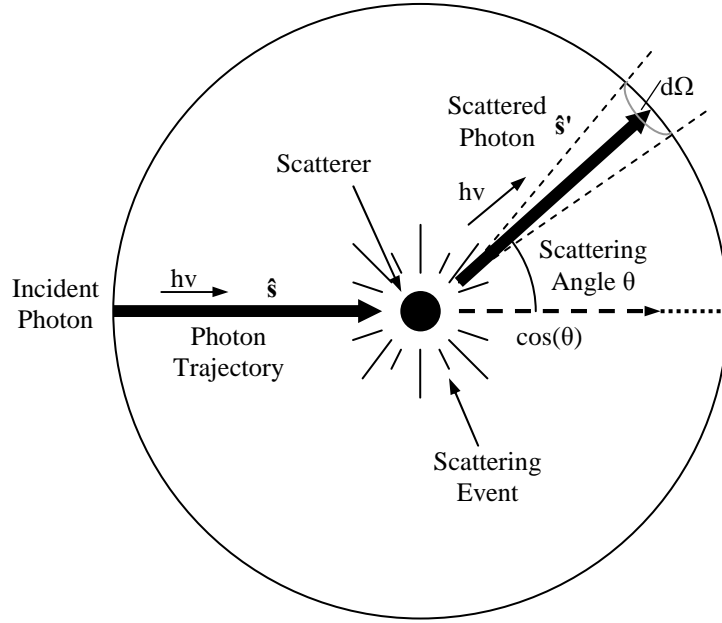
Figure 2.6 Photon scattering event in tissue, the angular distribution of the scattered light relative to the incident light is expressed in the differential scattering cross section. A photon travelling along the direction ŝ is scattered in the direction ŝ'. (Adapted from [11])

If the scatter object is assumed to be spherical symmetric, the differential cross section can be described by the cosine of the angle between $\hat{s}$ and $\hat{s}'$, this is called the phase function.

The fraction of light that gets scattered in the $\hat{s}'$ direction, from the $\hat{s}$ direction is described in the Scattering Phase Function (SPF). The SPF can be expressed in the differential cross section:

$$p(\hat{s} \cdot \hat{s}') = \frac{4\pi}{\sigma_s + \sigma_a} \frac{d\sigma_s}{d\Omega}(\hat{s} \cdot \hat{s}') \tag{6}$$

From this the average cosine of scatter is a measure of scatter that stays in the forward direction and is defined as:

$$g \equiv \frac{\int_{4\pi} p(\hat{s} \cdot \hat{s}')\hat{s} \cdot \hat{s}' d\Omega'}{\int_{4\pi} p(\hat{s} \cdot \hat{s}') d\Omega'} = \frac{1}{4\pi W_0} \int_{4\pi} p(\hat{s} \cdot \hat{s}')\hat{s} \cdot \hat{s}' d\Omega'$$
$$= \frac{1}{2W_0} \int_{4\pi} p(\cos\theta)\cos\theta \sin\theta d\theta \tag{7}$$

where W_0 is the fraction of the total cross section that is due to scattering (μ_s / (μ_a + μ_s))

If a medium contains a uniform distribution of identical scattering objects with a density of ρ the scattering coefficient μ_s is defined as:

$$\mu_s = \rho\sigma_s \tag{8}$$

The inverse of this coefficient is the mean free path between two scattering events.

Absorption
Absorption is the transfer of energy from a photon to matter. According to the quantum theory, molecules have energy levels corresponding to quantum states. The molecule can excited to a higher energy level when the difference in energy between the two levels is equal to the photon energy.

$$h\nu = \Delta E \tag{9}$$

where h is Planck constant and ν the frequency. When the molecule drops to a lower energy level, it releases the energy in the form of heat, or radiation.
The absorption bands of a molecule are the frequencies that are absorbed by a specific molecule. There are three modes of absorption: rotational, vibrational and electronic. Electronic transitions occur in atoms and molecules, vibrational and rotational only occur in molecules. Rotational levels represent the rotational state of the molecule and correspond to wavelengths ranging from the far IR to the submillimeter region. The vibration of a molecule can also be altered, the corresponding levels are in the IR region. [11]
Electronic levels are the most interesting here because this is what happens in the photosensitizer. Electronic transitions are induced by photons with energies from UV to IR regions. The electronic levels are associated with molecular orbitals. If a transition occurs the electron is moved from one orbital to another.

The absorption of a medium can be quantified in the same manner as scattering, the absorption cross section σ_a. It is the ratio between incident wave intensity I_0 and absorbed power P_{abs}:

$$\sigma_a(\hat{s}) = \frac{P_{abs}}{I_0} \tag{10}$$

An absorption coefficient μ_a for a uniform distribution of absorption particles with a density of ρ in a medium can be defined as:

$$\mu_a = \rho\sigma_a \tag{11}$$

The inverse is the mean free path between two absorption events.
From this the Lambert-Beer law is defined as

$$I = I_0 \exp[-\mu_a z] \tag{12}$$

which relates the transmitted intensity I with distance z in a homogeneous medium.[11]

2.2.2 Analytical method

Tissue has been modelled as a two-component system, randomly positioned scatter and absorption particles embedded in a homogeneous continuum. The multiple scattering is very important for the theory on light propagation. Because of multiple scattering, light loses coherence rapidly in tissue. This justifies the use of the Radiation Transport (RT) model in which coherent properties of light are not explicitly taken into account.

The RT model describes the flow of luminous energy through a medium. The medium is characterized by the absorption coefficient μ_a, the scattering coefficient μ_s and the scattering phase function (SPF) $p(\hat{s}. \hat{s}')$.

The intensity of light can be described with the radiation transport equation:

$$\frac{1}{c_m}\frac{d}{dt}I\left(r(t),\hat{s},t\right) = -\left(\mu_a+\mu_s\right)I\left(r(t),\hat{s},t\right)$$
$$+\frac{\mu_a+\mu_s}{4\pi}\int p\left(\hat{s}\cdot\hat{s}'\right)I\left(r(t'),\hat{s}',t\right)d\Omega' + Q\left(r(t),\hat{s},t\right) \tag{13}$$

The first term left is the incident light intensity, the first term on the right is loss in light intensity due to absorption and scattering out of the plane, and the second term is the increased intensity due to scattering from other direction into the direction of the plane. The third term is the source term.

The solution to this equation can be obtained in several kinds of media and in different geometries. In this case the solution for the scattering dominant limit is the most interesting. The scattering dominant limit ($\mu_a << \mu_s$) is also known as the diffusion limit. This situation can be described by means of photons that make a random walk through the medium, taking a series of steps of random length in random direction. The scattering is isotropic, which means that all angles are equally likely. This is modelled with the reduced scattering coefficient μ_s' and is related to the scattering coefficient μ_s and the average cosine of scatter g.[11]

$$\mu_s' = \left(1-g\right)\mu_s \tag{14}$$

The photons can also be absorbed, this is described by the absorption coefficient μ_a. The properties of the medium can be combined in the diffusion constant D.

$$D = \frac{c_m}{3\left(\mu_a+\left(1-g\right)\mu_s\right)} \tag{15}$$

The attenuation coefficient is given by

$$\mu_t \equiv \mu_a+\left(1-g\right)\mu_s \tag{16}$$

The diffusion equation can be obtained with under assumptions from the radiation transport equation. [11]

$$\frac{\partial}{\partial t}\Phi_d\left(r,t\right) = D\nabla^2\Phi_d\left(r,t\right) - \mu_a c_m\Phi_d\left(r,t\right) + Q_c + Q_s \tag{17}$$

Solutions for this equation are only valid for completely diffuse fields, this requires that the distance between source and detector needs to exceed $1/\mu_s$. The scattering should be dominant over absorption and the tissue should be homogenous.

2.2.3 Monte Carlo method, numerical modelling

Since analytical methods are difficult at best for realistic RT problems a widely used way to solve RT problems is the Monte Carlo method. Monte Carlo is a numerical method that uses probability distributions to determine the results. The method simulates the trajectory of a single photon by calculating the properties of each step of the photon (length, direction, "weight," etc). These properties are determined by statistically sampling randomly distributed variables.
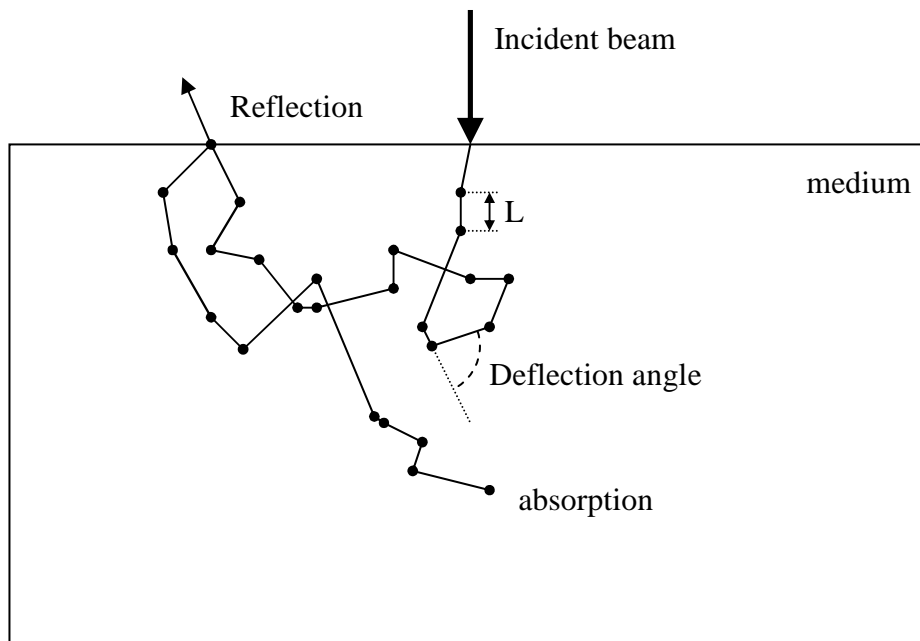
Figure 2.7 The Monte Carlo method for a single photon packet.

Advantages over the diffusion approximation are that MC simulations do not need the requirement that $\mu_s \gg \mu_a$ and accurate results can be obtained close to sources and boundaries. On top of that it is easily adapted to multilayered and three dimensionally heterogeneous tissue.[14]

In the basic Monte Carlo model first the step size of the photon packet is determined, the distance between an interaction between light and tissue. Beer's law relates the decrease in unscattered intensity of light with depth in tissue:

$$\frac{I(L)}{I_0} = p_L = \exp\left[-(\mu_a + \mu_s)L\right] \tag{18}$$

In the Monte Carlo method this is interpreted as the probability that a photon packet will cover a distance L without being scattered or absorbed, the mean free path. When L is expressed in the probability factor p we get:

$$L = -\frac{\ln p}{\mu_a + \mu_s} \qquad (19)$$

Now L can be determined each step by selecting a number p from a uniform distribution.

$$f(p) = \begin{cases} 1 & 0 < p \le 1 \\ 0 & otherwise \end{cases} \qquad (20)$$

The average of *ln p* with distribution *f(p)* is *–1*, thus the mean free path is $1/(\mu_a + \mu_s)$ as expected. [11]

Each photon packet has a weight that models the effect of the absorption of tissue. For the other computational option namely the photon is terminated according to a probability distribution, a lot of extra computing is needed to get the same results. Each step a fraction of the photon packet is absorbed:

$$\Delta W = W \frac{\mu_a}{\mu_a + \mu_s} \qquad (21)$$

After this the deflection and the azimuthal angle of the scattering event will be determined. The scattering Henyey-Greenstein function describes the probability distribution of the cosine of the deflection angle, and is a function of the anisotropy factor g. The azimuthal angle is uniformly distributed over the interval 0-2π.[15]

When the step size is large enough to encounter a boundary, the step size is shortened in a way that the photon packet stops at the boundary. The remaining part of the step is used for the next step. Then the probability of reflection at the incident angle is determined using Fresnel's formulas. Then a random number is sampled from the uniform distribution, if this number is smaller than the probability of reflection, the photon packet is reflected, and otherwise transmitted. According to this and to the remaining part of the step the location is updated.

Another possibility to handle reflections is to reduce the weight proportional to the amount reflected (transmitted part) and introduce a new photon packet on the reflected position with the remaining weight. This increases computing time but decreases variance in reflectance and transmittance.

When the photon packet is going out of the tissue, this is added to the resulting reflection vector [15].

After this step this procedure is repeated over and over until the weight of the photon packet reaches a certain threshold, absorption. This is shown in figure 2.7 [15].

2.3 Electronics Background

2.3.1 Photodiode

A photodiode is a device which converses light into current. This is achieved using the photoelectric effect. When photons are incident on a semiconductor, these photons can transfer their energy to individual silicon atoms. For each photon that is absorbed an electron hole pair results. This is equivalent to saying that an electron is transferred from the valence band to the conduction band. The only condition that has to be met is that the photon needs to have a higher energy than the bandgap E_g. [16]

To detect the electron-hole pairs, the electrons and the holes need to be separated before they can recombine. In a photodiode this is done by the built-in electric field in the depletion region. The electrons will flow to the n doped silicon, and the holes will flow towards the p-doped silicon (figure 2.8). As a result a reverse current is generated through the diode, the photocurrent. [16]
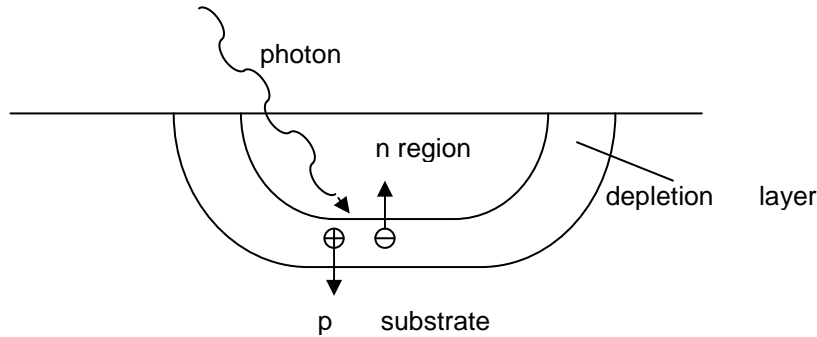
Figure 2.8 Generation of a photocurrent in a photodiode

The photodiode can be modelled as a current source parallel to an ideal diode with its parasitic elements. The parasitic elements of a diode are a parallel resistance Rd, which is the zero biased parallel resistance. Normally this is a very high resistance. Series resistance R_s is the resistance of the semiconductor and is very low. The last parasitic element is C_d, which has important performance effects. It depends on the area of the diode and on the voltage (the width of the depletion region).

The photocurrent is given by equation 22,

$$I_{photo} = qA\frac{P_{photo}\lambda}{hc}\eta \qquad (22)$$

In this equation, q=1.602 10-19 C is the charge of the electron, A is the area of the photodiode, P_{photo} is the optical power incident per unit of area, λ is the wavelength of the incident light, h=6.626 10-34 J · s is Planck's constant, η is the quantum efficiency of the device and c=2.1098 108 m/s is the speed of light in vacuum.

Most important parameter of a photodiode is the quantum efficiency, this is the percentage of photons that effectively produce electron hole pairs. This is, among other things, influenced by the amount of absorbed light within the depletion region. The absorption coefficient of silicon depends on the wavelength of the incident light, given by figure 2.9. As a result a photodiode has a different response for different wavelengths. [16]
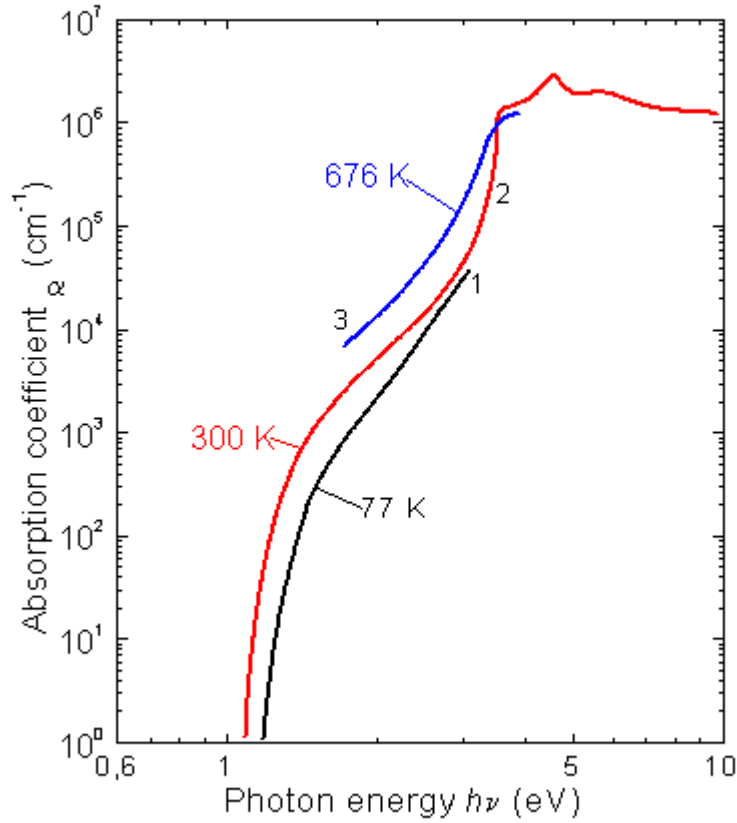
Figure 2.9 Absorption coefficient of intrinsic silicon

The intensity of an incident beam of photons at a specific depth z is

$$I(z) = I_0 e^{-\alpha z} \tag{23}$$

where I_0 is the intensity just beneath the surface and α is the absorption coefficient.
The width of the depletion region is determined by equation 24 and the parameters from the process from which the photodiode is made.

$$W = \left(\frac{2 \epsilon_s \left(V_{bi} + V_R \right)}{e} \left[\frac{N_a + N_d}{N_a N_d} \right] \right)^{1/2} \tag{24}$$

In this equation, W corresponds to the width of the depletion region, V_{bi} is the built in potential of the diode, e=1.602 10-19 C is the charge of the electron, V_R is the reverse voltage applied to the diode, N_a is the concentration of acceptor impurities in the p-side and N_d is the concentration of donor impurities in the n-side of the junction. With these two equations the spectral efficiency can be determined.
Other important parameters are dark current and the noise. Dark current is the current that flows when no optical signal is present. The dark current is generated by thermally excited electron hole pairs. The noise sources in a photodiode include shot noise, thermal noise and quantum noise.

2.3.2 Light Emitting Diode

The inverse mechanism of a photodiode is also possible. When a voltage over a pn junction is applied electrons and holes are injected into the depletion region where they are minority carriers. When they recombine with majority carriers in a direct band to band process, they emit a photon. The amount of photons emitted is proportional to the diode current. This effect is called injection electro-luminescence and is used in a Light Emitting Diode. The spectral output of a LED is about 30-40 nm wide.

An important parameter of a LED is the quantum efficiency, this parameter can be split up in two parameters, the internal quantum efficiency and the external quantum efficiency. The internal quantum efficiency is the fraction of the current that is converted to photons and depends on the injection efficiency and the ratio between radiative and non-radiative recombination. Both of these parameters depend on doping level and semiconductor. The external quantum efficiency is the fraction of generated photons that are emitted from the semiconductor. The external quantum efficiency is normally very low due to photon absorption, Fresnel loss (the loss due to the difference in refractive index, part is reflected back into the semiconductor) and critical angle loss (when the photon has an angle greater then the critical angle defined by Snell's law).

The wavelength of a LED depends on the bandgap energy, as stated in formula 25.

$$\lambda = \frac{hc}{E_g} = \frac{1.24 \times 10^{-6}}{E_g} \tag{25}$$

where E_g is the bandgap energy in eV.

The bandgap of silicon is indirect, which makes almost impossible to make a LED with. The bandgap of GaAs is direct and is 1.42 eV this gives a wavelength of 873 nm. To get a visible output bandgap energies between 1.7 and 3.1 eV are needed. For this purpose $GaAs_{1-x}P_x$ can be used. With x < 0.45 it is a direct bandgap material. At x = 0.4 the bandgap energy is 1.9 eV which corresponds with a wavelength of 652 nm.

With the advances in material science more materials with different direct bandgap energies became available. At this moment a wide range of source wavelengths within the visible spectrum is on the market.

2.3.3 Current to Voltage amplifier.

The output quantity of the photodiode is the photocurrent. This current is linear with the amount of light. It can be converted to a voltage with the use of a transimpedance amplifier. Ideally the amplifier has zero input impedance because in that case the diode is not loaded, and no voltage is across the diode. The transimpedance amplifier can be implemented with an operational amplifier as in figure 2.10.
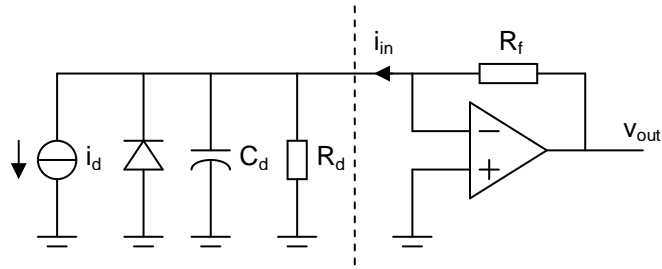
Figure 2.10 Transimpedance amplifiers with photodiode including its parasitic elements

The voltage between the + and – input of the amplifier is amplified by the open-loop gain of the amplifier resulting in a voltage at the output. This voltage appears across the resistor between the – input and output, resulting in a current through that resistor. Due to the feedback the current through the feedback resistor becomes equal to the photocurrent. If the photocurrent is a bit higher than the feedback current, a voltage will appear over the input, due to the high input resistance of the operational amplifier, and the output voltage will increase. As a consequence the feedback current increases to the same level as the photocurrent, and the voltage over the input of the operational amplifier goes down to zero.

The transimpedance amplifier will have low input impedance because the voltage will be almost zero over the input.

The output voltage will be proportional to the input current with the following relation:

$$i_{in} = \frac{v_{out}}{R_f} \qquad (26)$$

The feedback resistor determines the gain of the amplifier. Except for the gain, important parameters of an amplifier are the noise, distortion and the bandwidth.

Noise
The noise due to amplification is determined by the operational amplifier itself and by the feedback resistor. The noise of the operational amplifier is due to several physical processes can be described by the voltage noise density e_{ni} (V/ $\sqrt{Hz}$) and the current noise density i_{ni} (A/ $\sqrt{Hz}$) in front of the operational amplifier. These sources can also be converted to the output. At the output the current noise source is represented by:

$$e_{noi} = i_{ni}R_f \qquad (27)$$

the voltage noise of the operational amplifier at the output is equal to:

$$e_{noe} = (1 + R_f C_i s)e_{ni} \qquad (28)$$

The noise of the resistor is thermal noise and has spectral density:

$$e_r = \sqrt{4kTR_f} = e_{noR} \tag{29}$$

where k is the Boltzman constant and T is the temperature. This noise source is directly measured at the output.

The total noise is added according to equation 30. And assumes uncorrelated sources

$$e_{no} = \sqrt{e_{noR}^2 + e_{noi}^2 + e_{noe}^2} \tag{30}$$

Adding a capacitor in the feedback network can reduce the total noise, this results in a lower amplification of noise in the higher frequency band, but decreases the bandwidth of the amplifier [17]. If a feedback capacitor is used the total noise at the output is equal to:

$$e_{noe} = \frac{1 + R_f(C_i + C_f)s}{1 + R_f C_f s} e_{ni}$$

$$e_{noi} = \frac{R_f}{1 + R_f C_f s} i_{ni} \tag{31}$$

Distortion
The distortion of the amplifier is clipping distortion and harmonic (weak) distortion. The last one is usually not big and in our case it is not an issue. Clipping distortion occurs when the output voltage should be higher than the supply voltage. This is for example the case when the input current times the amplification factor exceeds the supply voltage, and as a consequence the output voltage is equal to the supply voltage. In this case there is no linear relation between the input current and the output voltage. This can be prevented by properly choosing the feedback resistor or increasing the supply voltage of the operational amplifier.[18]

Bandwidth
The bandwidth of the operational amplifier is determined by the source capacitance, the Gain-Bandwidth product of the operational amplifier and the feedback network. This is shown in equation 32 and 33.

$$BW = \sqrt{f_{FB} f_{OpAmp}} \tag{32}$$

where BW is the bandwidth of the amplifier, f_{OpAmp} the Gain Bandwidth product and f_{FB} the cut-off frequency of the feedback network which, can be calculated from:

$$f_{FB} = \frac{1}{2\pi R_f(C_{input} + C_f)} \tag{33}$$

where C_{input} is the diode capacitance and C_f the feedback capacitance that can be there for noise reduction or stability issues [17].

2.3.4 Microcontroller

A microcontroller is a single chip which includes at least a CPU and read-only memory. Usually the microcontroller includes also some peripheral functions, such as read/write memory, PWM, counters and AD converters. The microcontroller executes the program on the read only memory and can perform pre-programmed tasks using its peripheral devices. Compared to general-purpose processors it runs at low frequency, uses low power and is self-sufficient (it does not require extra devices like memory).

Analog to Digital Conversion (ADC) .

A method for analog to digital conversion is successive approximation, whose working principle is illustrated in figure 2.11
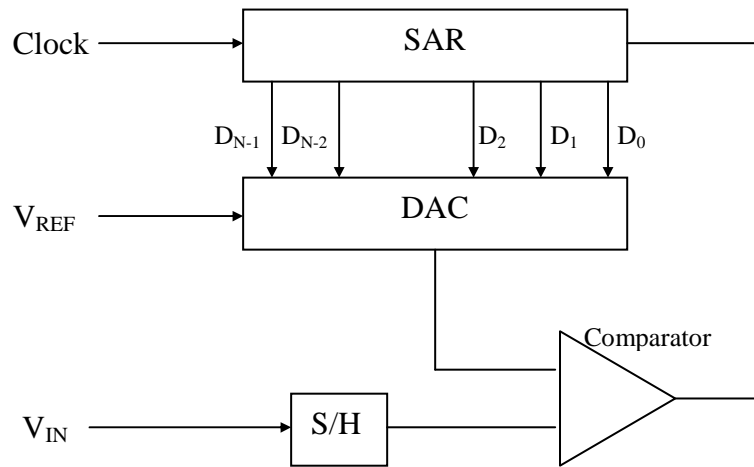
Figure 2.11 Successive Approximation ADC

The input is sampled with sample and hold (S/H) circuitry. A first approximation is made setting the Most Significant Bit (MSB) in the Successive Approximation Register (SAR). That first approximation is converted to a voltage using the Digital to Analog Converter (DAC) and compared to the input voltage. If the DAC voltage is smaller than the input voltage the MSB is reset and the next bit is set in the SAR, otherwise the MSB stays set and the next bit is set in the register. This next approximation is compared again until all bits are determined.

The accuracy of the ADC is determined by its resolution, the width of the SAR n. The value is approximated with steps of $V_{ref}/2^n$. Which gives quantization errors of maximal $0.5* V_{ref}/2^n$. The conversion result is according equation 34:[19]

$$ADC = \frac{V_{IN} 2^n}{V_{ref}} \tag{34}$$

Pulse Width Modulation (PWM)
PWM on a microcontroller is usually implemented using a counter. An output pin is set and when the counter reaches a reference value the output pin is reset. The output pin is set again when the counter reaches its maximum value. The counter is reset and the procedure is repeated. By altering the reference voltage a different pulse width can be obtained as shown in figure 2.12 [19]
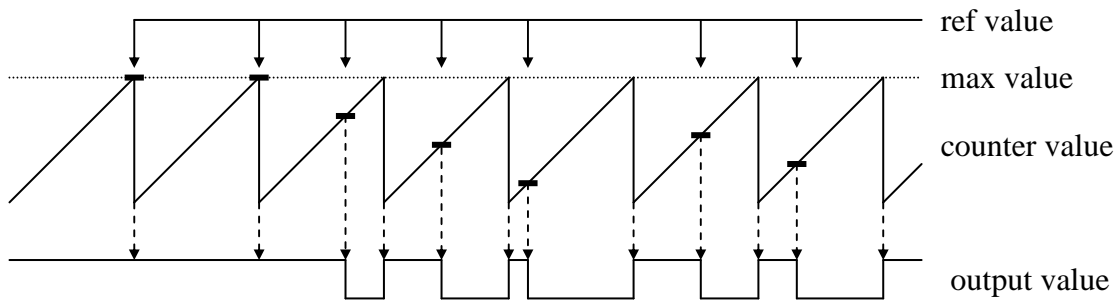
Figure 2.12 Pulse Width Modulation implementation using counters.

2.4 Wireless link

2.4.1 Wireless communications

There are several ways of implementing a wireless communications channel. A commercially available technique used in many applications is Radio Frequency Identification (RFID). For example, it is used in product tracking, public transport systems and in passports. It is also used in implanted devices, in animals for identification and in humans for identification and payment in nightclubs.

There are three types of RFID communications: passive, semi-passive and active . In the active type the transponder has its own power source and uses this to actively broadcast a response signal. The passive and semi-passive types use backscattering or load modulation of the RF field to do the communications. Semi passive has its own power source, but does not use it for the communication. Passive tags use the power from the RF-field.

RFID can be used with several frequencies, Low frequency (125 kHz), High frequency (13.56 MHz), and Ultra High Frequency (>300 MHz).

In the low frequency case the downlink of the RFID system uses On Off Keying as modulation technique. The time between two gaps in the field determines the data. For the Atmel demonstration kit the bit rate can be chosen between RF/2 to RF/64, which results in 64 kbit/s to 2 kbit/s.

For the uplink the primary coil voltage can be altered by the RFID transponder using a damping stage changing the Q factor of the secondary coil. By modulating primary the coil voltage in this way, data communication is possible between the transponder and the base station. The Atmel demonstration kit allows Manchester or bi-Phase encoding for modulating the coil voltage. The bit rate can be up to 64 kbit/s.
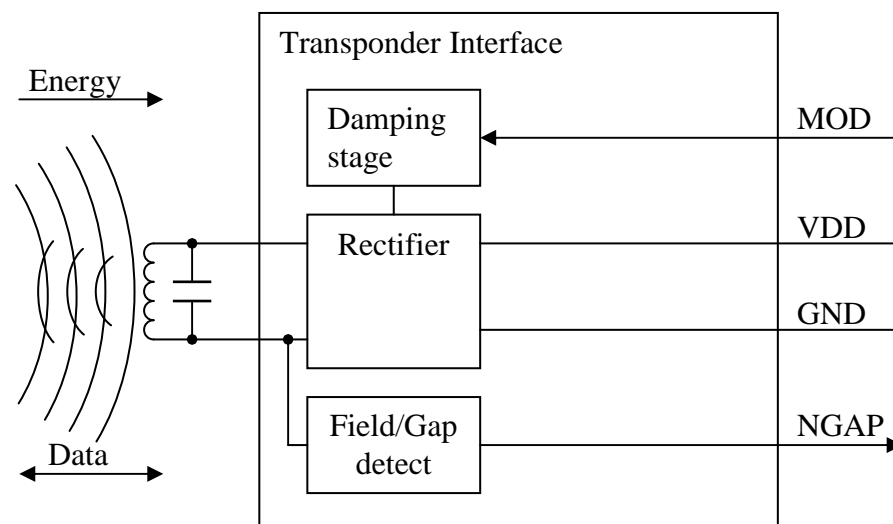
Figure 2.13 Transponder Interface for RFID.(Adapted from [20])

Normally a passive transponder constantly repeats its code. The base station just has to listen with the correct coding scheme and the correct header. If the communication needs to be more sophisticated, the base station initiates communications by querying for data. The corresponding tag or transponder replies. This response can contain the ID code of the tag, measurement data stored in the EEPROM of the tag or data that is supplied by a microcontroller.[20] A typical configuration for a transponder chip is given in figure 2.13. With a damping stage to modulate the field and Gap detection circuitry to detect the on-off keying modulation.

2.4.2 Inductive Power transfer

Wireless powering can be done using inductive power transfer. This consists of a primary coil, which produces an alternating magnetic field. The secondary coil is placed within this magnetic field and a current is induced. The amount of current induced depends on the magnetic field present.

Inductor

The coil is characterized by its self-Inductance value L, which is dependent on the dimensions and the number of turns. For several geometries approximations are available in literature. For a multiple layer short solenoid the value can be approximated with equation 35 which is given by the Radio Engineers handbook [21].

$$L_0 = \frac{0.315 r^2 n^2}{6r + 9B + 10C} [\mu H] \qquad (35)$$

where r is the average radius in centimeter, B the length of the coil in centimeter, C the height in centimeter as shown in figure 2.14.
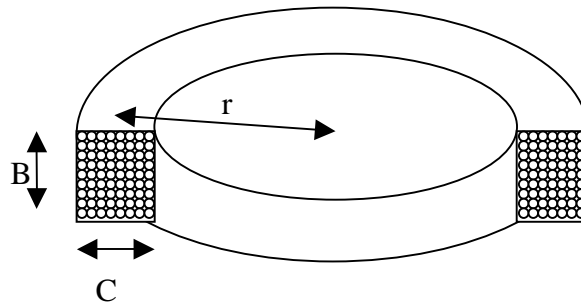
Figure 2.14 Multiple layer short solenoid.

Ideally an inductor does not have any resistance, but in the real world the inductor has a certain resistance. This is modelled as a series resistance R. The Q factor is a measure for this series resistance and is dependent on the oscillation frequency according to the relation given in equation 36.

$$Q = \frac{\omega L}{R} \qquad (36)$$

where ω is the angular frequency. The resistance is also dependent on the frequency because of the skin effect. The skin effect implies that current densities are higher at the side of a conductor and low at the centre of the conductor, this effect increases with frequency and contributes to the resistance in a conductor. To reduce the effect for frequencies in the range of few kHz to a few MHz, Litz wire is used. A litz wire consists of a number of individual insulated strands, which are woven in such a way that the current will be equally distributed over the strands, reducing the skin effect.
For coil resistance the frequency dependent resistance is modelled as an Effective Series Resistance (ESR).

To determine the ESR extensive analysis is needed, but a simple approximation is given by Kendir [22] and is given by formula (37)

$$ESR = R_{dc}\left(1 + K_c\left(\frac{N_s \times ID}{OD}\right)^2\left(\frac{ID\sqrt{f}}{0.262}\right)^4\right) \tag{37}$$

where R_{dc} is the DC resistance of the coil, K_c is a factor which considers the shape of the coil, N_s is the number of strands in the Litz wire, ID is the diameter of an individual strand in meters, OD is the outer diameter of the Litz wire and f is the frequency. The last term $\left(\frac{ID\sqrt{f}}{0.262}\right)^4$ is the Eddy current basis factor.

The power dissipated in the coil can be approximated using [22]

$$P = i^2 ESR \tag{38}$$

Secondary side
The secondary side of an inductive power link can be modelled like the circuit given in figure 2.15.
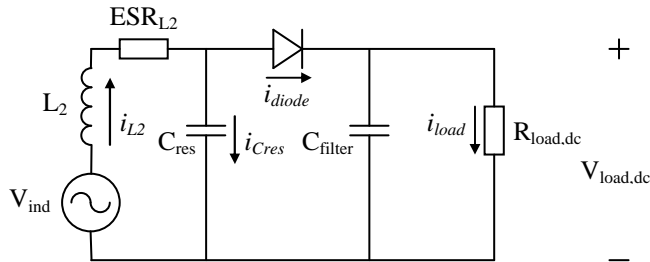
Figure 2.15 Non-linear model of the secondary side.

The load of the secondary side is modelled as $R_{load,dc}$, the rectifying circuit is modelled with diode D_1 and capacitor C_{filter}. The resonance circuit consists of the lossy inductor L_2 with its series resistance ESR_{L2} and the capacitor C_{res}. [22]
The secondary side can also be approximated with a linear model, given in figure 2.16.
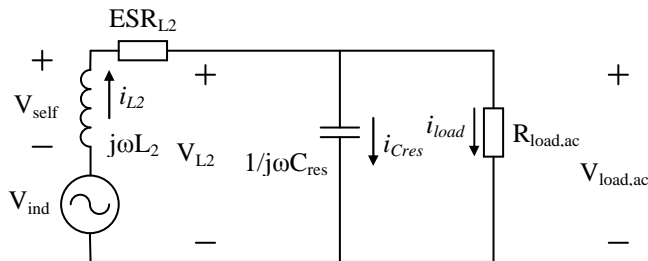
Figure 2.16 Linear approximation of secondary side

To justify this approximation the DC load must be transferred to a linear AC load. The formula to approximate the AC load is given in equation 39.

$$R_{load,ac} = \frac{\frac{1}{2}\left(V_{load,dc} + V_{diode}\right)^2}{P_{diode} + P_{load}} \qquad (39)$$

The same voltage over the coil and resonance capacitor must be maintained. The effective ac load voltage is approximated by equation 40.

$$V_{load,ac} = \frac{V_{load,dc} + V_{diode}}{\sqrt{2}} \qquad (40)$$

This model is only valid if the following relation is valid.

$$\frac{1}{\omega C_{res}} = R_{load,dc} \qquad (41)$$

When the linear model is not valid the various parameters can be determined using SPICE analyses. With this analysis the induced voltage can also be determined.
With the linear and non-linear analyses the optimal inductor value can be determined, such that it minimizes the loss in the inductor, and the required induced voltage can be calculated. From the required induced voltage the corresponding magnetic field can be calculated using equation 2.5-8.[22]

$$H_{ind} = \frac{V_{ind}}{N_2 \pi^2 a^2 2 f \mu_0} \qquad (42)$$

Primary side
The primary side can be modelled using the circuit shown in figure 2.17:
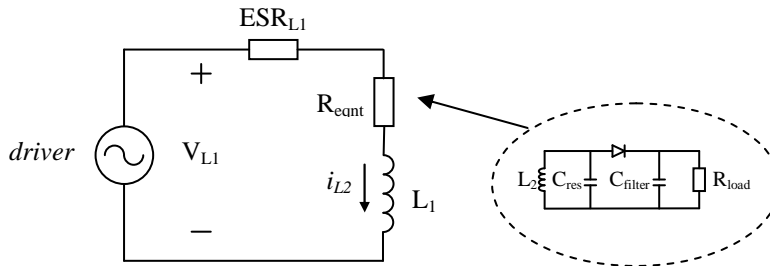
Figure 2.17 Model of the primary side of the inductive power link.

The driver can be a class E driver, described in the next paragraph. The ESR_{L1} corresponds to the losses in the primary coil, R_{eqnt} equals the equivalent load of the secondary side and is given by:

$$R_{eqnt} = \frac{P_2}{i_{L1}^2} \qquad (43)$$

where P_2 equals the power delivered to the secondary coil.[22]

To induce the needed voltage in the secondary coil, the current through the primary coil needs to be:

$$i_{L1} = \frac{V_{ind}}{\omega k \sqrt{L_1 L_2}} = \frac{V_{ind}}{\omega M} \qquad (44)$$

where k is the coupling coefficient, which depends on the geometric position of the two coils, the number of turns and the size. M is the mutual inductance and is given in µH by the Radio Engineers Handbook [21] as:

$$M = n_1 n_2 M_0 \qquad (45)$$

where n_1 is the number of turns in the primary coil, n_2 the number of turns in the secondary coil. M_0(µH) is given by:

$$M_0 = 2.54 N \sqrt{Aa} \qquad (46)$$

where A is the radius of the largest coil, a the radius of the smallest coil and N is depends on the relative position of the coils and is tabulated in the radio engineers handbook.[21]
If equation 37, 38 and 44 are combined equation 47 is obtained:

$$P_{loss} = \frac{V_{ind}^2}{\omega^2 k^2 L_1 L_2} \times \frac{2\pi r \rho}{K_s bc} \left(1 + K_c \left(\frac{N_s \times ID}{OD} \right)^2 \left(\frac{ID\sqrt{f}}{0.262} \right)^4 \right) \qquad (47)$$

If the coil is operated at a frequency where the skin effect is negligible (the second term goes to zero) one can conclude that the loss decreases when L_1 increases [22]. This only valid if the operating frequency is far below the self-resonance frequency of the coil.

Class E driver

A class E driver is a power efficient driver for a given load. The class E driver is characterized by the fact that at the switch time, zero voltage is over the switch and no current is flowing, while the voltage over the switch is close to zero when the current is flowing. This minimizes the power dissipated in the switch. [23] Figure 2.18 shows a possible implementation.
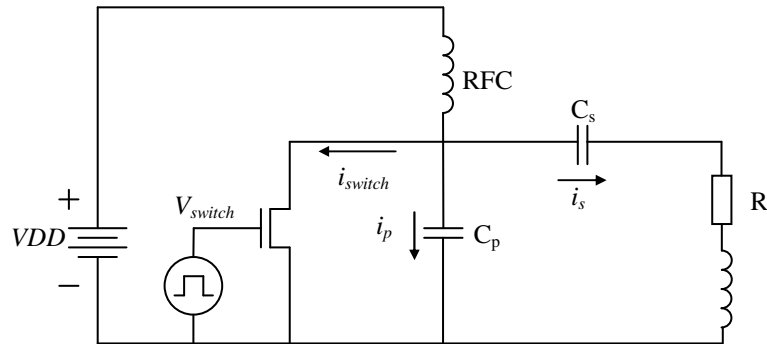
Figure 2.18 Class E topology with a multi frequency load.

While the switch is closed, current from L and C_s (I_s) flows through the switch and not to C_p, as a consequence of the fact that no voltage builds up over the switch. When the switch opens, L and C_s continue to supply current and C_p is loaded, increasing the voltage over the switch. When the current I_s changes direction C_p supplies the current through C_s and L, decreasing the voltage over the switch. When the voltage is diminished, the switch is closed again and the process starts again. The typical waveform is given in figure 2.19.
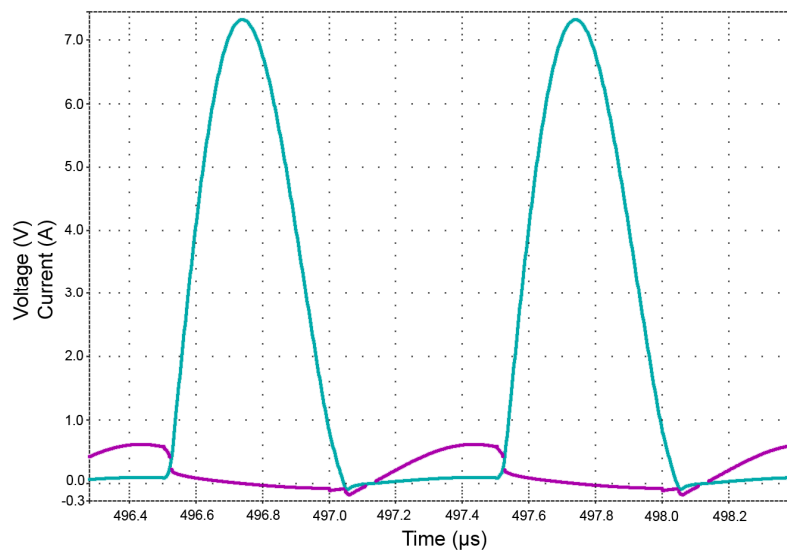
Figure 2.19 Simulation of class E driver, current through and voltage over the MOSFET.

The component values can be calculated with the methodology proposed by Kazimierczuk [24]. First, the two resonant frequencies (ω_{01}, ω_{02}) with its quality factors (Q_1 Q_2) are determined. When the switch is closed:

$$\omega_{01} = \frac{1}{\sqrt{LC_s}} \tag{48}$$

$$Q_1 = \frac{\omega_{01}L}{R} = \frac{1}{\omega_{01}RC_s} \tag{49}$$

And when the switch is open,

$$\omega_{02} = \frac{1}{\sqrt{\dfrac{LC_sC_p}{C_s+C_p}}} \tag{50}$$

$$Q_2 = \frac{\omega_{02}L}{R} = \omega_{02}R\frac{C_sC_p}{C_s+C_p} \tag{51}$$

Where R is the load and the ESR of the coil.
Kazimierczuk defined A_1 and A_2 as the ratio between the resonant frequency ($f_s = \omega_{01}/2\pi$, $f_p = \omega_{02}/2\pi$) and the operating frequency f:

$$A_1 = \frac{f_s}{f} \tag{52}$$

$$A_2 = \frac{f_p}{f} \tag{53}$$

With these parameters, Kazimierszuk set up a set of equations, which can be solved numerically. The results were tabulated in a lookup table, and with these results the several component values can be calculated. [24]

2.5 Biocompatibility

During the last century many artificial materials and devices have been developed that can perform functions within the human body. These materials (biomaterials) have to keep functioning within the human body, where they are in contact with biological fluids and living tissue, without causing rejections or adverse reactions. Devices created form these materials are generally known as implants or biomedical devices. Implants are generally accepted and the most common are orthopedic prostheses, cardiovascular implants, neural implants, plastic and reconstructive implants, dental implants, ophthalmic implants, catheters and bladder stimulators, drug dispensing implants, general surgical systems (for example staples). [25]

The traditional the term biocompatibility is given to materials that evoke a minimal biological response. It suggests that a biocompatible material display only harmonious behaviour in contact with tissue and body fluids. And it does not state anything about the effect of biological processes on the material. Black [26] states that the real biocompatibility "is not whether there are adverse biological reactions to a material, but whether the material performs satisfactorily in the application under consideration". This defined by Williams as "the ability of a material to perform with an appropriate host response in a specific application" in The Williams Dictionary of Biomaterials [27].

The appropriate host response in a specific application is the medical function of the implant. Which has results in the potential benefit of the implant.

Black defines Biological performance to replace the traditional idea of biocompatibility as: The interaction between materials and living systems. Two closely related terms are the host response: the local and systemic response other then the intended therapeutic response of living systems to a material. And the material response: The response of materials to living systems.[26]

Host response

Apart from the intended host response, the host can respond to the biomaterial in a different non-intended way. This can be local, systemic or remote.

Inflammation is a local non-specific response to tissue damage. It can also be triggered by intrusion of foreign materials. The result from the inflammation response can be:

- Extrusion, if the implant is in contact with epithelial (tissue composed of layers of cells that line the cavities and surfaces of structures throughout the body) tissue, the response will be the formation of a pocket continuous with the adjacent epithelial membrane.
- Resorption, if the implant is resorbable the implant eventually resolves.
- Integration, the implant is embedded with nearly normal tissue
- Encapsulization, the implant is encapsulated. This is the most common case.

Local Specific response to blood vessel damage and blood tissue damage are respectively coagulation (thrombosis) and hemolysis (thrombus). This is the response induced by PDT. The first one is acute, caused by direct damage and/or contact with foreign materials, and the second one is chronic caused by damages to the blood cells. Another local host response is adaption to the implant. For example growth of a new tissue layer (neointima). After insertion of the implant clotting takes place and a fibrin surface is formed and within 24 hours it is stable. Within a few weeks the implant is covered with granulation tissue.

Systemic specific host response is the immune response. The system of cells and mediating agents mediating this response to foreign or non-self materials is called the immune system. If something, foreign tissue or an implant, is recognized as non-self it produces an inflammatory response called rejection.[26]

The material response, discussed in the next subsection, can cause remote host response. Degradation of the biomaterial can cause particles of the biomaterial to be transported to other parts of the body or organs where they can cause problems. [26]

Material response

Material effects can be swelling, fluids or ions moves from tissue to the biomaterial, and leaching, components of the biomaterial move in to the tissue. Swelling can cause the material to exceed its stress limit, or can experience static fatigue. Leaching can cause undesirable biological reactions of the released product.[26]

Other material effects can be corrosion in metals, and dissolution in ceramic materials (for example silicone) . The biomaterial is solved in the fluids surrounding it. This can cause defects in the material, causing leaching for example. Dissolution depends on material properties like composition, processing and final form, and on local properties such as pH and pO_2. On the contrary to corrosion it is not dependent on local applied potential because these materials act as insulators. [26]

Implant life history

The implant life history is "the total combination of requirements that the biomaterial must meet to be successful in an application". [26] The implant life history varies considerably from application to application and from patient to patient. A hip replacement is a different problem for a 35 year old and a 70 year old. The implant life history can be used for demand matching at can help to construct a 'good enough' device. Objective measures for the implant life history are age (life expectancy) and gender. [26]

In-Vitro biocompatibility tests.

In Vitro tests are necessary before implantation. It is desirable that the material is tested under circumstances that the material encounters during operation and after implantation. Four classes of exposure environments are distinguished for this reason: Physiological (chemical (inorganic) and thermal conditions), Biophysiological (physiological with cell products, enzymes, proteins etc), Biological (Biophysiological with viable, active cells), Pericellular (biological but with cells of the immediate vicinity). In vitro tests are usually only carried out under the first two classes. [26]

Encapsulation

Encapsulation of an electronic circuit is a suitable way to make a device biocompatible. Silicone is a suitable material for biocompatible sealing of an implant. [28] Medical grade silicone is commercially available and is suitable for extended duration implantation. [29]

Studies on the effect of medical grade silicon have been done. It was shown by Swanson that during a 2-year implantation a weight increase of 0.91% was measured. This was due to absorption of lipids. The mechanical parameters such as elongation and tensile strength changed considerable during the implantation period. The data from the experiment of Swanson also suggests that no silicone is leaching during the implantation period. [30]

The silicone from Applied Silicone is especially made for long-term implantation and meets the ISO 10993 requirements for long-term implantation. [29]

The front-end of the implant will be encapsulated with biocompatible epoxy. The epoxy does is not flexible, it is used to prevent the bondwires from breaking.

3 Implementation of the System

3.1 General Overview

The main purpose of the system to be developed is the delivery of light to a specific volume of tissue. The light source should be controlled externally to the body. The number of sources would be ideally moderately large; in this way the targeted volume can be illuminated in a controllable and well-defined manner.

The secondary application is monitoring the treatment. This consists of monitoring the temperature, the fluence rate, the concentration of the photosensitizer and the oxygen level. This data has to be available for the physician supervising the treatment.

The system is meant for long term operation, meaning more than 6 months, thus battery operation is not desirable and the implant should be externally powered. Further, the implant should be packaged in a biocompatible way. The system should be modular in a way that it can be adapted to different types of PDT and different treatment volumes.

The system consist of three main parts: the optodes which deliver and monitor the treatment, a central unit which communicates and manages the power and a base station which acts as an interface between the system and the operator at the outside.
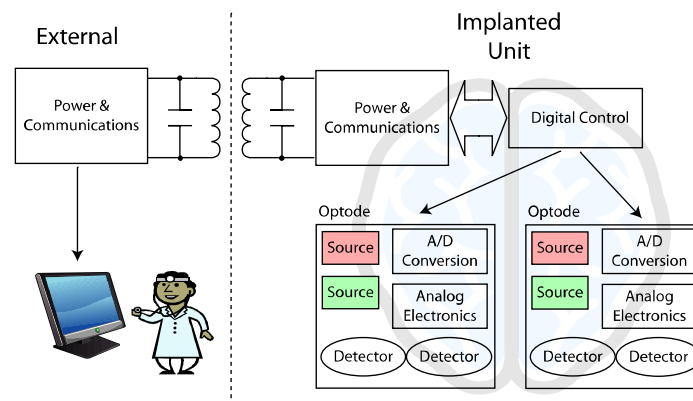
Figure 3.1 Impression of the telemetric PDT system.

Figure 3.1 shows a schematic diagram of the full telemetric system. Two main elements are visible in the proposed concept, namely the external unit and the implant. The external unit should take care of inductively powering the implant and communicating with it. The implant includes communication electronics to exchange data digitally with the external unit and a digital control unit. This unit is in charge of multiple optodes, which are combinations of light sources and detectors with suitable signal conditioning and readout electronics. The first prototype that we describe here should be applicable to laboratory rats. For this reason, only one optode is implemented and the optode and main unit are combined.

3.2 Functions of the implant

The optodes have two main functions, activating the photosensitizer and monitoring the treatment. In order to fulfil their first task, the optodes need to deliver a controllable amount of light in the activation wavelength region of the photosensitizer. For the second function the optode needs to monitor the three main ingredients that are necessary for PDT: light, photosensitizer and oxygen. Other functions of the device could be to monitor the temperature and potentially pH.

3.2.1 Activation of the photosensitizer
For the activation a light source with the suitable wavelength is needed. This is obtained from Light Emitting Diodes (LED). These are available in a large variety of wavelengths, can deliver the needed optical power of 5mW, can be obtained in chip form, and they are moderately power efficient light sources. [31] Compared with lasers the optical power is less, a few milli Watts instead of a several Watt, and the beam is not coherent. The output spectrum is much wider then for laser, the spectral width is about 20nm.
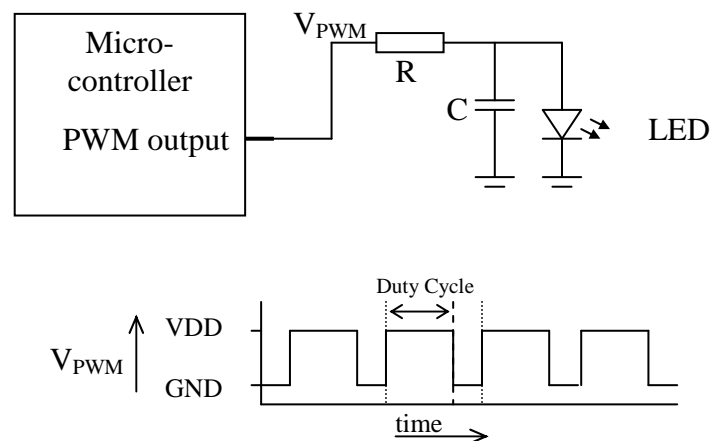
Figure 3.2 A) LED drive circuit B) PWM signal.

A micro controller drives the LED with Pulse Width Modulation as seen in figure 3.2. The amount of light is determined by the current through the LED, which is determined by the supply voltage, the resistor value and the duty cycle of the PWM. The last quantity is controlled by the micro controller, and can be altered from the outside.

3.2.2 Fluence rate
The scattered fluence can be measured by a set of photo detectors. The radiated light is known if the radiation pattern of the LED is properly measured. By fitting a model of light propagation in tissue, an estimation can be made on the fluence rate absorbed by the tissue.

Monte Carlo simulation

A Monte Carlo simulation has been made to determine how much optical power is available at different distances from a 5 mW source. The simulation used the input parameters given in table I. These are parameters that are characteristic for the gray matter in the brain.[11]

TABLE I. INPUT FOR MONTE CARLO SIMULATIONS

	Transparent Layer	Brain Tissue[3]
Absorption Coefficient (1/cm)	0	1.5
Scattering Coefficient (1/cm)	0	400
G	1	0.9
Refractive Index	1.8	1.37
Thickness	0.00-0.04	15e8

Only gray matter was simulated and the content of the blood was not taken into account. First a point source is simulated which results in the reflection photon probability as a function of radius. This simulation has been repeated with different thickness of a transparent layer between the optode and the brain tissue, simulating the effect of a passivation or packaging layer. The packaging layer was assumed transparent because no data on the packaging layer was available. The use of medical grade epoxy satisfies this assumption. The results from the point source are convoluted to a round flat source with a radius of 0.01 cm. The results are plotted in figure 3.3.
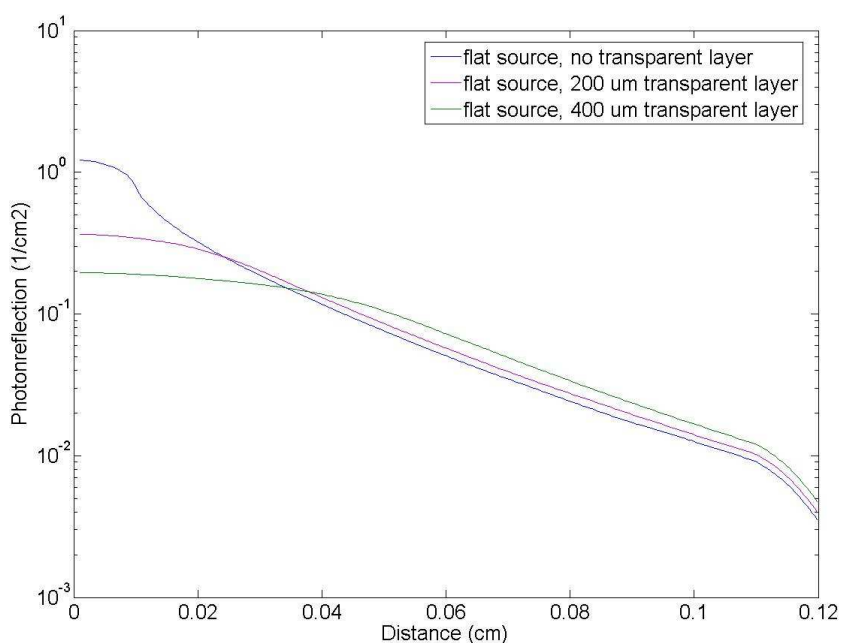
Figure 3.3 Photon reflection versus distance from source.

As shown in the picture the transparent layer has a significant effect on the distribution of light within tissue when the detector distance to the source is smaller than the width of the transparent layer. At larger distances the effect is less significant. The shape of the source is also clearly visible in the figure.

3.2.3 Photosensitizer measurement

A property of many photosensitizers of interest is that they are fluorescent. This means that the photosensitizer can be promoted by photons with a specific wavelength to an excited state, and after a certain amount of time it will fall back to its ground state, radiating a photon. These radiated photons are an indication of the amount of photosensitizer and can easily be measured by a photo detector after the source is switched off. A drawback of this is that the surrounding tissue will influence the measurement.

A fluorescent measurement can be implemented using the microcontroller. The fluorescent lifetime of the photosensitizer in the triplet state is rather long, in the order of a few μs [32]. Thus a fluorescent measurement can be done with a micro controller with a clock of a few megahertz.

Another option is to do the fluorescent measurement with a light filter to distinguish between the excitation wavelength and the fluorescent wavelength. It was chosen not to do this because the first method is easily implemented in this configuration of the implant. A filter can be applied in a later stadium if required.

3.2.4 Oxygen measurement

The amount of oxygen available in tissue is a difficult parameter to measure. Differential Pathlength Spectroscopy (DPS) has been developed to this end by Amelink et al [33]. This method uses the difference in reflectance spectrum of two collection fibers. One of the fibers delivers white light and detects the reflected spectrum, the other one detects only the reflected spectrum. By combining the information coming from both spectra, we can isolate the properties of the volume just before the first fiber. From the optical properties of this region an indication of oxygen level can be calculated [34].

For implementation of DPS with sufficient spectral resolution a rather large amount of wavelengths is needed. Several sources with a very small bandwidth (1 to 2 nm) might be used, but this poses important integration challenge. Quantum dots could be used to achieve this by producing different wavelengths at the same time, especially when combined with filters on the detector. Another option is to place a fluorescent dye on the optode which can be activated by a LED and which radiates a broadband spectrum. With this last option a spectral detector is also needed.

Other oxygen sensors are under investigation. Currently efforts are being done to miniaturize the pO2 sensor made by TNO quality of life. This sensor consists of a coating at the tip of an optical fiber. This coating (ruthenium) is excited by a blue LED (470 nm) and under influence of O2 present the excited coating is deactivated under the emission of light with a wavelength of 600 nm. This light is detected with a photodiode. [35]

3.2.5 Temperature measurement

The measurement of temperature is a very common quantity to measure in medicine. It is a good measure for local inflammation. It can also monitor the heat generated by the treatment. If the temperature becomes too high (hyperthermia), tissue can be damaged.

A very simple way to measure the temperature, is to measure the voltage over a diode at a constant current I. The temperature coefficient can be expressed by:

$$\alpha = \frac{dV}{dT} = \left(\frac{k}{q} \ln I \right) \tag{54}$$

where $q = 1.602 \times 10^{-19}$ C is the charge of the electron, $k = 1.38 \times 10^{-23}$ m^2 kg s^{-2} K^{-1} is Boltzman Constant. This temperature coefficient is approximately 2.0 mV/K. The circuit in figure 3.4 could be used for a simple temperature measurement, the 'constant' current is determined by the digital output voltage (VDD), the voltage over the diode, and the resistor R. This will give a small error because of the temperature dependence of the resistor. For a resistor the temperature coefficient is about is 0.0001 R per Kelvin. [33]

With a reference voltage of 1.1V and a 10 bit ADC, steps of

$$\frac{1.1V}{2^{10}} = 1.07 mV / step \tag{55}$$

are possible. When carefully calibrated, it should be possible to make an appropriate measurement of the temperature.
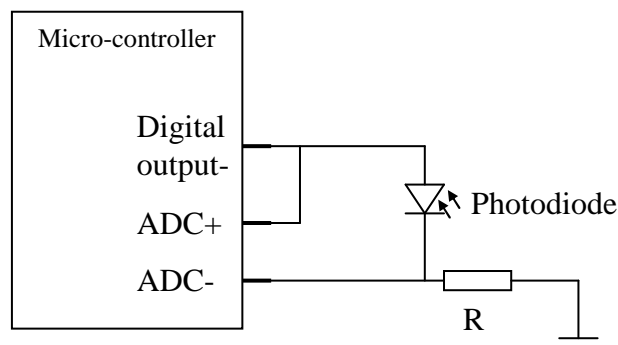
Figure 3.4 Temperature measurement schematic.

3.3 Implementation of the optode

The optode should contain the sensors and actuators and electronics capable of doing all the functions of the implant. In figure 3.5 an impression of the optode is given.
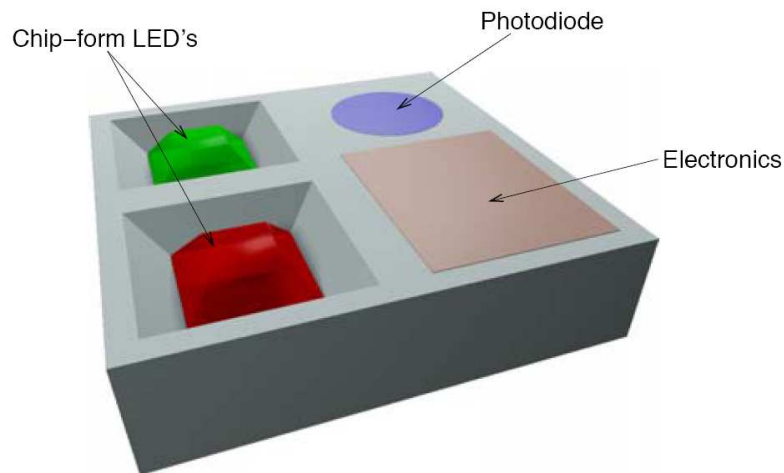
Figure 3.5 Impression of the optode.

Because a short development time is required the electronics are not included in the optode and are implemented with discrete components instead.

For actuation a LED is used, and for measuring photodiodes are used. The measurements techniques described can all be done with a photodiode (fluorescence, reflectance and temperature measurement). The optode is made of a silicon wafer as a carrier for the LEDs and as a substrate for the photodiodes. Four different types are made with different configurations on the amount of LEDs and photodiodes.

3.3.1 Photodiode design
The photodiode is designed using the DIMES 02 bipolar process. In order to dimension the photodiode, several steps have been taken. In the first place, estimation on how much optical power would be available at the photodiode was calculated using Monte Carlo simulations, figure 3.3.

The photodiode is constructed from the junction between the P-substrate and an N-epi layer. The contacts were made with a deep P diffusion, a highly doped P implantation and a highly doped N implantation. If the contacts are not highly doped, a Schottky diode will be formed, and the contact will only conduct in one direction.

With the properties of the process the depletion width is determined and with this the quantum efficiency is estimated using the absorption coefficient of silicon from Green et al [36]

Given the expected quantum efficiency the size of the photodiode was chosen to be 160*160 μm. This gives an expected photocurrent of a few microamperes. With the absorption coefficient the spectral efficiency has been calculated for several reverse voltages and is shown in figure 3.6.
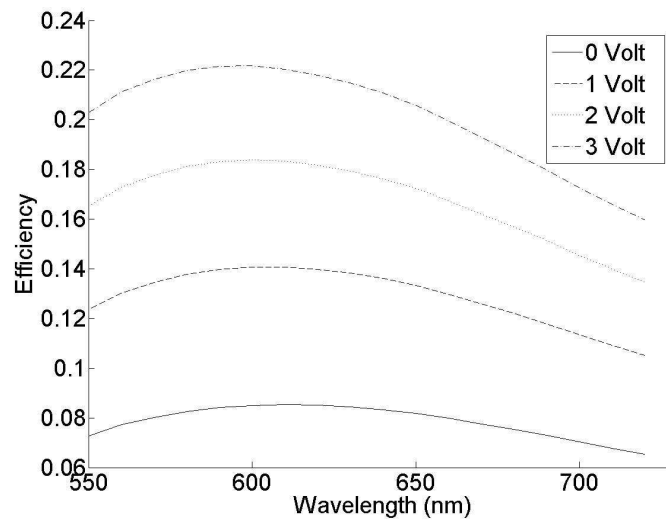
Figure 3.6 Spectral efficiency of photodiode with several reverse voltages.

The diodes have the layout given in figure 3.7
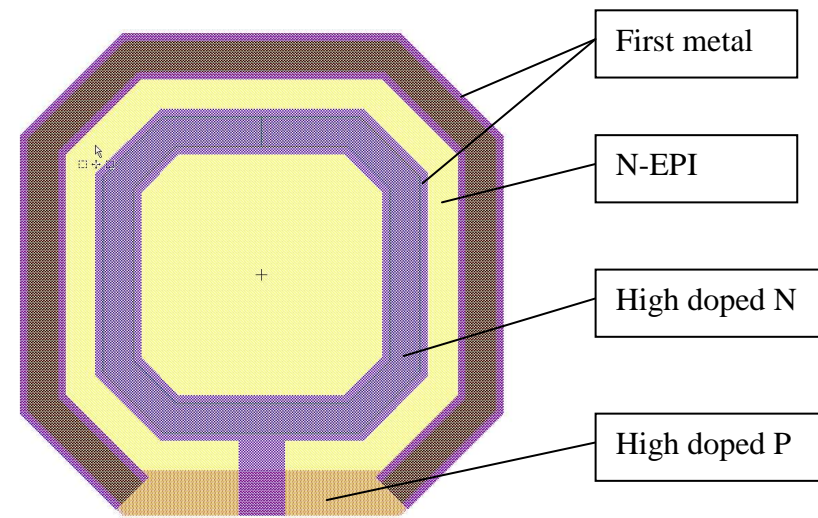
Figure 3.7 the designed photodiode.

The inner ring is for contacting the N-Epitaxial layer. The contact consists of a highly doped N implantation with a width of 15 μm. That implantation is contacted with the first metal (aluminium) through a ring form contact window of 10 μm wide. The ring shape is used to insure that the contact has low resistance.

The outer ring is the contact to the P-substrate. A high-doped P implantation is used for contacting the first metal. The contact window is 10 μm wide and the implantation and metal are 15 μm wide. Again a ring is used for low contact resistance.

The shape was chosen to be octagonal to reduce the electric field in the corners and to avoid corner breakdown. [36]

3.3.2 Implementation of the LED

The light source will be implemented with a LED in a chip form. This LED will not be constructed on the chip itself because the bandgap of silicon is not of the appropriate size and the fact that silicon is an indirect bandgap semiconductor. The LED chip has to be placed on the carrier chip. LED chips are available for several wavelengths, small sizes (<300μm) and connections configurations. Most LED chips have a contact on top and on the bottom, but chips with both contacts on top are also available. It was chosen to make the carrier chip compatible with both.

The LED chips are placed in a hole covered with metal. This prevents light from penetrating directly into the silicon, and the metal can be used as the back contact for the LED.

The hole is made by means of the following processing steps. First the rest of the wafer is passivated using Silicon Nitride. After that the wafer is patterned and the holes are etched in Tetramethylammonium hydroxide (TMAH). Because of the anisotropic etch rates of TMAH the walls of the pits resulting from the etching are tilted with 54.7 degrees, thus the holes in the corresponding mask are 640μm by 640μm to get the desired space to mount the LEDs. After this step the second metal is deposited using lift off. With lift off a larger variety of metals can be used, which is useful for the through wafer contacts.

3.3.3 Contacts

To use the optode in the circuit there should be contacts to the other, discrete, components in the circuit. With normal chips these contacts are made with bondpads to which bondwires are bonded. These bondwires are very fragile, but this is not a significant problem because the chips are protected by the package. In this application the chip is the front-end of the application and is in close contact to tissue. The chip will be protected with silicone as shown in figure 3.8. This silicone is flexible and when bondwires are embedded in the silicon the probability that they break is high.
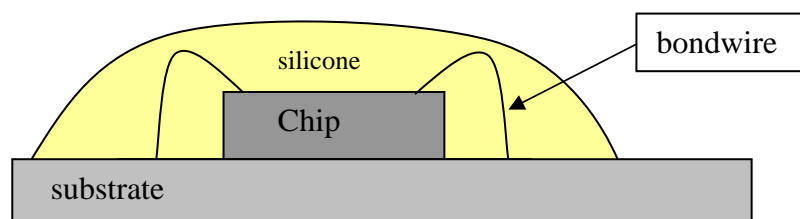
Figure 3.8 Contacting the chip with bond wires, protected with silicon

For this reason bondwires are not preferred in this application, and the possibility of contacts at the bottom of the chip is investigated. These contacts are called through wafer contacts. To experiment on this topic extra features have been made on the chip. For now it was chosen to embed the front end chip in an epoxy, this is rigid and will not break the bondwires.

The proposed through wafer process is as follows. First pads (100μm by 100μm) are made on the front of the wafer where the through wafer contacts have to be made, all these pads are connected to each other. They are disconnected when the chips are diced. At the end of the process, the wafer is turned and on the places where the though wafer contacts have to be made, holes of 50μm by 50μm are etched using Reactive Ion Etching (RIE). The RIE process stops on the metal pads. After this step copper, is grown from the pad (seed) using copper plating. Because this technique is experimental normal bondpads are also made.

3.3.4 Lay out

There are several photodiodes on the wafer with spacings from the source ranging from 300μm to 1200μm can be measured enabling DPS measurements. All the diodes have the same dimensions. In the different configurations there is room for one or two LEDs. All the contacts have a though wafer pad (100 um*100 um), and bondpads (200μm by 200μm).

The layout with 4 photodiodes and 2 LEDs is given in figure 3.9
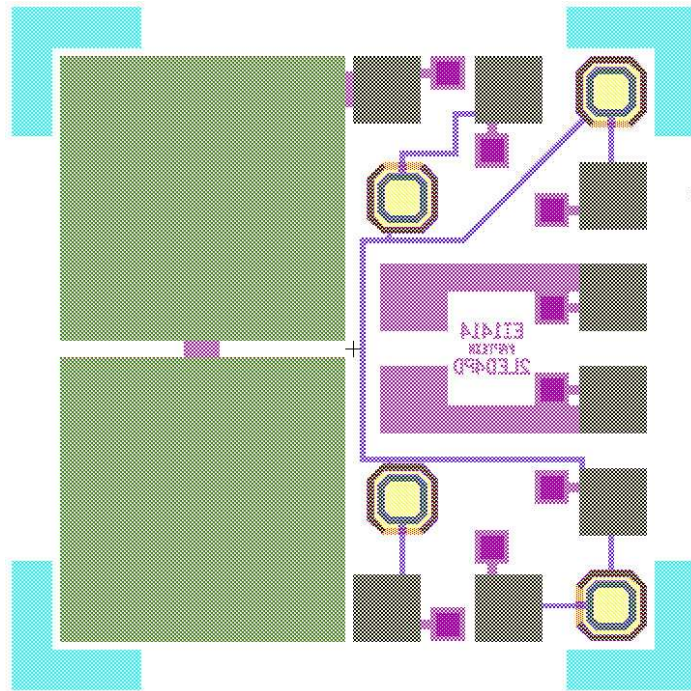
Figure 3.9 Layout of a single optode with 4 photodiodes and 2 LEDs

The total optode size is 1450μm by 1450 μm after dicing, the blue markings are the saw lanes. The four configurations are placed in a cell and 9 of these cells are repeated in a 10*10mm cell given in figure 3.10. Second metal lines are added to make the connections between the through wafer pads.
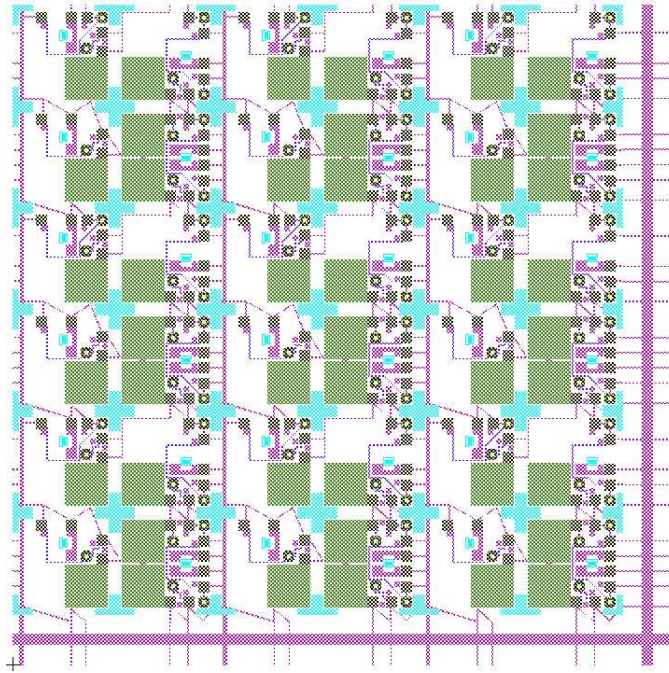
Figure 3.10 Cell of 10 by 10 mm with support lines for electroplating.

These 10*10 mm cells are used in the process for all steps except the second metal. For the second metal a full wafer mask is used. This is because extra metal lines are used to supply the current for the electroplating. The full wafer mask is given in figure 3.11
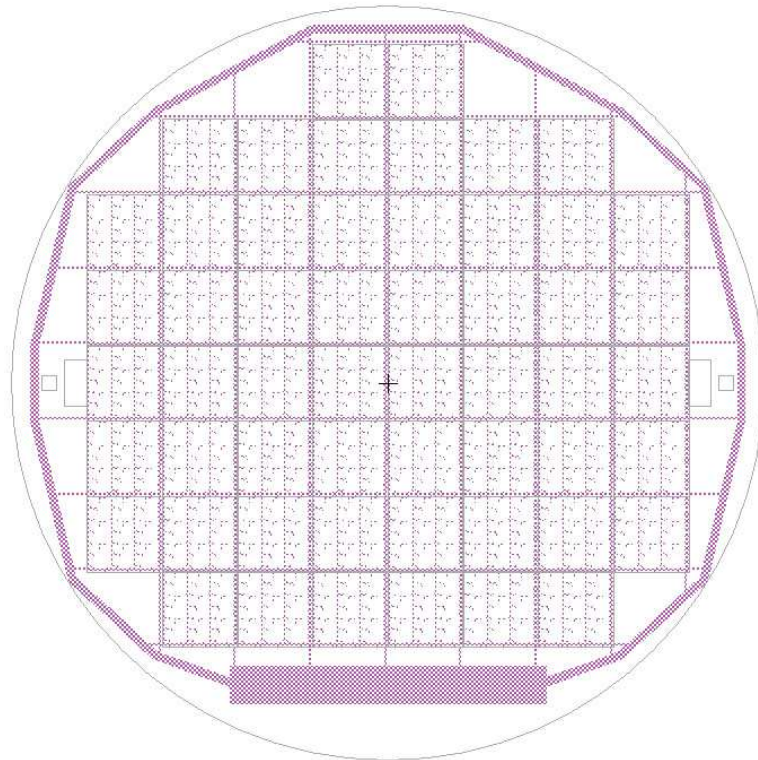
Figure 3.11 Full wafer mask for patterning of metal 2.
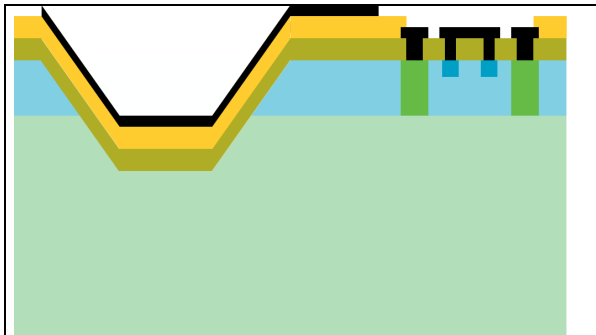
3.3.5 Process Flow

The process to make the optode is given in table II. The whole process is given in the Appendix. A

TABLE II. PROCESS FLOW FOR THE OPTODE
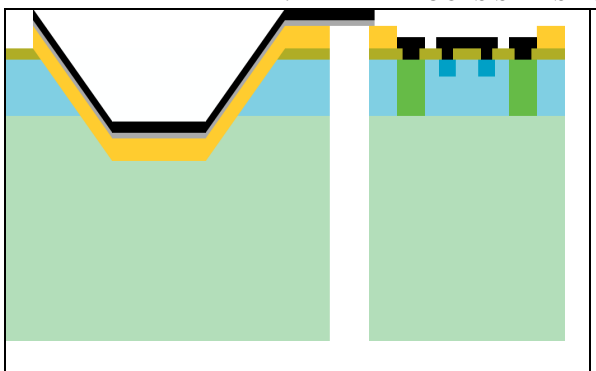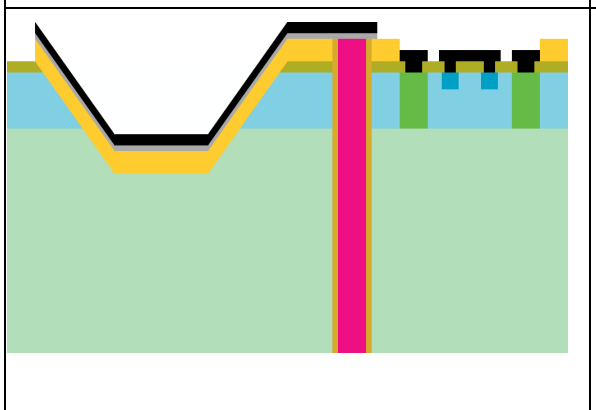
	Start wafer, P-type Boron (doping level +/- 3 x 10^{15})
	N-type epitaxial layer, Arsenic (doping level 1x 10^{16})
	Boron diffusion, deep P.
	Arsenic Implantation, N+
	Oxide mask for TMAH

	TMAH etch, and stripping of oxide
	Create contact windows in the oxide for first metal
	Deposition of first metal, (0.6um Aluminium). Etch of first metal.
	Oxide deposition for isolation of second metal.
	Apply photoresisist (green), develop photoresists. Sputter second metal.

	Remove photoresist.

From this point the optode is ready. The next steps, given in table III, are for creating the through wafer contacts.

TABLE III. EXTRA PROCES STEPS FOR THROUGH WAFER CONTACTS

	Reactive Ion Etch from backside, land on Oxide Plasma Etch Oxide
	Passivate sidewalls, Plasma Etch Oxide Copperplate from TiN seed.

3.3.6 Assembly of optode

The LED's are mounted by hand. Because the mounting of the LED is done after processing in the clean room, it is possible to install different LED's on different substrates, which gives flexibility in choosing the photosensitizer and the measurement setup. An optode can for example be equipped with a LED with a short wavelength, which is capable of exciting the fluorescence of the photosensitizer in order to measure its concentration. Another option is just to equip it with a LED for activating the photosensitizer.

The LED back contact is made with conductive glue and the front contact with a bondwire.

The contacts to the other components are made with the bondwires to the flexible backplane or by means of the flip-chip technique when the though wafer contacts are made.

3.4 Electronics

The electronics in the implant are implemented using discrete components. The main part of the electronics is the micro controller; this controls the LED, has the A/D conversion on chip and controls the communications. This topic is further developed in subsection 3.4.3. The signal from the photodiodes needs to be converted to a voltage with the help of a transimpedance amplifier. The circuit for that is designed in subsection 1.

The communications are implemented with the microcontroller and a transponder chip, and antenna. This is described in subsection 2.

3.4.1 Transimpedance amplifier

The input of the amplifier is a current of several microamperes. The output is a voltage between 0 and 2.7 V, the supply voltage. The feedback resistor is given by formula 26, and is dimensioned to 1 MΩ.

The choice of the operational amplifier depended on several factors. The input bias current should be as low as possible, because the current from the photodiode is very small. This in requires a very high gain and the offset could lead to amplifier saturation.

The input current noise should be very low as it is amplified with the feedback resistance.

The bandwidth of the amplifier should be high, at least 1 MHz, for the dynamics of the fluorescence measurement.

For these reasons the OP462 was chosen, with a bias current of 360 nA, Gain Bandwidth Product is 15 MHz and current noise < 1pA/√Hz.

Noise

The output noise due to the feedback resistor is $e_r = \sqrt{4kTR_f} = 0.12 \mu V / \sqrt{Hz}$

The noise due to the op-amp is equal to $i_n = 0.4\,pA/\sqrt{Hz}$ and $e_n = 9.5nV/\sqrt{Hz}$. If C_f is not implemented, this gives $e_{noi} = 0.4 \mu V / \sqrt{Hz}$ and $e_{noe} = (1 + 8e^{-6}s)9.5nV/\sqrt{Hz}$ (with C_i = 8pF)

The total noise is dominated by the operational amplifier current noise, and is equal to $e_{no} = 0.41 \mu V / \sqrt{Hz}$.

Bandwidth

The bandwidth is given by the GBA and the input capacitance in combination with the feedback resistor according to equations 32 and 33. This gives $f_{FB} = 19.8kHz$ and a total bandwidth of 546 kHz.

3.4.2 Transponder chip

For the communications a standard RFID solution is chosen. The U3280M is a transponder chip that is widely used in similar applications and is used as interface between micro controller and the communications coil [37]. The chip has its own power supply that can also be used to power a low power micro controller, but this is insufficient for this application.

The chip also contains an EEPROM memory, which can be read and written to with RFID, using the onboard bi/phase modulator. The memory can be written to with the serial interface. Unfortunately, the serial interface of the micro controller and transponder chip are not compatible. For that reason these two features of the chip will not be used.

The damping stage is used for the communications from the transponder and is controlled by the MOD-pin. The communication signal to the transponder will be available on the NGAP-pin. This is an on-off keying signal.

The antenna will be a coil in the shape of the implant. The Q factor needs to be around 40 for read and write operations. The coil L_a has a value of 47.3 μH with a Q factor of 37.4. This requires a capacitance C_a of

$$C_a = \frac{1}{L_a (2\pi f)^2} = 34.3 nF \tag{56}$$

for a resonant frequency of 125 kHz. The resonant capacitor is then tuned until the coil picks up a maximal signal. It was found to be 30.2 nF.

3.4.3 Microcontroller

All the activity of the implant is coordinated by the microcontroller. This gives the functional requirements of the microcontroller. First of all the microcontroller needs to be able to drive the LED, which is done with PWM. At least two pins need to have PWM output. The second requirement it needs to be able to do A/D conversion, 10 bits is enough for the temperature measurement which is showed in subsection 3.2.5. For communication only two digital I/O ports are needed (NGAP and MOD). One of them needs to be able to generate an interrupt to wake up the device (NGAP). The memory needs to be sufficient to store all functionality needed for the several measurements and communications. Further demands for the microcontroller are size and power consumption.

We chose to use the ATTiny861 as it has all the functional demands, has relatively large memory size and small power consumption. [37]

3.5 Inductive Power Link

The inductive power link consists of a driving circuit, primary coil, secondary coil and rectifier circuit. The most critical design issues are on the secondary side. The main factor is the loss in the secondary coil that will cause heating of the surrounding tissue. The power link is designed from that point of view. The design procedure proposed by Kendir et al is followed.[22]

Most important parameters to consider for an implant are coil size, losses (heat dissipation), and magnetic field limitations.

First the frequency of the field is chosen to be 1 MHz, this is a trade off between magnetic coupling (better at high frequencies) and absorption by the skin (low at low frequencies).

3.5.1 Secondary side

The secondary side of the system consists of a coil which has the geometry given by the implant geometry given in subsection 3.7. The coil that can be constructed on that area has the same area as a coil with a radius of 1.5 cm. The rest of the design is based on a coil with a radius of 1.5 cm, because the theory on that kind of geometry is available. The approximation of a multiple layer short solenoid is given in subsection 2.4.2. The height (C) of the coil was set to 2 mm and the length (B) was varied between 1 and 5 mm.

Three types of Litz wire are available, five bundles of 14 single twisted wires with a diameter of 0.04 mm (5*14*0.04), 10 single twisted wires with a diameter of 0.05 mm (10*0.05) and 16 single twisted wires with a diameter of 0.04 mm (16*0.04). The last two have the same outer diameter, and form those two the last one has the lowest resistance, thus only the first one and the last one are considered.

All the geometries with the two kinds of lit wires were evaluated for loss and needed magnetic field.

The loss of different configurations of number of strands and turns is determined using formulas and data of Litz wires from literature [22] and from simulations using Spice with the circuit given in figure 2.15 found in chapter 2. The load resistance was determined to be 521 Ω: the supply voltage divided by the supply current of the microcontroller, amplifier and the LED's. This is shown in table IV.

TABLE IV. LOAD CALCULATION

device	Supply current (mA) @ 2.7 V
microcontroller	0.38
amplifier (4)	2.00
LED	1.40
LED	1.40
total	5.18

The non-linear model was simulated in SPICE to determine the optimal resonance capacitor value and the needed induced voltage. From the data of the simulations the loss and H-field are calculated, they are given in figure 3.12 and figure 3.13.
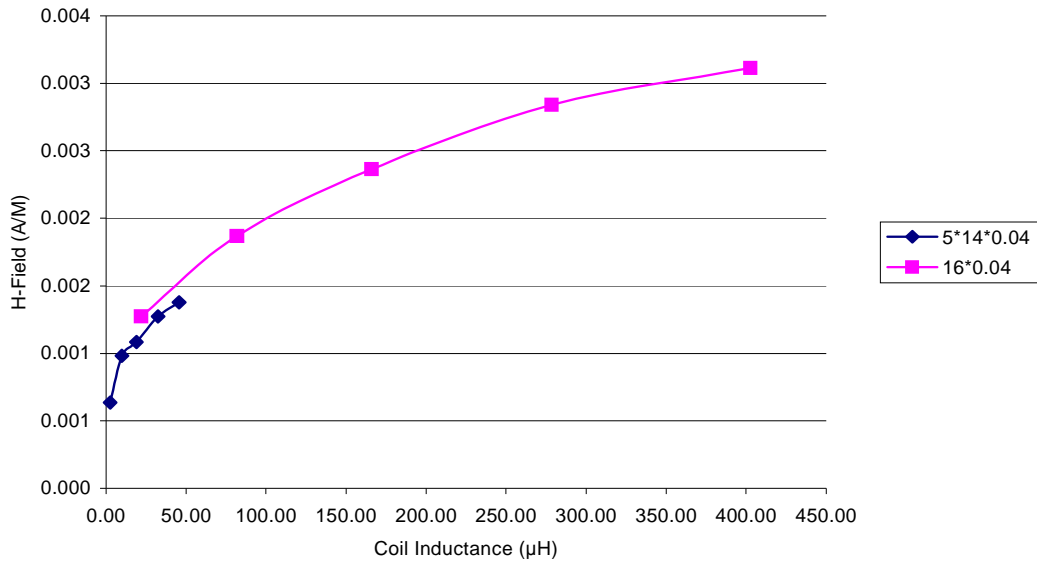
Figure 3.12 Loss in the secondary coil for different kinds of litz wire as a function of inductor value
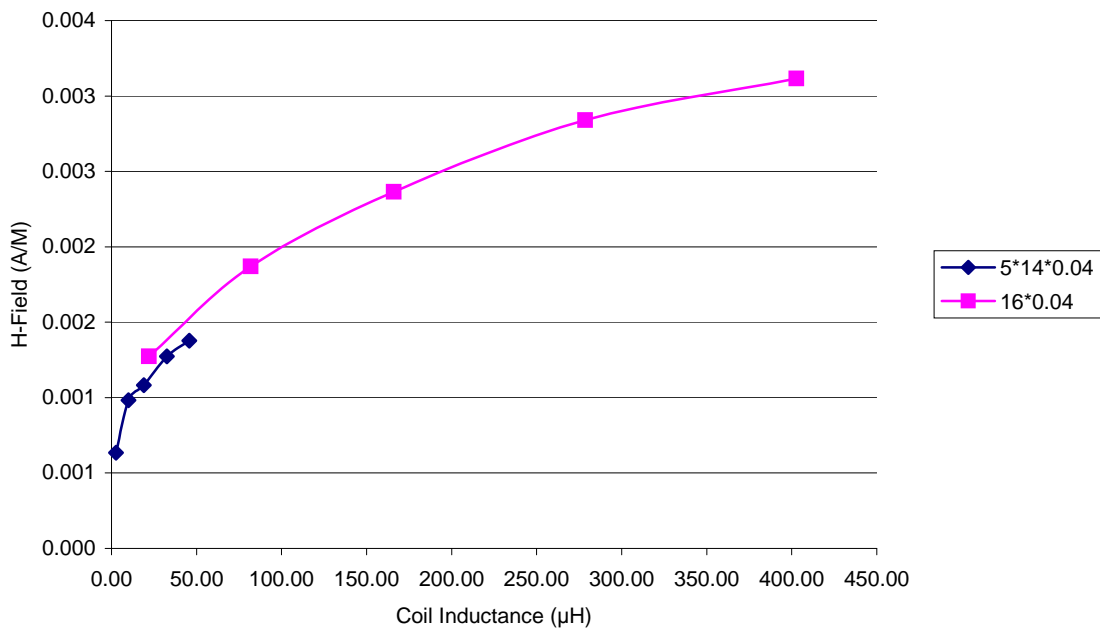
Figure 3.13 Needed induced H field for the different kinds of litz wire as a function of inductor value

The 5*14*0.04 litz wire has a relatively large outer diameter, thus in the same area less turns can be constructed. From figure 3.12 one can see that the loss is gets lower for larger inductance for the 5*14*0.04 wire. For the 16*0.04 wire that is a minimum just below 100μH.

From figure 3.13 it can be seen that the higher the inductance the higher the H-field is that is needed. A lower inductance is thus preferred.

The 3 mm high inductor made with the 5*14*0.04 wire was chosen with an inductance of 19.1 μH and 20 turns.

Rectifier circuit

For the rectifying circuit the circuit given in figure 3.14 is used. The diode is used to rectify the signal, the Zenerdiode is used to prevent the rectified voltage from exceeding the input range of the regulator. When the voltage is to high, the voltage regulator will not work. The LDO makes sure that the output voltage is constant at 2.7V.
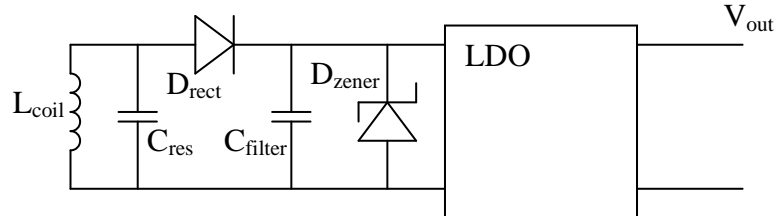
Figure 3.14 Rectifier circuit at the secondary side.

3.5.2 Primary side

The primary side needs to induce the magnetic field that is required to power the implant. The geometry of the primary coil is large to induce the field over a big area. The radius is 15 cm, further there are no other constraints.

The primary coil is made from plain copper wire. The wire, which is used to make coil, is very long due to the large diameter this is why the resistance would be very high if one of the available litz wire is used.

The mutual conductance is given by equation 45 and 46, it was calculated for a distance of 5 cm. With equation 44 the needed current in calculated.

Class E driver.

A class E driver is used for driving the coil, the capacitances are calculated with the help of the equations of 2.4.2. The MOSFET that is used is IRF330, and the polarization inductor for supplying the current is 500µH. With the help of SPICE simulations the circuit is tuned.

Three configurations are simulated with different primary coils are simulated, one with 7, 14 and 27 windings, respectively 50.7 µH, 192 µH, 659 µH. For these values a class E driver is simulated with the circuit given in figure 3.15. The circuit is tuned in such a way that the losses in the MOSFET are minimized. This is done by adjusting the capacitors.
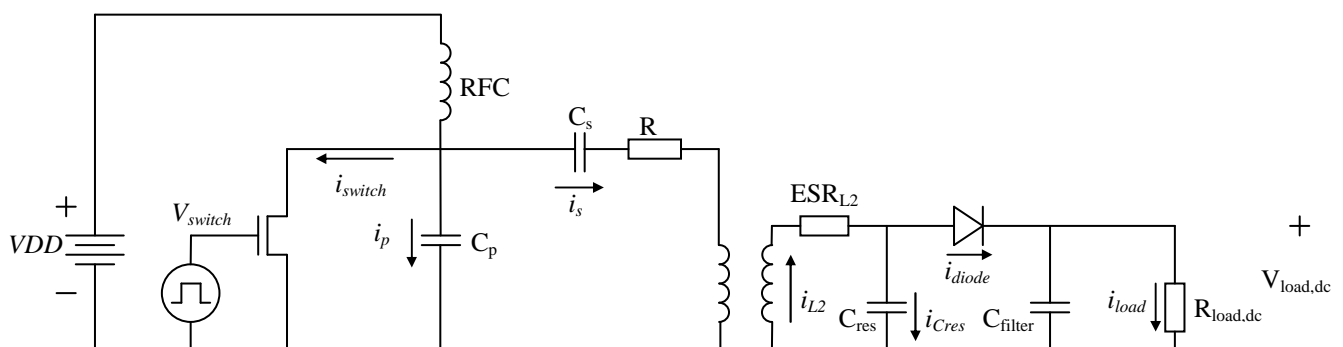
Figure 3.15 Power coupling circuit

Practical implementation

The primary coil was made in base plate that will be on the bottom of the cage where the rat will be when treated. In this plate a circular cutout is made where the primary coils can be placed. One for communication and one for the powering. Two coil holders are made which can be placed in the cutout. The base plate and coil holders are shown in figure 3.16.
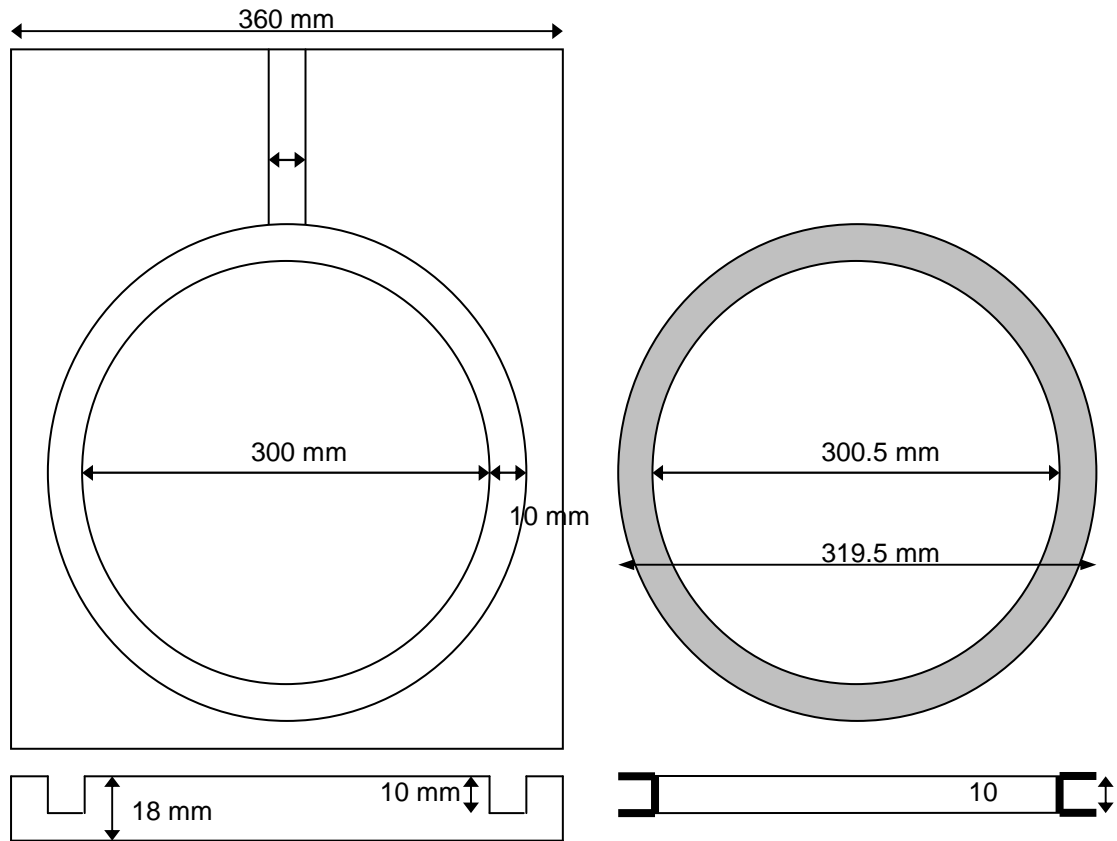
Figure 3.16 left: base plate, right: coil holder for the primary coils.

The three coils were made and measured with the spectrum analyzer. The measurement data is given in table V. From the measurements it was found that the stray capacitance is significant. This has some consequences for the C_s and C_p. The inductor value with which the capacitor values are calculated is somewhat larger, according to formula 57

$$L_{new} = \frac{L}{1 - \omega^2 C_{stray} L} \tag{57}$$

Two coils are made, one with 7 and one with 14 windings. The smaller one is also made, because the smaller the coil gives a smaller stray capacitance.

TABLE V. PROPERTIES OF
PRACTICAL PRIMARY COILS

N	14	7
L (µH)	170	44
R (Ω)	1.66	0.829
C (pF)	46.1	33.9
L_{new}(µH)	246	46.8

Due to this stray capacitance the self-resonance is a significant problem. This is why we chose for the 7-turn implementation of the coil.

Tuning the practical circuit
The capacitors of the Class E driver are implemented with tuneable capacitors. The circuit is given in figure 3.17. The tuneable capacitors allows simple tuning of the primary
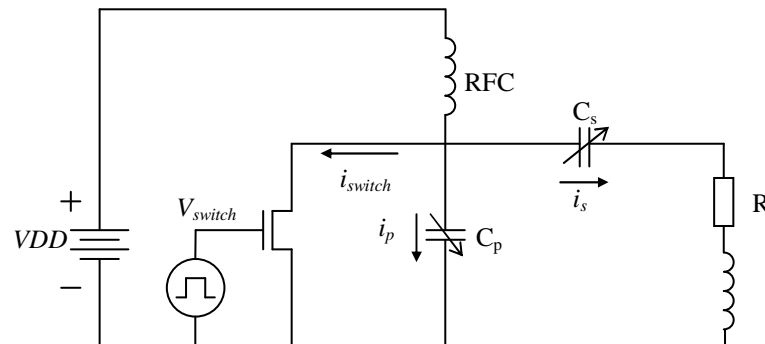
Figure 3.17 Implementation of the Class-E driver

circuit. This is needed because the resonant frequency of the secondary coil is not exactly 1 MHz. The tuning procedure starts with measuring the resonant frequency of the secondary side. This resonance frequency is used as input for the class E driver, V_{switch}. The capacitors are then tuned until the desired behaviour, minimal loss in the MOSFET, is accomplished. Then the supply voltage is increased until the current through the primary coil is enough to supply the implant; the needed induced voltage is supplied.

3.6 Software

An important part of the software of the microcontroller is the communication. The Finite State machine depends highly on the chosen protocol. For that reason the communication protocol is first described in section 3.6.1. After that the code is described with a FSM and several flowcharts for the several functions of the implant in section 3.6.2. In section 3.6.3 the program, which is used to control the implant from the PC, is described.

3.6.1 Communication protocol
The PC initiates all the communication. Several measurements and treatments can be done by the implant. The PC can initiate a procedure by sending a message to the implant using the standard on-off keying procedure, and the implant can answer with Manchester encoding.

PC to micro controller uplink, On Off Keying
Time between gaps determines the value of the bit being transmitted namely, zero or one. The temporal parameters of this encoding are given in table VI.

TABLE VI. TIMING FOR ON OFF KEYING

Symbol	Typical Time (µs)	Length @ 200kHz (cycles)
0	80	16
1	324	64
gap	276	55

The data is fed through the transponder gap detect circuit to the NGAP pin.
The uplink is implemented by generating an interrupt on pin change of NGAP and generating a counter interrupt 64 cycles after a change of NGAP. The stop condition is when NGAP is one for more then 64 clock cycles. This is shown in figure 3.18.
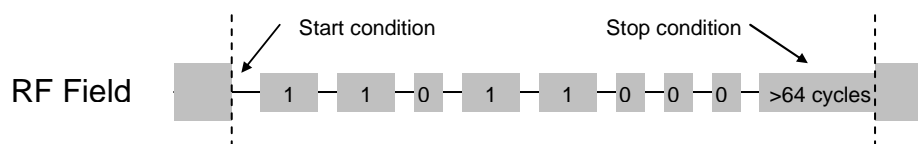
Figure 3.18 On-Off Keying.

Every time there is a pin change on NGAP the procedure in figure 3.19 is evaluated.
When the start condition is met, NGAP is zero for the first time, the microcontroller goes to send state and the counter is started. When the NGAP changes to 1, the counter is reset. When it the value is 0 again, the amount of time passed is evaluated and the symbol is stored in the memory. When the time between two gaps was not within a range that corresponds with a symbol the microcontroller goes to an error state.
The stop condition is monitored by the counter interrupt at 64 cycles. When the stop condition is met, the instruction is evaluated.
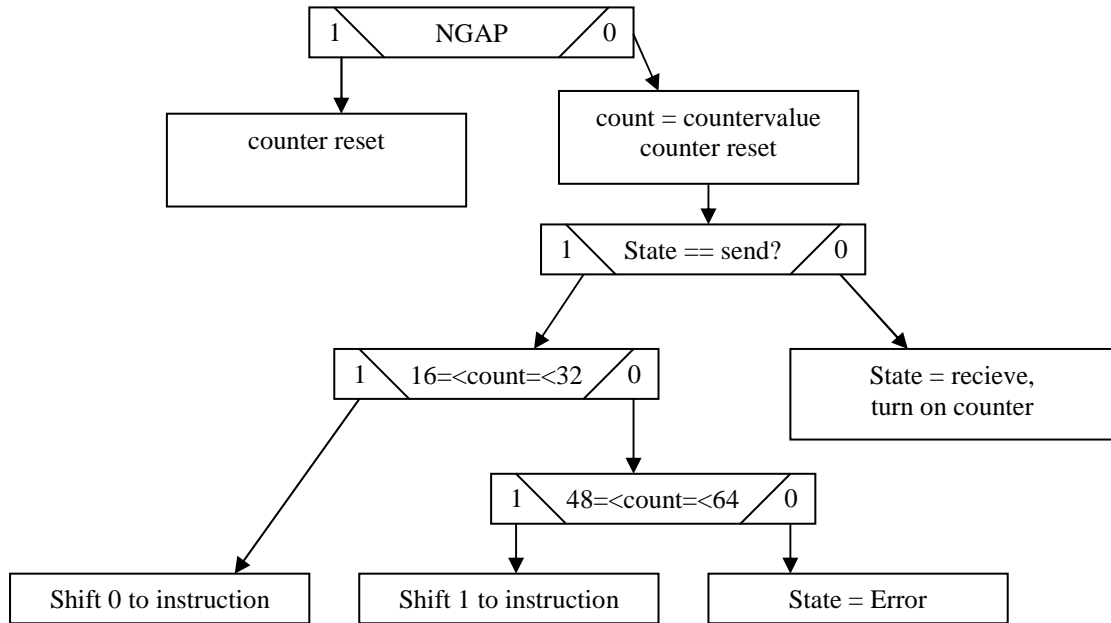
Figure 3.19 Flowchart of the NGAP-interrupt procedure

Microcontroller to PC downlink, Manchester Encoding
The data stream is generated on the MOD chip of the transponder chip and is Manchester encoded. The data is encoded in the following matter, in the middle of the clock cycle an edge in the data signal is made, a positive edge in the data stream is associated with a one and a negative edge in the data stream is associated with a zero. This is shown in figure 3.20.
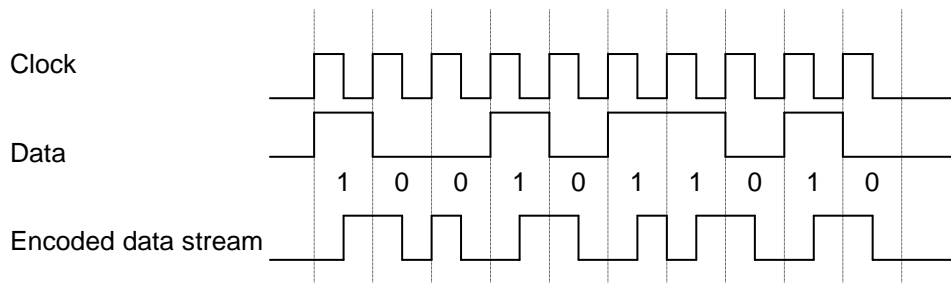
Figure 3.20 Manchester Encoding

The downlink has a speed of 125/32 kbit/s, this is a standard for RFID. One clock cycle is thus 0.256 ms. The value of the data stream needs to be updated every half clock cycle, every 0.128 ms. On the positive edge of the clock cycle the encoded data stream is updated with the inverse of the data, and on the negative edge the encoded data stream is updated with the value of the data.
A normal RFID transponder chip constantly sends out its code in to the atmosphere when it is within the field. The code contains a header, and if the header is known by a base station the code can be obtained by that base station by listening.
Thus to send a message from the microcontroller to the PC the message has to be sent several times to make sure that the PC listens when the message is send. A repetition of 15 times was enough in the experiments that were done.
The procedure is implemented according the flowchart in figure 3.21.

```
                    ┌─────────────────────────┐
                    │  Startcounter @ 125 KHz  │
                    │        Count = 7         │
                    └─────────────────────────┘
                                 │
                    ┌────┬───────────────────┬────┐
                    │ 0  │   Sendcount<15    │ 1  │
                    └────┴───────────────────┴────┘
              ┌──────────┘                   └──────────┐
   ┌─────────────────┐                       ┌─────────────────┐
   │  Stop counter   │                       │  Bytenumber = 1 │
   │       End       │                       │  Reply = 0xE6   │
   └─────────────────┘                       └─────────────────┘
                                                      │
                          ┌────┬──────────────────────────┬────┐
                          │ 1  │  Bytenumber < replylength  │ 0  │
                          └────┴──────────────────────────┴────┘
                        ┌─────┘                            └─────┐
            ┌────┬──────────────┬────┐            ┌─────────────────┐
            │ 1  │  counter<16  │ 0  │            │   Sendcount++   │
            └────┴──────────────┴────┘            └─────────────────┘
                 │
      ┌─────────────────────┐
      │  MOD = reply(count) │
      │    Reset counter    │
      └─────────────────────┘
                 │
            ┌────┬──────────────┬────┐
            │ 1  │  counter<16  │ 0  │
            └────┴──────────────┴────┘
                 │
      ┌─────────────────────┐
      │  MOD = reply(count) │
      │    Reset counter    │
      │       Count --      │
      └─────────────────────┘
                 │
            ┌────┬──────────────┬────┐
            │ 1  │  Count = 0xFF │ 0 │
            └────┴──────────────┴────┘
                 │
      ┌──────────────────────────┐
      │        Count = 7         │
      │ Reply = answer[bytenumber]│
      │      Bytenumber++        │
      └──────────────────────────┘
```
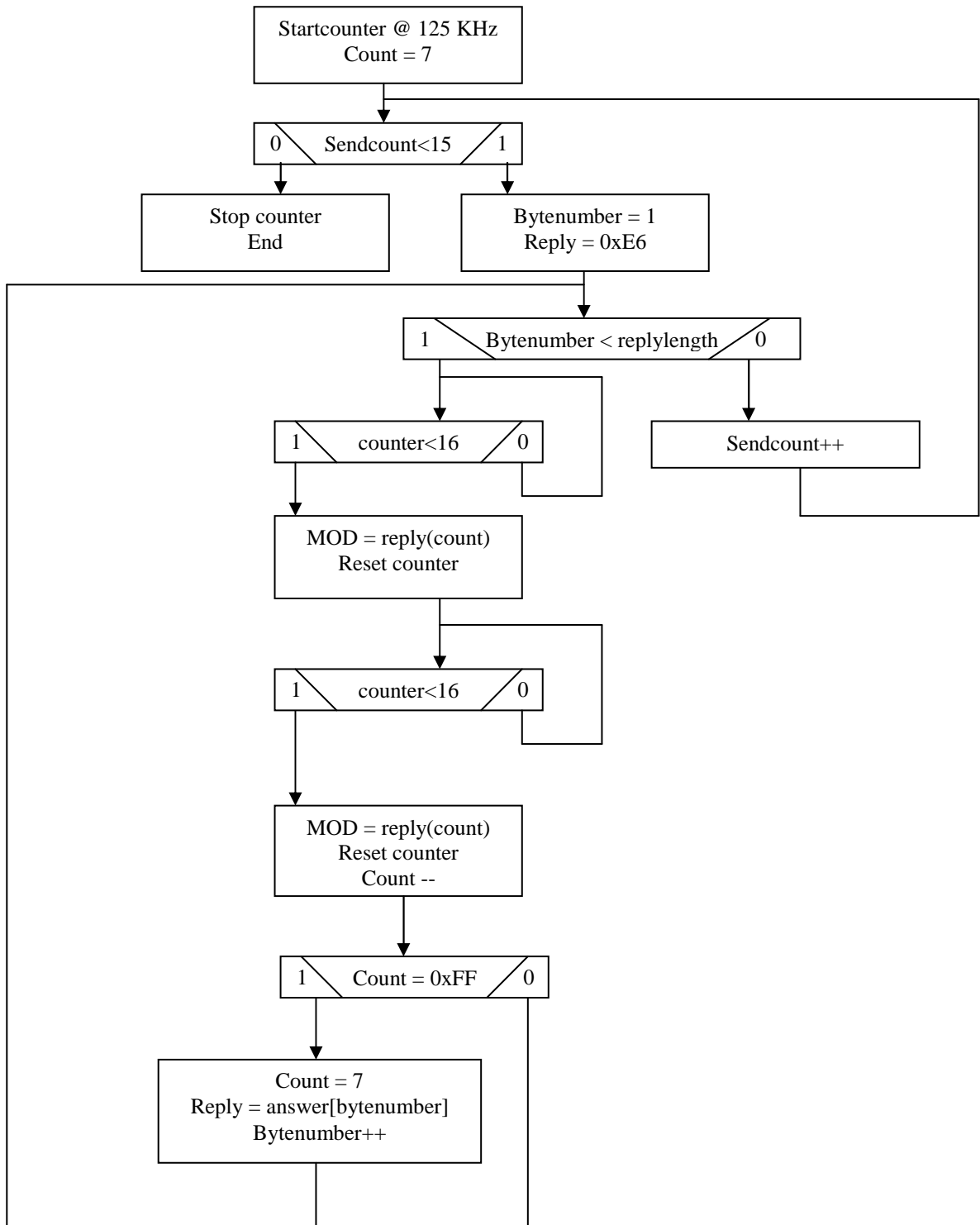
Figure 3.21 Flowchart of the Manchester Encoder procedure

The message that has to be sent is in the variable answer. The length of this variable is stored in the variable replylength. Every half cycle, 16 cycles of a 125kHz clock, the MOD output is updated. The variable count counts which bits are sent. After a byte has been sent the count is reset and the next byte is loaded. When all bytes are sent the sendcount is updated and the message is send again until it is sent 15 times.

Protocol

PC initiates action by sending 4 bytes with instructions to the microcontroller. This message concludes with a parity bit. If the instruction is correctly received (parity check), the microcontroller answers by sending an Acknowledge byte. After the Acknowledge byte has been sent the UC performs the instruction. If the instruction has measurement results, these are stored in the memory of the microcontroller. These results can be downloaded with a special instruction, read result.

An instruction consists of a procedure (4 bits), parameter TIME (1 byte), parameter AMOUNT (1 byte), INTENSITY (1 byte), 3 bits 0, parity bit as shown in table VII.

TABLE VII. INSTRUCTION

bit	31-28	27-20	19-12	11-4	3-1	0
content	Procedure	Time	Amount	Intensity	0	parity

The procedures are defined as in table VIII

TABLE VIII. PROCEDURES

0000	LED1 on with INTENSITY for TIME unit time, do AMOUNT of reflection measurements
0001	LED 2 on with INTENSITY for TIME unit time, do AMOUNT of reflection measurements
0010	Fluorescence measurement
0011	Temperature measurement
0100	LED1 and LED2 on with INTENSITY for TIME unit time, do AMOUNT of reflection measurements
0101	Tune measurement
1111	Read result

The micro controller acknowledges the instruction when received correctly or acknowledges a data request with the data, else it gives a not acknowledge. A not acknowledge can have three reasons:

- timing error: the time between two gaps was not within a range that corresponds with a symbol or the gap was too long.
- Parity error: The last bit is not correct with the rest of the message
- Instruction error: The message was received correct, but the procedure does not exist

The reply is constructed as in the table IX.

TABLE IX. MICROCONTROLLER REPLY

	Header 8 bit	Ack/nack 4 bit	Procedure 4 bit	Previous procedure 8 bit	Data length 8 bit	data n*8 bit	Checksum 8 bit
Acknowledge, no data	E6	F	Procedure				Checksum
Acknowledge with data	E6	F	F	Previous Procedure	Data length	data	Checksum
Timing error	E6	0	0				Checksum
Parity Error	E6	A	procedure				Checksum
Instruction error	E6	A	procedure				Checksum

The possible communication scenarios are given in table X.

TABLE X. COMMUNICATION SCENARIOS

	PC	Microcontroller answer
Correct instruction:	1-12-FF-04-0	E6-F-1
Timing error	1-12-FF-04-0	E6-0-0
Parity error	1-12-FF-04-1	E6-A-1
Instruction error	5-12-FF-04-1	E6-A-5
Data request	F-00-00-00-0	E6-F-F-0X-04-XX-XX-XX-XX-checksum

The first instruction means that LED 2 needs to be on with an intensity of 18/255, for 255 times the time unit and 4 reflection measurements will be done.

3.6.2 Micro controller software.

The software of the microcontroller is written according to the finite state machine given in figure 3.22.

```
        ┌──────────────┐
        │     IDLE     │
        │      0       │
        └──────────────┘
               │ Start condition
               ▼
   ┌───────────┐  Invalid Bit   ┌───────────┐
   │  RECEIVE  │ ─────────────► │   ERROR   │
   │     1     │                │     2     │
   └───────────┘                └───────────┘
        │ Valid data   Invalid Data   │ Stop condition
        ▼                              ▼
  ┌──────────────┐              ┌──────────────┐
  │ SEND ACK (+  │              │  SEND NACK   │
  │    data)     │              │      4       │
  │      3       │              └──────────────┘
  └──────────────┘                    Nack Sent
        │ Ack sent
        ▼
  ┌──────────────┐
  │Perform Action│
  │      5       │
  └──────────────┘
        Action done
```
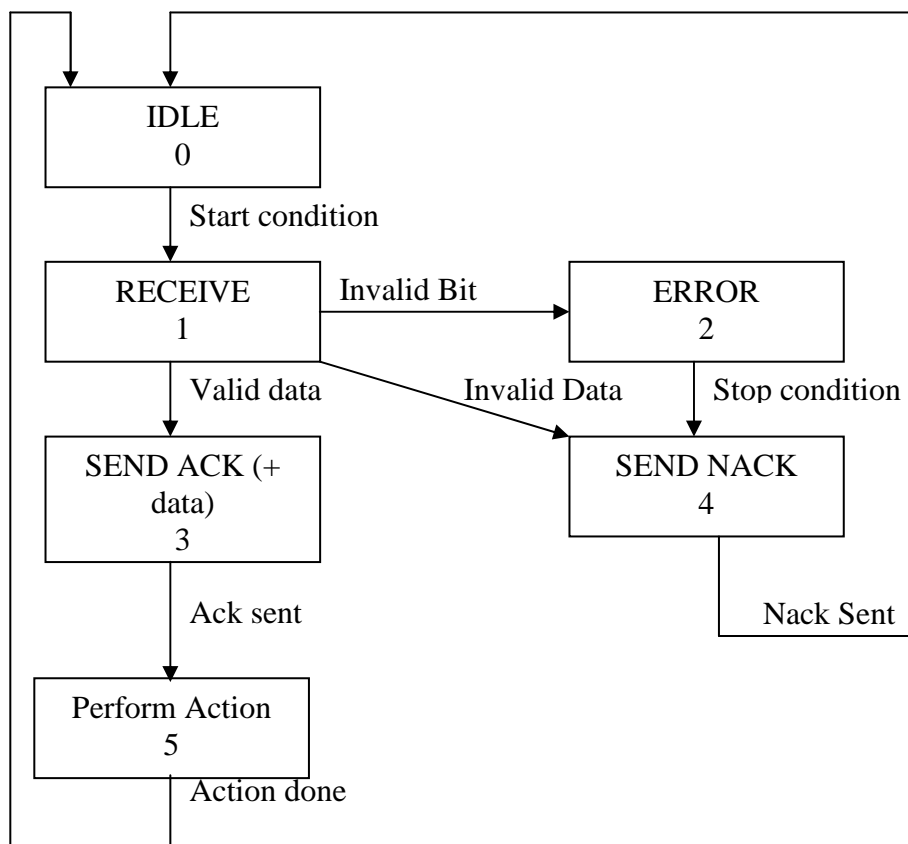
Figure 3.22 FSM of the program in the microcontroller

When the microcontroller is introduced to a magnetic field, the microcontroller is switched on and is in the IDLE state. When the NGAP pin of the microcontroller is pulled low, the start condition, a message will be received. The microcontroller gets to state 1, in this state it receives the message according to the procedure given in figure 3.19. From here an error can occur due to timing (state 2). When the complete message is received, the stop condition is given (NGAP low for more the 64 clock cycles) and the message is interpreted. The message can either be valid (go to state 3) or invalid (state 4). When in the error state the stop condition will cause a transition to state 4. In state 2 an acknowledge is sent and after that an action is performed which was in the received message (state 5). After the action is performed the microcontroller returns to the idle state. After the not Acknowledge the microcontroller returns to the idle state as well.

For the several functions: treatment with reflection measurement, temperature measurement, fluorescence measurement and the tune measurement the following procedures are implemented and described in the following subsections.

Treatment with reflection measurement

This procedure has three input parameters: the time the LED needs to be on (variable time), the intensity (variable intensity) and the amount of measurements to be done (variable amount). The intensity and time are controlled by the method LED_on. The measurements are done with a standard interval (variable ADCInterval) that is equal to the treatment time divided by the number of measurements.

The intensity is equal to the duty cycle of the PWM output (variable PWMcompare).

The method has the following procedure: every time interval an interrupt is generated, in this case the time interval equals four seconds. The implant is used for long low dose treatments, thus a minimum length of four seconds is acceptable.

In the interrupt handler the treatment time is updated (variable LEDonTime), then it is determined whether it is time for a measurement (variable ADCTime). When this is the case an AD conversion is done and the ADCTime is updated. When the time for the treatment has passed, the procedure is terminated. The flowchart is given in figure 3.23.
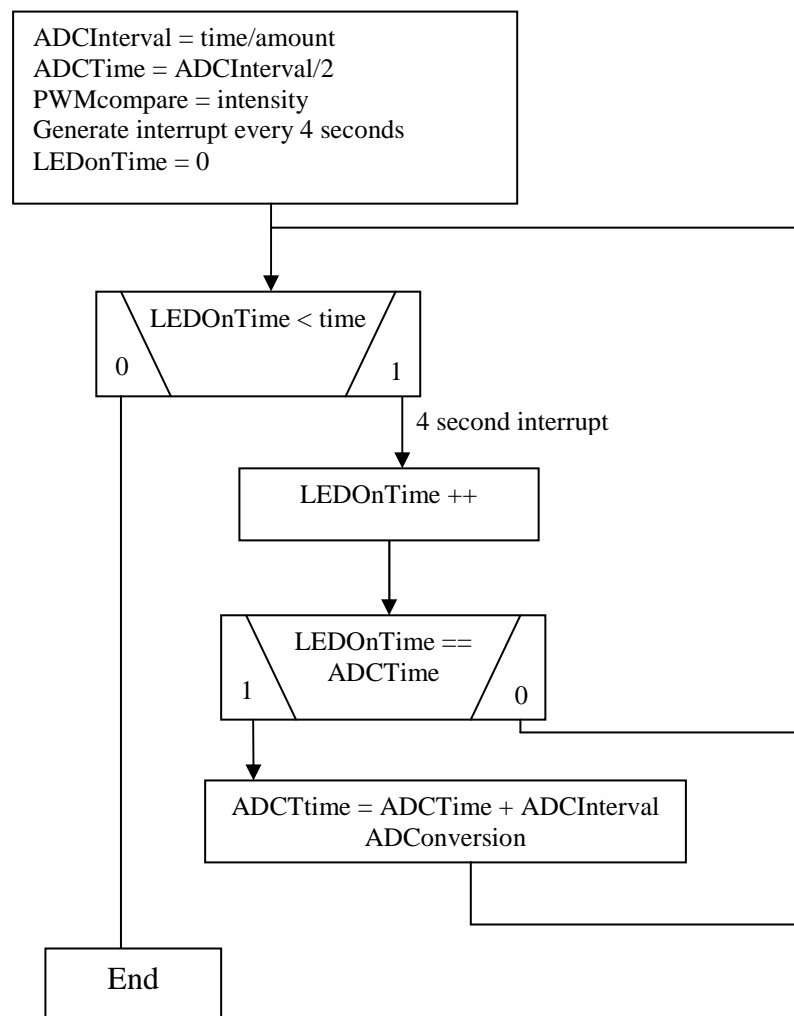
Figure 3.23 Flowchart of treatment *and reflection measurement procedures*

Temperature measurement
The temperature measurement uses one photodiode as transducer. This photodiode needs to be connected in different way from the usual configuration for light intensity measurement. Since this photodiode will alternate between the two functions, a switch is used as it is sketched in figure 3.24:
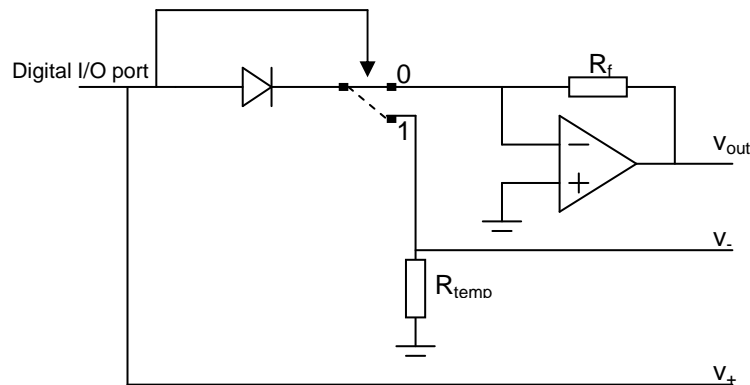
Figure 3.24 Circuit for temperature measurement and reflection measurement

When the digital output port is set, the switch is in temperature mode, which allows measuring the temperature dependent voltage over the photodiode. When the digital output port is switched to zero, the port acts as ground and the reflectance measurement can be done. The flowchart of the temperature measurement procedure is given in figure 3.25.

Set Temperature measurement pin
Initialize ADC
Differential AD Conversion(s)
Clear Temperature measurement pin
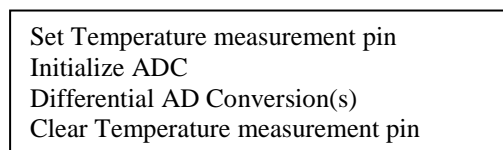
Figure 3.25 Flowchart Temperature measurements.

Fluorescence measurement
For the fluorescent measurement the LED has to be switched on in order to provide the excitation and then switched off to prevent disturbance of the measurement. Within a few microseconds the ADC needs to sample and hold the voltage that is at the output of the amplifier.

When the ADC is auto-triggered the sample and hold will take place exactly two clock cycles after the triggering event. The ADC-clock is 125 kHz, thus a clock cycle takes 8 µs.

To get a sample and hold within 8 µs of switch off of the LED the following procedure is used.

- ADC triggered on Timer/Counter1 Overflow
- Set timer 1 on 8MHz, period 125 ns
- Set TOP value to 256 (32us)
- Set COMPARE value to 128 – x, time between turn off and measurement is x*125ns.

The timing diagram is then given by figure 3.26:
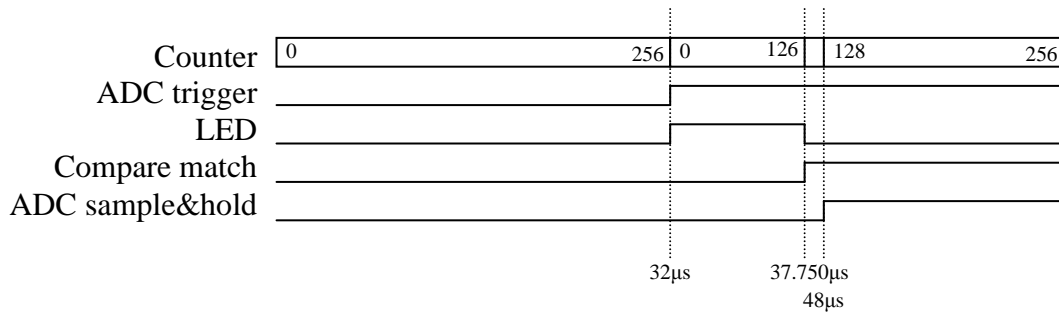
Figure 3.26 Timing diagram for the fluorescent measurement

The ADC is triggered on a positive edge on the trigger signal. If another positive edge occurs during the conversion this edge will be ignored.

This procedure can be repeated for several values of x, which allows a time resolved measurement of the fluorescence of the tissue.

Tune measurement

The tune measurement does 10 ADC conversions of the NGAP pin. The voltage on this pin is an indication of how well the communication coils are coupled. When communication is possible, the communication can be fine tuned with this method.

3.6.3 PC interface

The PC interface is implemented with the development kit for RFID from ATMEL, TMEB 8704. This kit comes with a board, antenna and standard software package which controls the board via the serial interface. The software is just for demonstrating purposes thus a java program is written to control the board in a direct way. This java program is written to translate the instructions from the user the instructions for the development board, in such a way that the correct messages are sent. The flowchart of the program is given in figure 3.27.
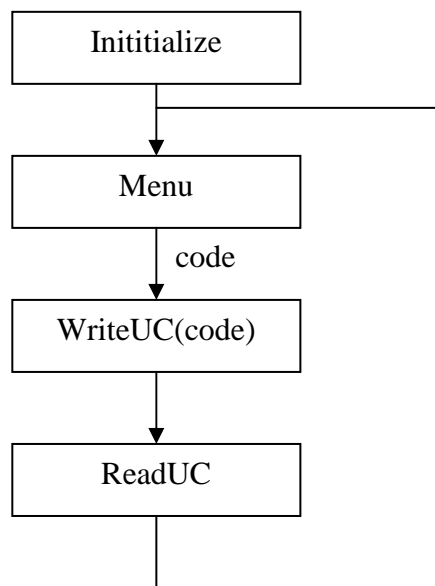
Figure 3.27 Flowchart of the PC Interface program

At start up the serial port is initialised in the initialise procedure. The main part of the program is a menu in which the user can select the different procedures:

- Therapeutic illumination with reflection measurements
- Temperature measurement
- Fluorescence measurement
- Read last results
- Tune measurement

When a procedure is selected additional information needed for the procedure is obtained. The procedure and variables are translated into the instruction for the implant and is written to the serial port with the method writeUC2. When an instruction is send to the implant, a reply is expected. To get the information the implant must be 'read' this is done directly after the sending of the instruction with the method readUC.

Besides this structure the method dataAvailable constantly monitors the serial port for data from the serial port.

The three mentioned methods are described in the next subsections.

After the data is received the field is turned off, to reduce the amount of interference during a measurement. The program is halted during a treatment until the treatment is over. The field will be turned on again when the user wishes to write a new command to the implant.

WriteUC

The writeUC2 method adds instructions for the development board. The protocol is given in table XI.

TABLE XI. PROTOCOL OF THE WRITE COMMAND

Byte 1	Byte 2	Byte 3-4	Byte 5-6	Byte 7-8	Byte 9	Byte 10..X
Function code	Number of Bytes	Gap time	Zero Time	One Time	Number of bits	Code

The function code (write, 80), the zero time, the one time and the gap time (for on-off keying), the total number of bytes in the message and the number of bits in the code that has to be written. This information is needed by the development board to send the instruction to the implant.

ReadUC

The development board only listens to (reads) a transponder when it is asked to do that. When data is expected, after a write command for example, the development board is asked read the transponder. The protocol for the read request is given in table XII.

TABLE XII PROTOCOL OF THE READ COMMAND

Byte 1	Byte 2-3	Byte 4-5	Byte 6-7	Byte 8-9	Byte 10-11	Byte 10-12	Byte 14	Byte 15
function code	TS min	TS max	TL min	TL max	TT min	TT max	Header	code type

This instruction consists of the function code (C0), the half a clock cycle time (TS), the full clock cycle time (TL), time-out time (TT), the header (E6) and the type of

coding used (bi-Phase or Manchester). The information is used to let the development board listen to the implant. When data is received, the data is put on the serial port by the development board.

dataAvailable
The program constantly listens to the serial port. As soon as data is available the method dataAvailable receives the whole message. The flowchart of the dataAvailable procedure is given in figure 3.28
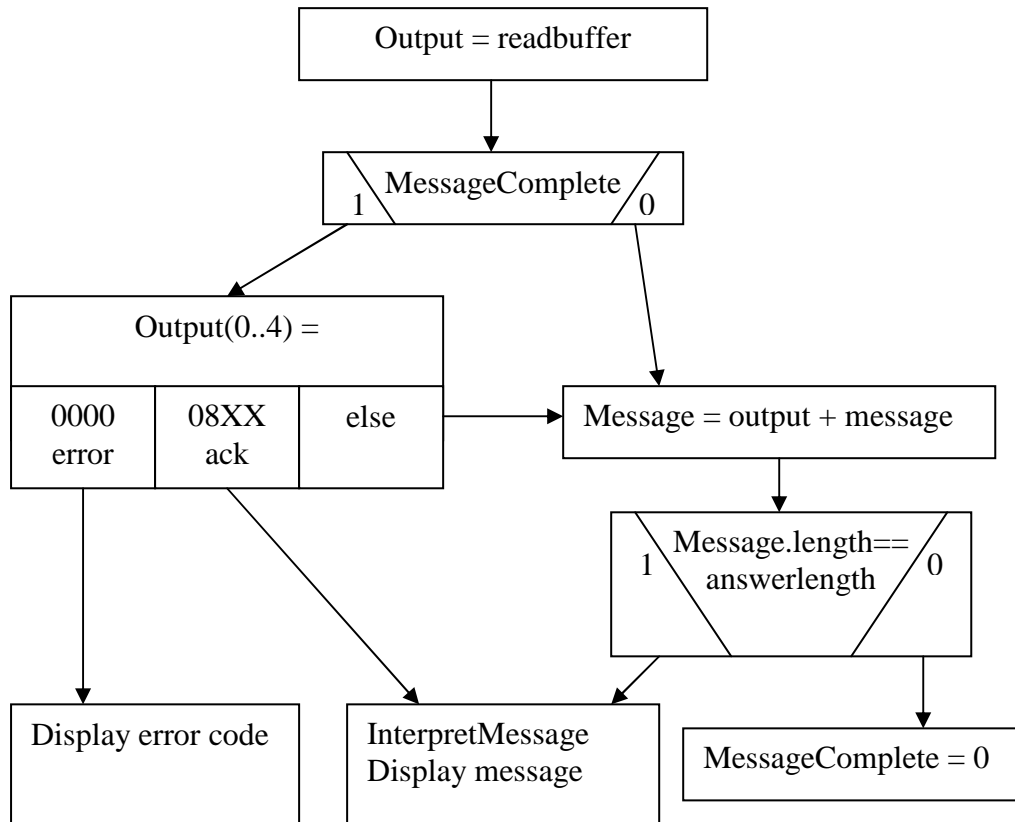
Figure 3.28 Flowchart of the Method that implements the receiving of the data from the serial port

The data is available in the readbuffer. The length of the message is stored in the first received bytes of the message. When the whole message is not received yet, a flag is put up (messageComplete) and the program waits until the rest of the message is available before it starts to interpret the message. When the whole message is received it is interpreted and displayed on the screen.

3.7 Biocompatibility

The shape and the encapsulation material are the most important issues for the biocompatibility of the implant. A laboratory rat is not a big animal and preferably the rat has to be able to move during treatment time. For this reason, a flexible circuit board is used. Because the head of the rat is not big enough to host the implant, the shape in figure 3.29 is chosen. The dimensions are given in figure 3.32. The optode is on the end of the 'wire' and is fixed to the head. The big part with the electronics is placed on the shoulders of the rat.
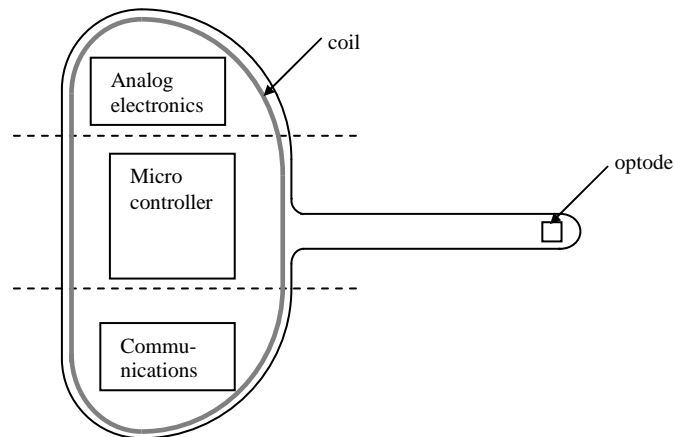
Figure 3.29 Shape of the implant

The big part is designed in such a way that it can fold in the direction of the dashed lines. The small part is also flexible. To test the size, experiments are done with dead animals as shown in figure 3.30.
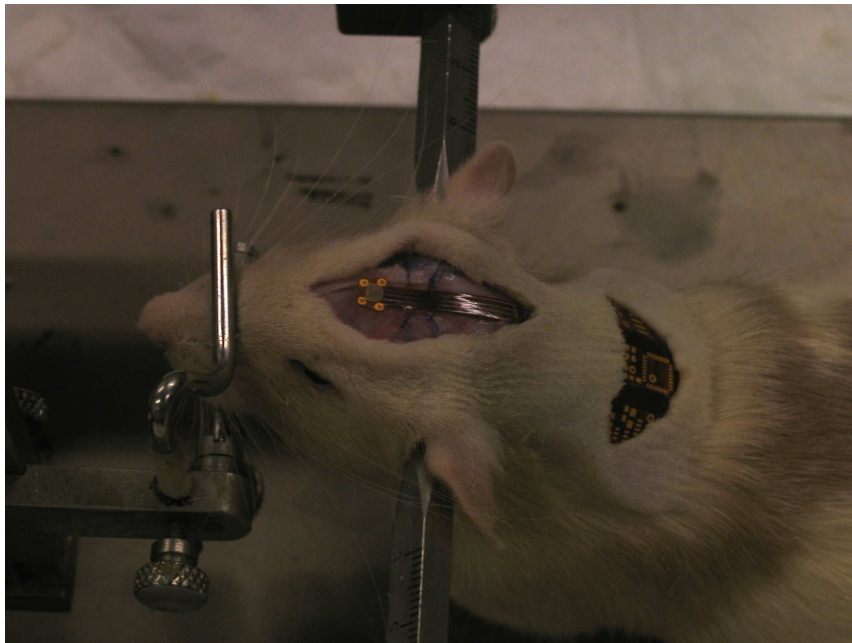
Figure 3.30 Testing the shape of the implant

The flexible substrate is made of polyimide, which is a biocompatible material, and has been used in implants before [38]. But the electronics are on top of the substrate and the tissue needs to be protected from the electronics too. Further more, the electronics cannot work if in contact with the tissue.

Implant grade silicone is used to encapsulate the implant. [29] The encapsulation of the optode itself is done with a biocompatible epoxy, Epotek 301. The epoxy is more rigid which is desired for the fragile wire bonded chip. The silicone is used for the rest of the implant because it is flexible and allows the implant to bend with the movement f the animal.

3.8 Implant Layout

The lay out is made according to the schematic, which consists of all the separate circuits presented in the chapter. A double layer board is used, with a substrate of 1 mil thick, and stiffeners of 2 mills thick. These are needed to make the connections to the electronics robust. The traces are all 200 μm wide and are orthogonal on the bending direction to improve flexibility. The pads are made of bondable gold, thus the optode chip can be mounted directly on the flexible substrate. The layout is given in figure 3.31
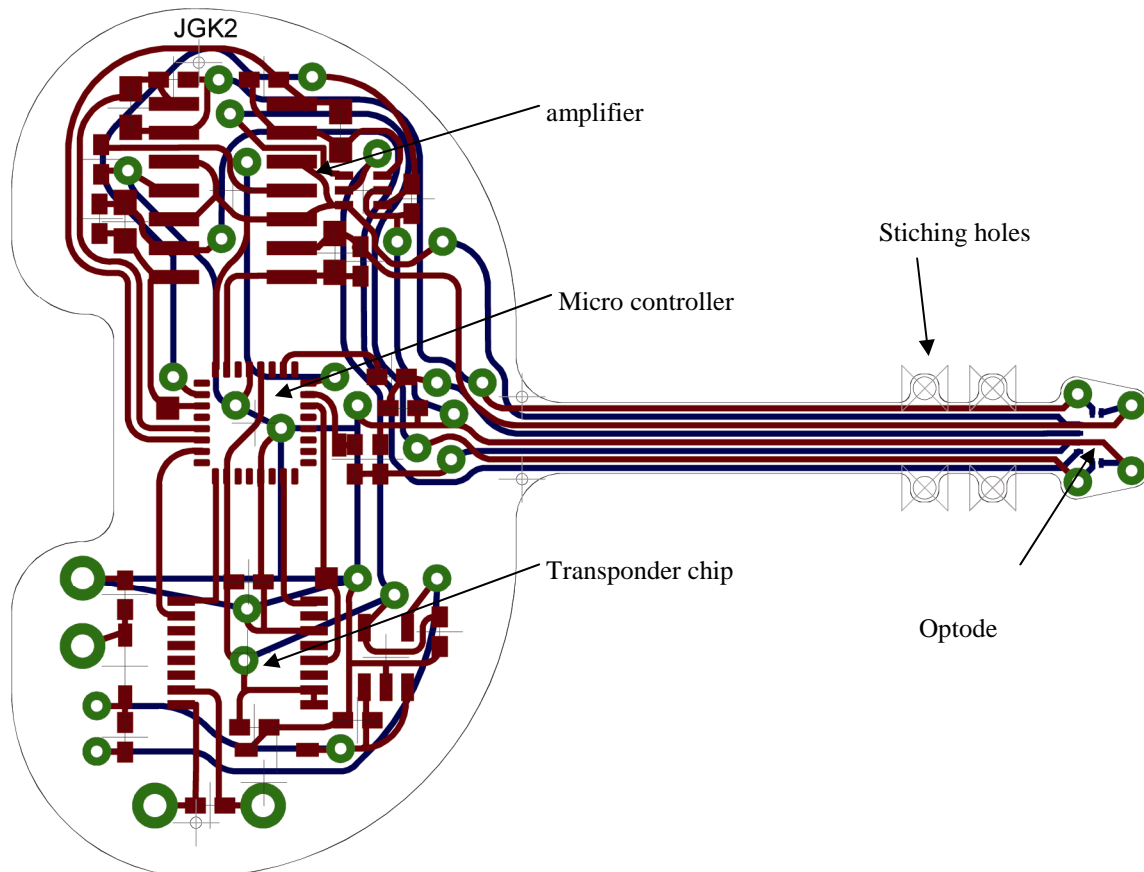
Figure 3.31 Layout of the implant

On the right the optode is placed, on the bottom. On the left are the amplifier, micro controller and transponder chip are placed. The red traces are on top, and the blue traces on the bottom. A ground plane is not used because it reduces the flexibility of the substrate. The bending lines are clearly visible. The electronics are supported by the stiffeners, as can be seen in figure 3.32. The dimensions of the implant are also given in this figure.
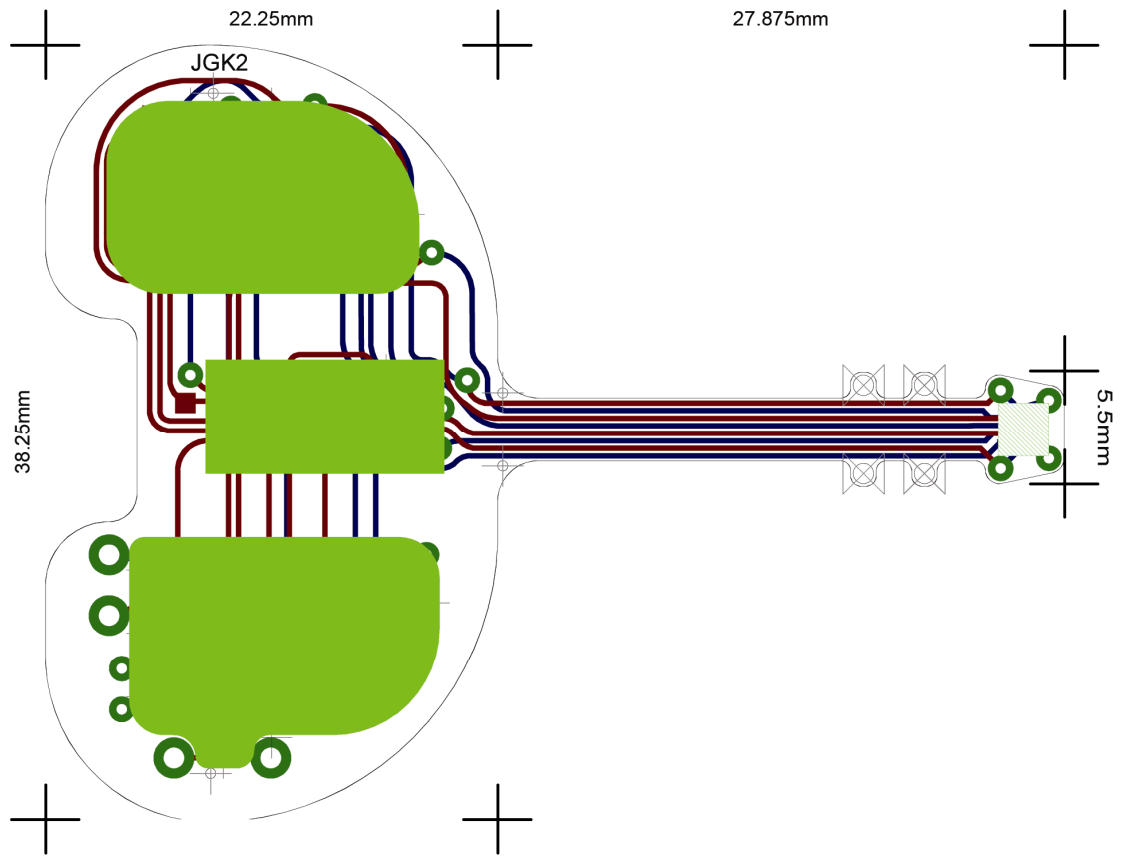
Figure 3.32 Layout of the implant with stiffeners

Multiple fixation rings are implemented in the design to attach the device to the anatomy of the rat using stitches and bone cement.

4 Results

4.1 Optode

The Optode was made in the DIMES facility. The picture in figure 4.1 shows the optode during processing after the fabrication of the holes for the LEDs and the photodiodes and the first metal.
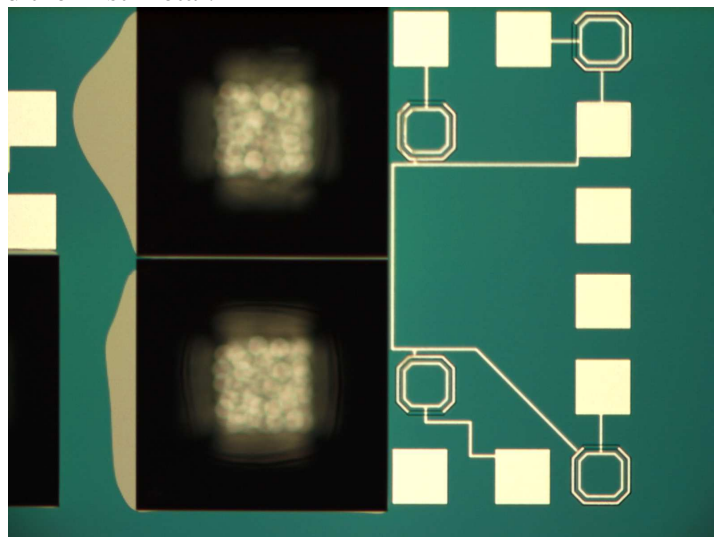
Figure 4.1 Picture taken from the optode during the manufacturing process.

As it can be seen in the figure the holes for the LEDs are deep, the bottom is completely out of focus. In this picture the second metal is not deposited yet.
The picture also shows the ground line is very close to the LED holes. This was not an optimal design choice. It would have been better if the ground line were at a larger distance from the holes. Potentially it is the cause of two problems; as shown in the picture the holes affect the flow of the photoresist during spinning on the resist to define the second metal. This gives problems when the chip is not in the left part of the chip. When on the right part, the ground line and photodiodes are not covered with photoresist and the chip becomes useless. The other problem that could occur was under etching during etching the hole. Both problems are shown in figure 4.2.
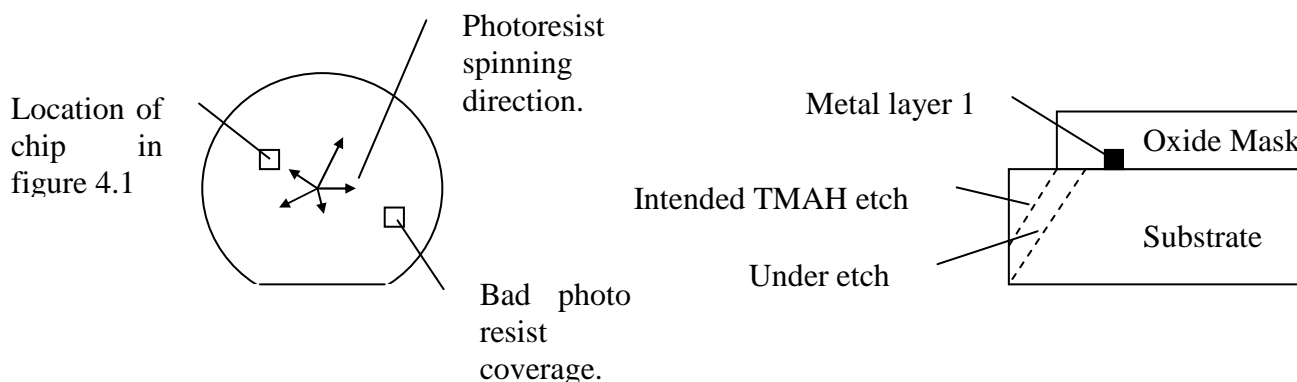
Figure 4.2 Left: the holes affect the photo resist spinning. Right: under etching during the etching of holes.

The wire was placed there for LED contacting reasons; the front contact of the LED is connected with a bondwire to bondpads that are in the big empty spot in the middle. This could also go directly to the correct bondpad, at the time of designing this was not carefully considered. Also a different kind of contacting which is more robust was under investigation.

4.1.1 Photodiode

The photodiode is characterized with the current to voltage characteristic of several photodiodes on different chips. A voltage was applied over the photodiode with the Delta Elektronika E018-0.6D power supply. This voltage was measured using the HP 34401 multimeter. After this the current was also measured with this multimeter. The resulting curves and is given in figure 4.3.
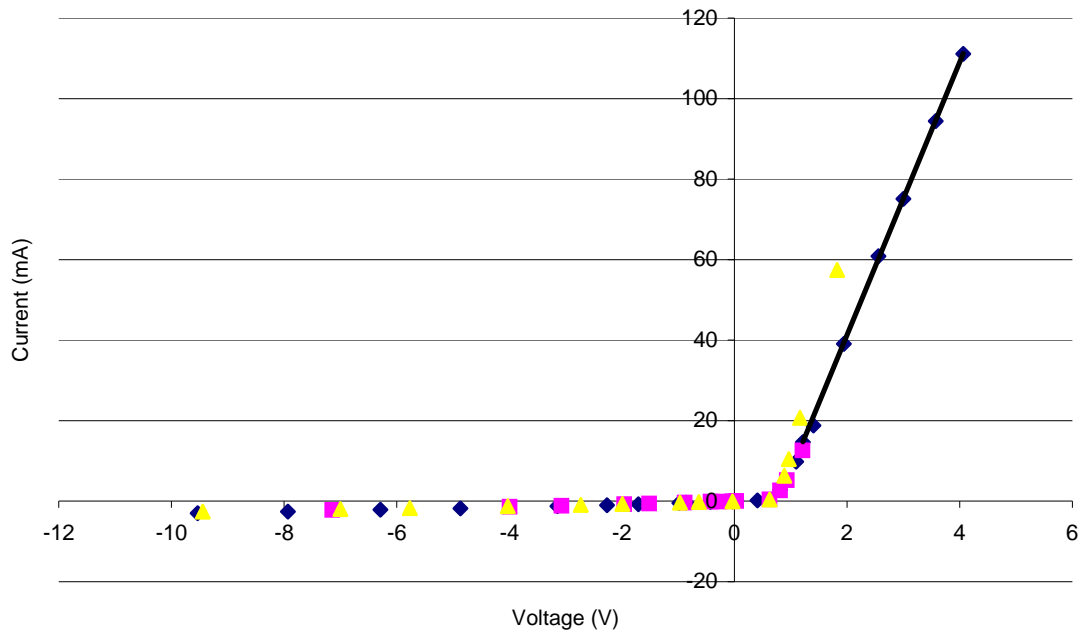
Figure 4.3 Current to voltage characteristic of the photodiodes.

From this curve two important parameters can be determined, the serial and parallel resistance of the diode. The serial resistance can be determined form the slope of the curve when a high positive voltage is applied. The curve will be linear in that part because the resistance of the diode will be negligible compared to the serial resistance. From the slope of the forward polarization a series resistance of 30 ohms was found. If we zoom in to the reverse current we get the graph given in figure 4.4.
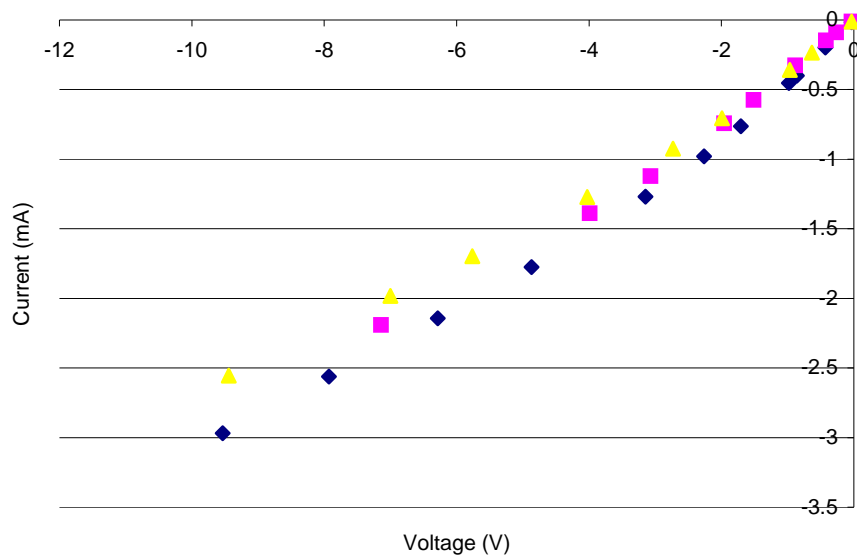
Figure 4.4 Reverse current of the photodiode

From the slope in this figure a parallel resistance of 3.5 kOhm can be concluded. Under normal conditions a very high parallel resistance is expected, well over 1 MegaOhm. A closer look at the design of the photodiode is needed to explain this unusual low parallel resistance. This can be explained using the figure in figure 4.5.
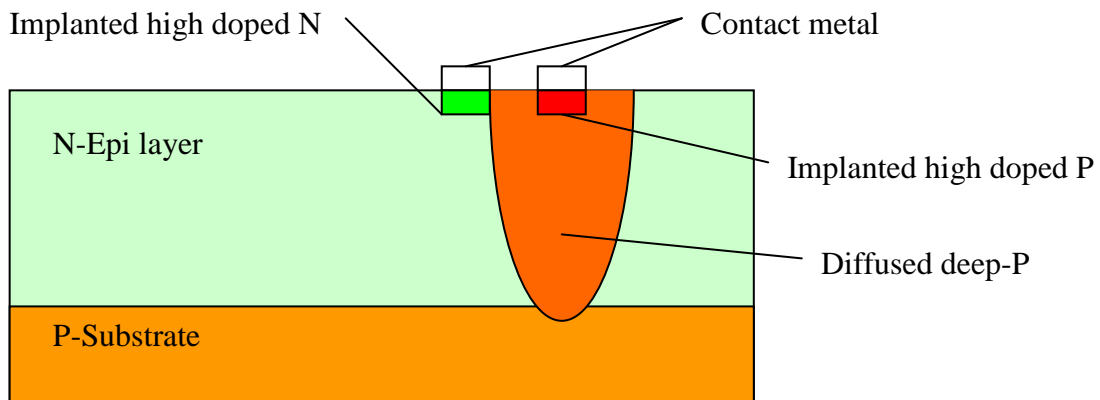
Figure 4.5 Contacts of the photodiode

The contact to the P-substrate was made using a deep P diffusion. This region not only diffuses vertically but also horizontally. This caused the P region to have not only ohmic contact with the P contact window but also with the N window. This ohmic contact is thought to be source of a lower then expected the parallel resistance. The solution to this problem is making the distance between the contacting metals larger.

4.1.2 Light Emitting Diode
Several LED chips were obtained and mounted in the cavity for the LED. Two types of LEDs were placed, with both contacts on the front, or with one contact on the back and one on the front. The ones with a backcontact were mounted with conductive glue. In this way the backcontact was connected to the rest of the chip. The front contact was made using a bond wire. For the LED chips with both contacts on the front, both contacts were made with a bondwire. This can be seen on SEM photograph shown in figure 4.6.
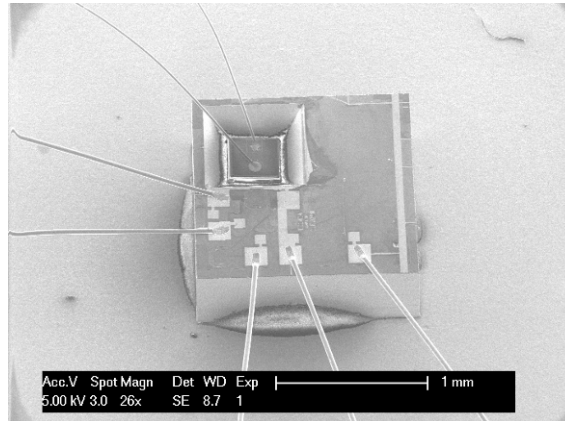
Figure 4.6 LED mounted in the cavity

In the picture the LED is directly connected to the casing of the chip.

4.1.3 Contacts
The contacting to the implant is implemented with normal bondwires. This due to the fact that the through wafer interconnect is still under investigation. The connections are shown also in figure 4.6. The bond wires are protected with a biocompatible epoxy. This is shown in figure 4.7.
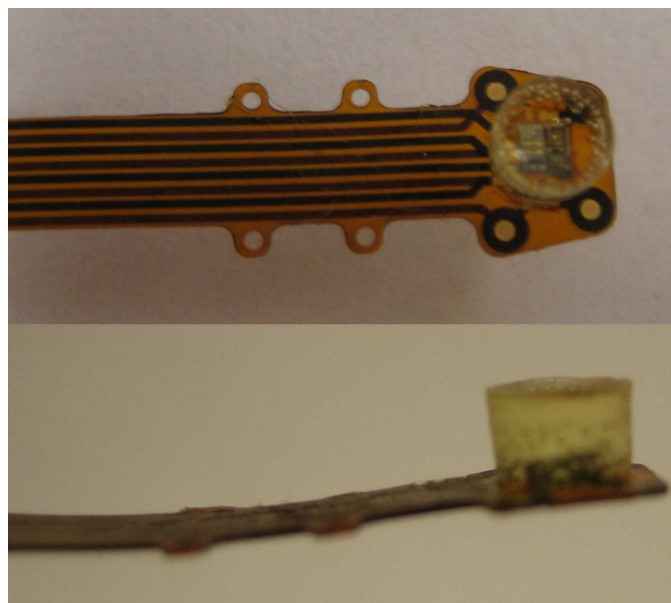
Figure 4.7 Optode mounted on the flexible PCB, protected with epoxy

4.2 Results Electronics

4.2.1 Transimpedance amplifier

The transimpedance amplifier was tested and simulated separately from the implant. The simulations were done using SPICE software and the practical setup is shown in figure 4.8.
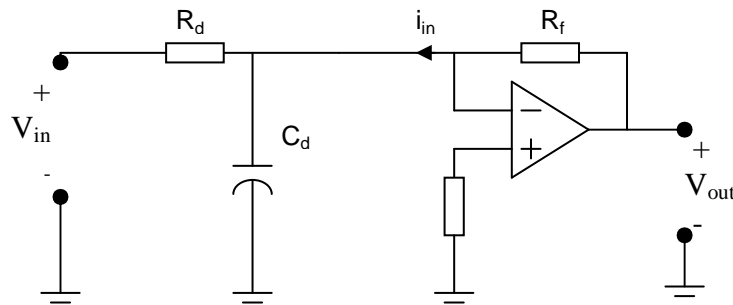
Figure 4.8 Measurement setup for the transimpedance amplifier.

The source resistance was 683 kOhm and the source capacitor was 3.3 pF. A measurement with and one without the compensation resistor was done. The compensation resistor was also 683 kOhm. The operational amplifier was supplied with a Delta Elektronika power supply E 060-0.6. The input was made using the Norton-Thevenin equivalent and was supplied by a Delta Elektronika dual power supply E 018-0.6D. The input voltage was varies between 100 mV and –1V that corresponds to an input current between 0 and 1.4 µA. The input and output voltage were measured on the Tektronix TDS 2012 oscilloscope. The results for the DC analyses are shown in figure 4.9.
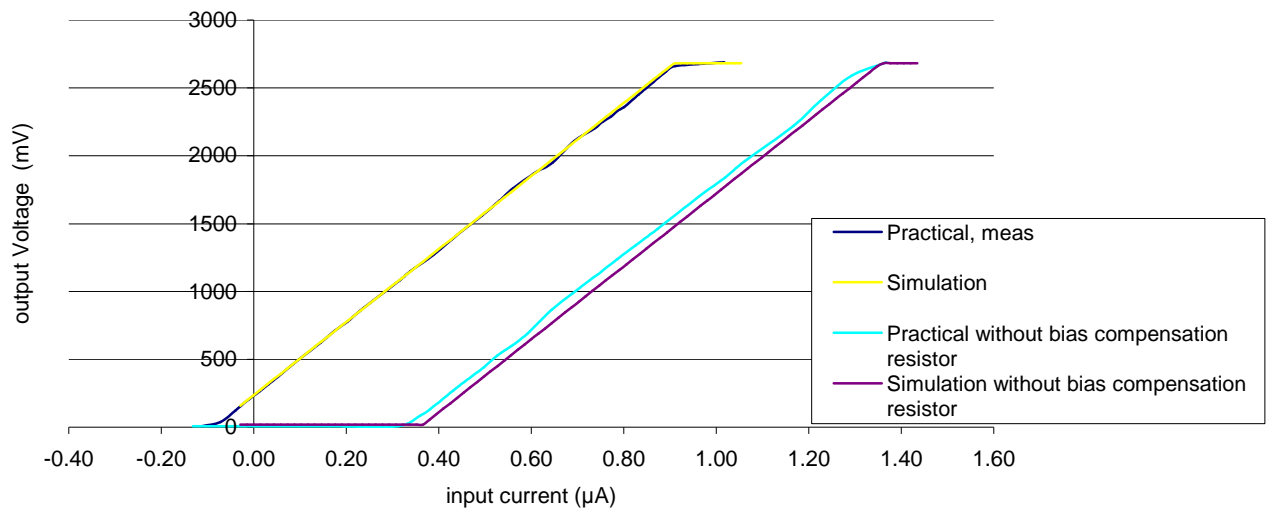
Figure 4.9 DC analyses of the transimpedance amplifier.

As shown in the figure the input bias current of 360 nA has a significant influence on the result. The compensation resistor for this would be a resistor on the positive input of the operational amplifier that is equal to the parallel resistance of the feedback resistance and the input resistance. The compensation resistor in this case was not chosen correctly which is the cause of the offset in the graph.

Due to the fact that the parallel resistance of the photodiode is very low, the input resistance is very low. As a consequence the offset of the influence is much less then

with a diode with high parallel impedance. The DC behaviour of this implementation of the transimpedance amplifier is good enough for this prototype. But in a later design when the parallel resistance is high, a compensation resistor is necessary to prevent a large offset.

The AC behaviour of the transimpedance amplifier was also investigated. Again the simulations were done using SPICE software. A similar setup was used as in the DC analyses. In this case the input voltage was a 350 mV ptp sine wave with –180mV offset. In the feedback network a capacitor was added to have a stabile amplification without resonant peaks. The Agilent 33220A arbitrary waveform generator supplied the input voltage. The frequency was varied and the in and output peak-to-peak voltage was measured using the Tektronix TDS 2012 oscilloscope. From this the gain of the amplifier was calculated. The results are shown in figure 4.10
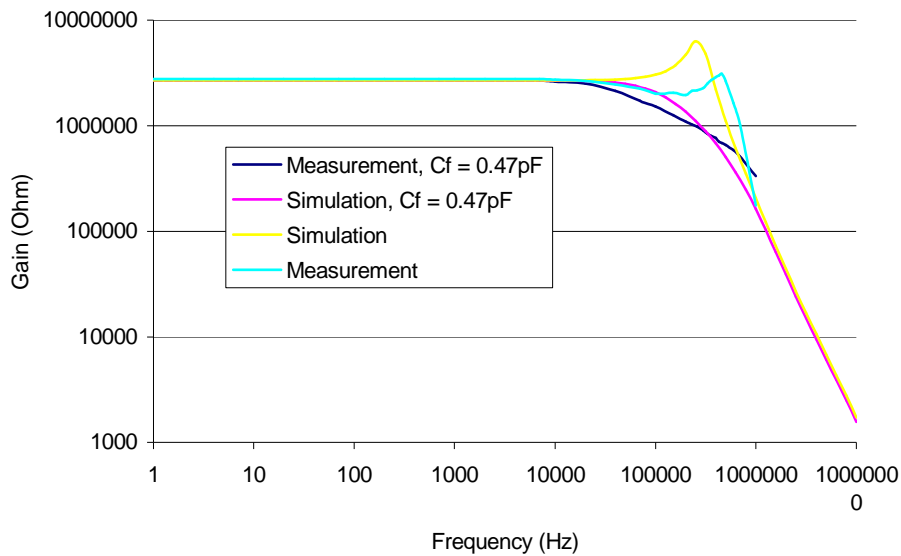
Figure 4.10 AC analyses of the transimpedance amplifier.

The bandwidth of the circuit without the feedback capacitor is higher than with the feedback capacitor, but peaks close to the corner frequency. This is the case for both the simulation and the measurement. The measurement shows a smaller amplification just before this peak, a similar behaviour is observed for the case with the feedback capacitor. The reason for this could be parasitic elements that were not simulated. This behaviour also reduces the bandwidth of the amplifier; the measurement and simulation of the amplifier with feedback capacitor show bandwidths of 50 kHz and 100 kHz respectively. The amplification factor does not decay with an expected 20dB per decade until about 1 MHz. The corner frequency for the measurement without the feedback capacitor is about 550 kHz, the simulation gave 500kHz.
Consequences for the limited bandwidth are that time-resolved fluorescence measurements are not possible with this amplifier.

- 88 -

4.2.2 Temperature measurements

The temperature was also tested separately from the implant. The setup is given in figure 4.11, the circuit was placed in an oven with three wires to the outside, ground, Vdd and the voltage over the diode. The photodiode is on chip and a 1k resistor is placed in series. The chip was connected to a large metal block to stabilize the temperature. The reference temperature was measured with a platinum temperature sensor.
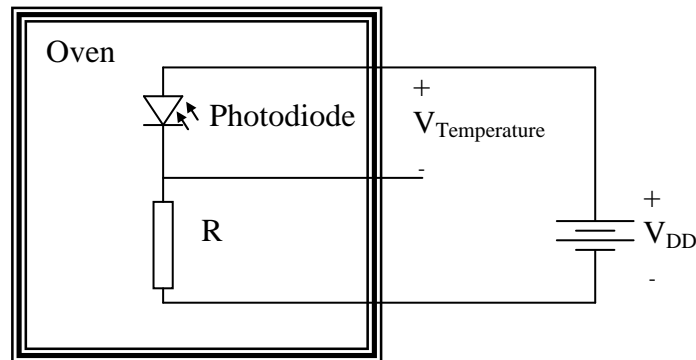
Figure 4.11 Temperature measurement setup.

The temperature of the oven was first increased from 30 to 50 degrees Celsius and after that decreased form 50 to 30 degrees Celsius. The measurement results, the voltage over the diode versus the temperature determined by the platinum temperature sensor, are plotted in figure 4.12.
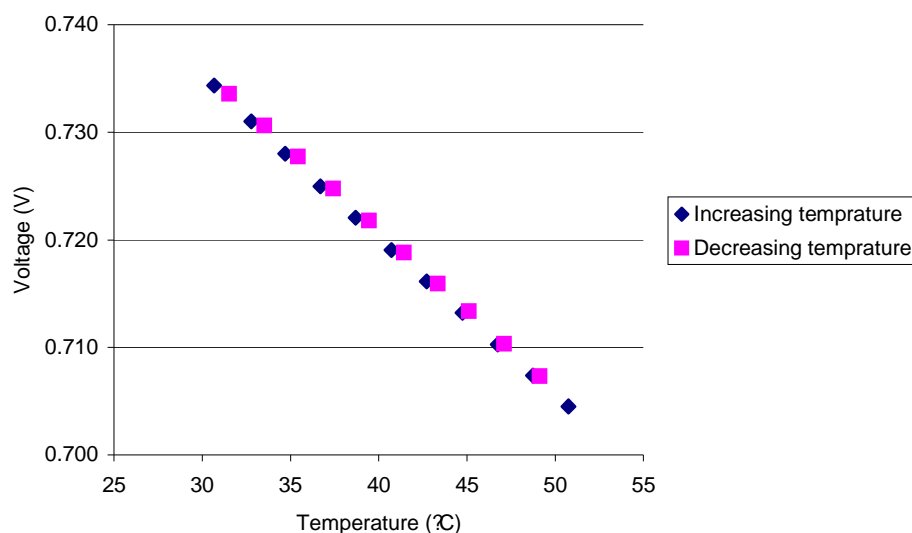
Figure 4.12 Photodiode voltage versus temperature

The temperature coefficient is 1.493 mV/K. With a 10 bit AD converter with a reference of 1.1 V, the voltage resolution will be 1.074 mV. This gives a temperature resolution of 0.71 K, which determines the quantization error to be 0.207 K.

The difference between increasing and decreasing temperature is caused by the settling time of the oven. The chip was not perfectly attached to the metal block, this causes small temperature differences between the chip and the platinum sensor when

a short settling time is chosen. The temperature differences could occur due to different heat capacities between the block and the chip, one heats up faster than the other. In later experiments it was shown that the difference is less when longer settling time was used. With longer settling times the value for R squared improved from 0.99884 to 0.99905 and with the longest settling time to 0.99972

The resolution of the measurements is high enough to do the necessary temperature measurements, which only require detection of temperature increase over a threshold of 1 Kelvin.

4.2.3 Power Link

Class E driver

The resonant frequency of the secondary side was determined to be 1.155 MHz. The values of the capacitors were determined with the equations in paragraph 2.4.2. They were determined to be 410 pF and 7.51 nF for the serial and parallel capacitor respectively. These values were used as start values to tune the practical circuit. The tuning of the circuit was done using the Tektronix TDS 3034B and the voltage and current waveform over the MOSFET was observed until the right behaviour was obtained, no voltage when the MOSFET was on, and no current when the MOSFET was off.

The parts used in the final implementation of the circuit given in figure 3.15 are given in table XIII. The current and voltage waveforms of the practical circuit are given in figure 4.13.

TABLE XIII. PARTS USED IN
CLASS E DRIVER.

MOSFET	IRF330
$L(\mu H)$	500
$C_p(pF)$	1500
$C_s(pF)$	310
$L_{primary}(\mu H)$	46.8
$L_{secondary}(\mu H)$	19.7
$R_{s, secondary}(Ohm)$	1.7
$C_{res}(pF)$	1000
Diode	BAS316
$C_{filter}(\mu F)$	1.0
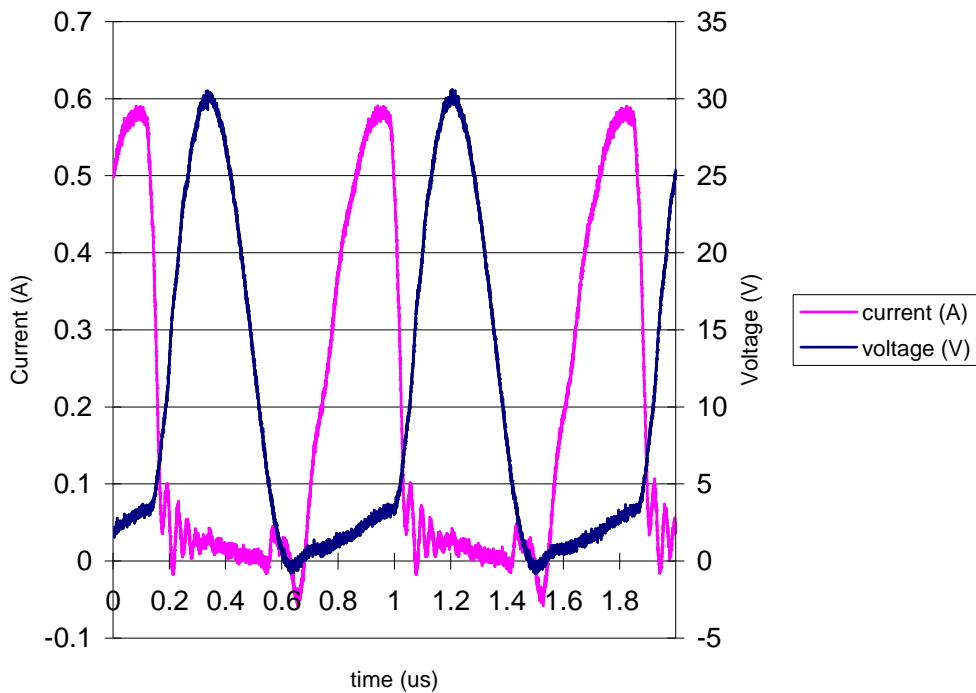
Figure 4.13 Practical current and voltage waveforms of the Class E amplifier

The values for the parallel and serial capacitor are much different then the calculated ones. The reason for this could be the fact that a MOSFET is used and not using an ideal switch. The MOSFET has parasitic elements that are not considered in the calculation of the capacitor value. Another reason could be the fact that the inductor value of the coil is changed due to the coupling with the communication coil. A significant change in behaviour is observed when the coil is moved around relative to each other.

When the Class-E amplifier is tuned correctly only 0.65 W of power is wasted in the MOSFET, this is much less then the maximum of 75 W. The Class-E amplifier can be tuned to another frequency in the case that other excitation frequencies are needed.

Efficiency

The power link efficiency was determined by measuring the peak-to-peak voltage on the circuit given in figure 4.14. It consists of the secondary coil with the resonant capacitor and a load resistance of 120 ohm in parallel.
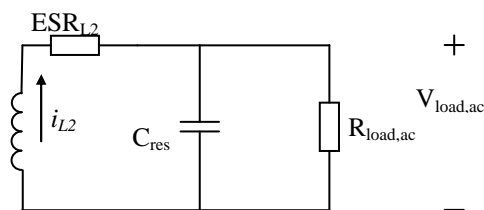
Figure 4.14 Secondary side of the power link with the load approximated with a resistor

The primary coil was driven by the class E driver. The class E driver was controlled by the Agilent 3320 A arbitrary waveform generator and supplied by a Delta Elektronika E060-0.6 power supply. The secondary circuit was moved from the centre of the coil (radius = 0cm) to the perimeter off the coil (radius = 15 cm). This was done for several heights. The results are plotted in figure 4.15.
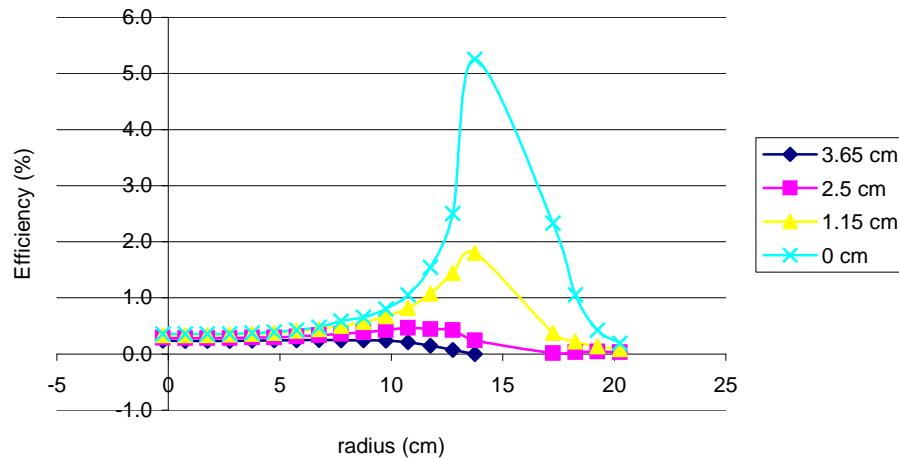
Figure 4.15 Efficiency of the power link for several distances from the primary coil

After this the induced voltage was determined using SPICE and the corresponding mutual inductance was calculated using equation 44. The theoretical calculated mutual inductance and the practical measurement of mutual inductance in the centre of the primary coil at different heights are given in figure 4.16.
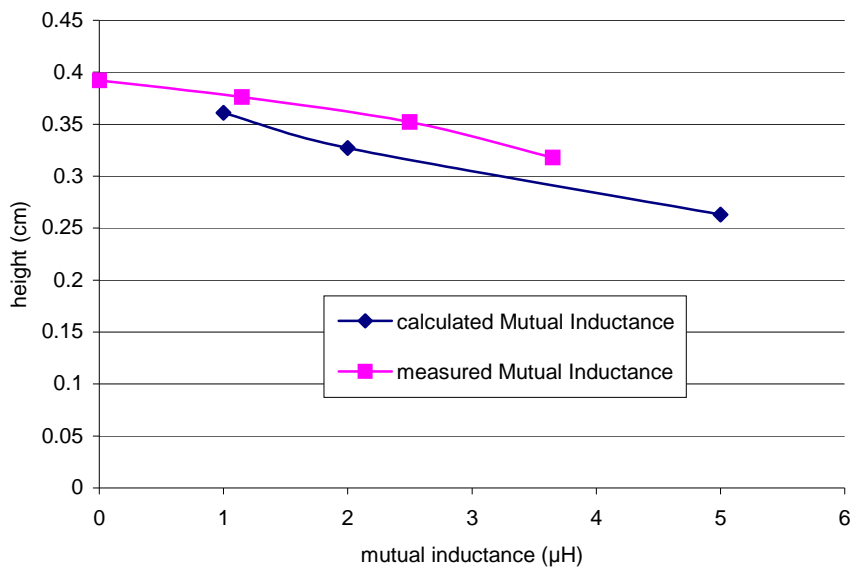
Figure 4.16 Theoretical approximation of the mutual inductance, and the practical measured mutual inductance

As it can be seen, the practical mutual inductance is higher than the theoretical mutual inductance. A reason for this could be the fact that the secondary coil is approximated with the model for a round coil with a radius of 1.41 cm, which has the same area of the actual secondary coil.

The overall efficiency at the centre of the primary coil is also determined. The input voltage was 10 V and the input current 145 mA, thus the power to the input equals 1.4W. The secondary coil picked up 2.69 mW of power at the center of the coil, which is an efficiency of 0.2 percent.

The peak power usage of the implant equals 14 mW, which corresponds to 1 percent efficiency with this power source, and is thus only achieved within 4 cm distance from the side of the coil. But normal power consumption is much lower; thus, with a buffer the power source is sufficient.

The buffer is implemented in with 0.3 F capacitor placed in front of the voltage regulator.

4.2.4 Flexible PCB

The amplifier, microcontroller and transponder chip are successfully implemented on the flexible PCB. As shown in figure 4.17.
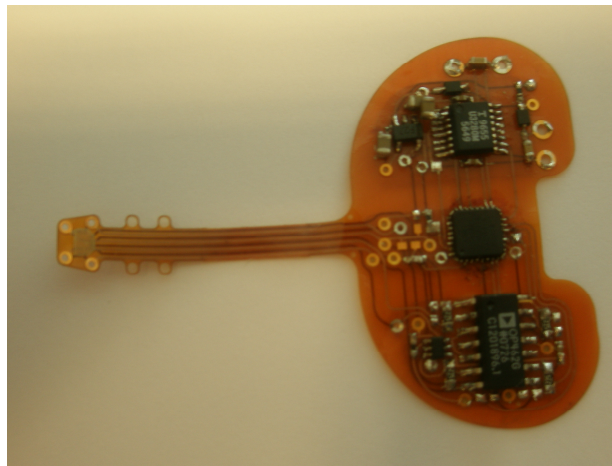
Figure 4.17 Flexible PCB with all components soldered except the coils and optode

Due to some mistakes in the design not all components are placed and some extra components are soldered on the PCB. In a later phase of the project it was found that the flexible PCB is not as robust as needed. All the vias were not reliable, especially the four bigger ones which are supposed to contact the coils. For this reason a hardwired solution was made to contact the coils to the rest of the circuit.

After mounting all the components the board was encapsulated in silicone as shown in figure 4.18.
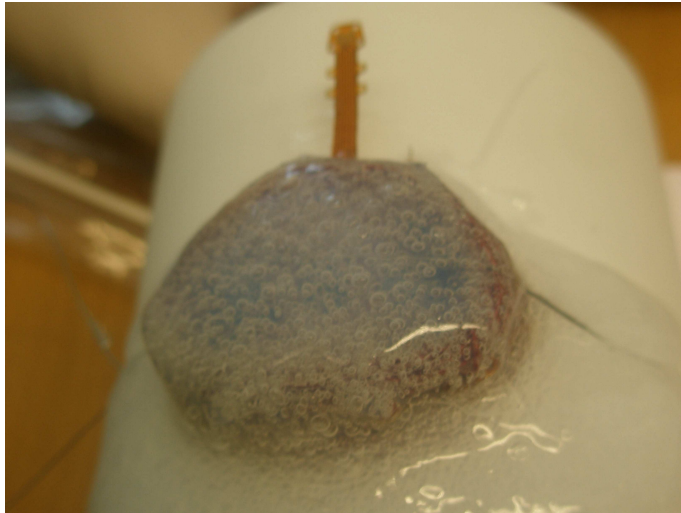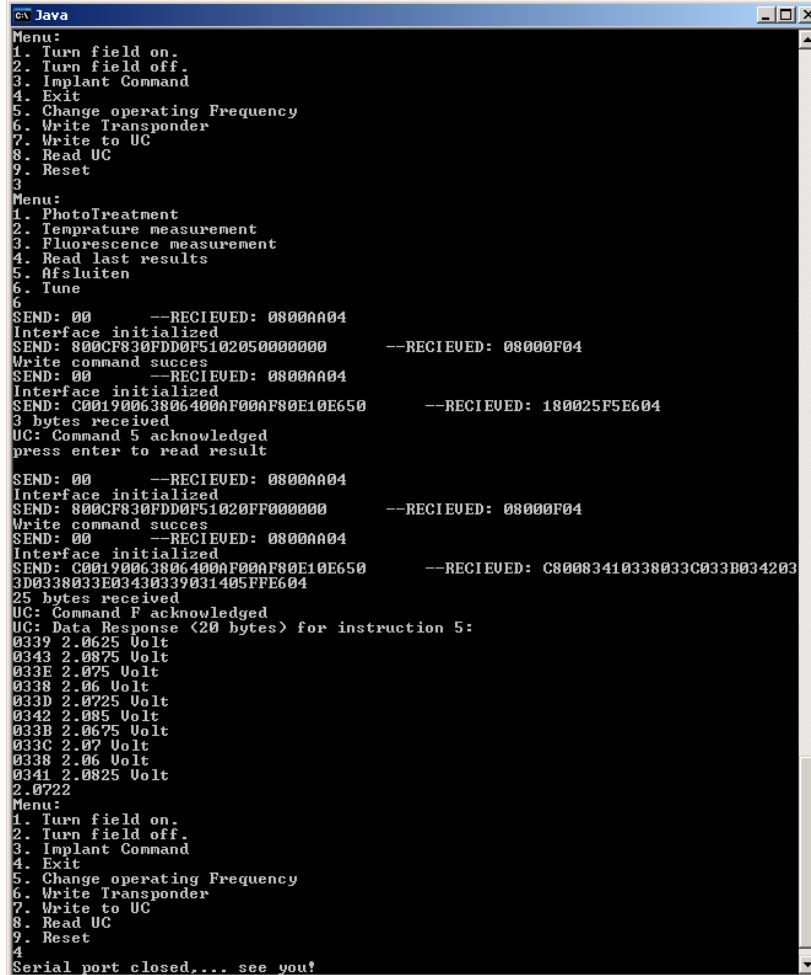
Figure 4.18 Flexible PCB encapsulated with medical grade silicone

In the picture air bubbles can be seen in the silicone. The air bubbles are possible leaks of the implant and are thus unwanted. In this case it was not harmful because it is just a first prototype but in the future this should be prevented. When special equipment is used airless silicone rubber can be made. This can for example be done by specialized packaging companies.

4.3 Software

4.3.1 PC Interface

The Pc interface is a text based input screen. Several treatments can be chosen in the menu, after which the treatment parameters can be altered. The results are stored in a comma separated excel file for easy access. A screen dump for a tune operation is given in figure 4.19.

```
Java                                                          _ | □ | X

Menu:
1. Turn field on.
2. Turn field off.
3. Implant Command
4. Exit
5. Change operating Frequency
6. Write Transponder
7. Write to UC
8. Read UC
9. Reset
3
Menu:
1. PhotoTreatment
2. Temprature measurement
3. Fluorescence measurement
4. Read last results
5. Afsluiten
6. Tune
6
SEND: 00        --RECIEVED: 0800AA04
Interface initialized
SEND: 800CF830FDD0F5102050000000        --RECIEVED: 08000F04
Write command succes
SEND: 00        --RECIEVED: 0800AA04
Interface initialized
SEND: C00190063806400AF00AF80E10E650        --RECIEVED: 180025F5E604
3 bytes received
UC: Command 5 acknowledged
press enter to read result

SEND: 00        --RECIEVED: 0800AA04
Interface initialized
SEND: 800CF830FDD0F51020FF000000        --RECIEVED: 08000F04
Write command succes
SEND: 00        --RECIEVED: 0800AA04
Interface initialized
SEND: C00190063806400AF00AF80E10E650        --RECIEVED: C80083410338033C033B034203
3D0338033E034303390314405FFE604
25 bytes received
UC: Command F acknowledged
UC: Data Response (20 bytes) for instruction 5:
0339 2.0625 Volt
0343 2.0875 Volt
033E 2.075 Volt
0338 2.06 Volt
033D 2.0725 Volt
0342 2.085 Volt
033B 2.0675 Volt
033C 2.07 Volt
0338 2.06 Volt
0341 2.0825 Volt
2.0722
Menu:
1. Turn field on.
2. Turn field off.
3. Implant Command
4. Exit
5. Change operating Frequency
6. Write Transponder
7. Write to UC
8. Read UC
9. Reset
4
Serial port closed,... see you!
```

Figure 4.19 Screen dump of the PC interface during a tune operation.

4.4 Complete Setup

The complete external setup is shown in figure 4.20.
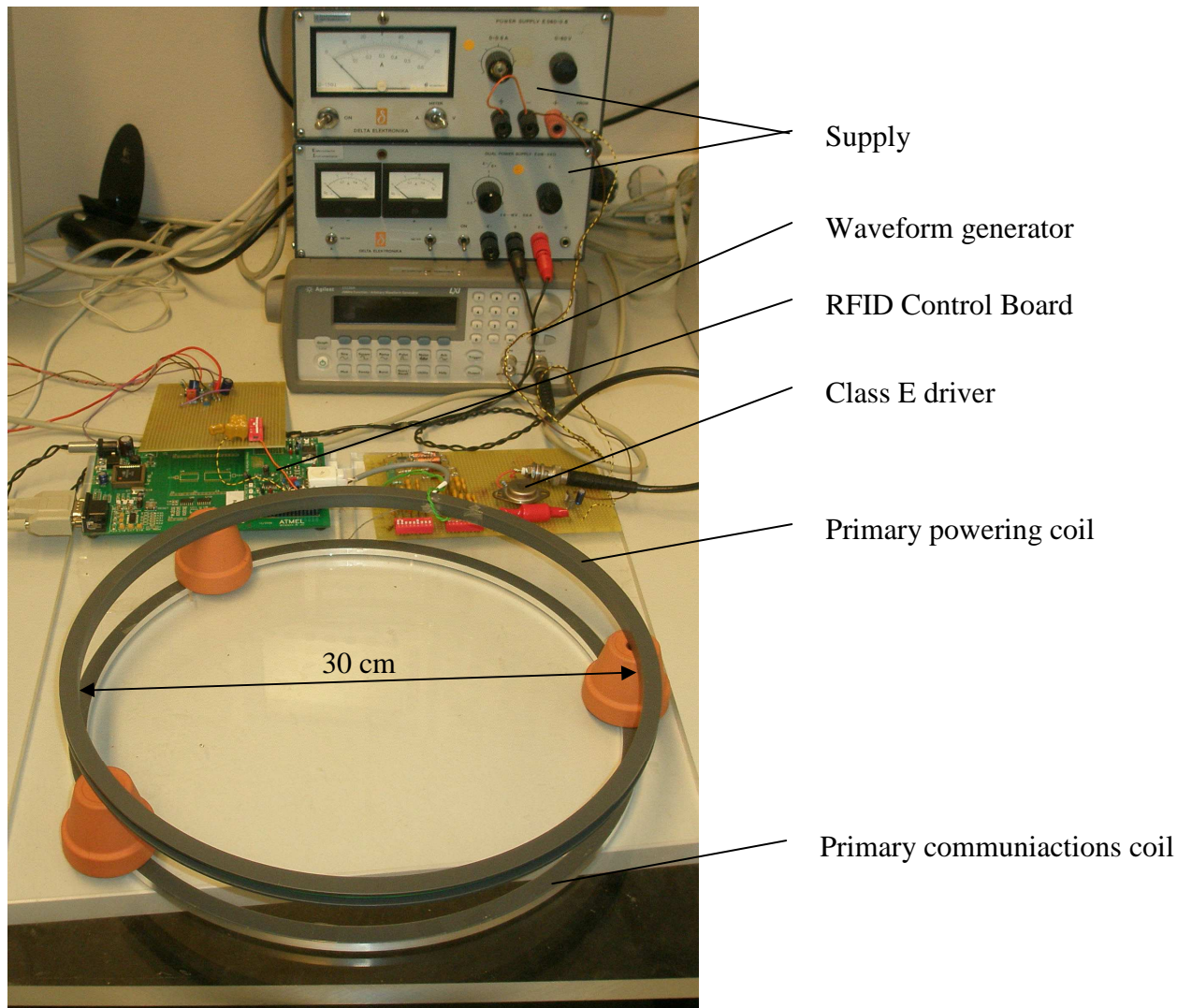
Figure 4.20 Complete External setup.

The different parts of the system can be seen in the picture. The treatment area is a circle with a diameter of 30 cm. This is enough to do a treatment in a rat. The spacers used are temporary and will be replaced with a solid cage like structure in such a way that the rat cannot get out of the treatment area.

5 Conclusions and outlook

A system has been developed which can administer and monitor metronomic PDT. It has been shown that the main function of the system, namely illuminating a specific volume with a specific wavelength at regular intervals over a period of several weeks has been successfully implemented. The other requirements on communication and powering are fully implemented, but not all the requirements on the monitoring of the treatment are available at this stage.

Optode
The front-end chip for the system, an optode containing photodiodes and used as carrier for a LED was designed and manufactured. The optode is manufactured at the DIMES facility with a custom process based on a standard bipolar process with added micro machining steps. These were necessary to create a cavity to carry solid-state sources. Different LEDs were mounted successfully, allowing up to two wavelength sources per optode. Because the LED is placed on the same substrate as the photodiodes are made, the sources and detectors are in close proximity. The photodiodes were successfully made in the same process. Although a low parallel resistance was measured due to a design flaw, the photodiodes are useful for the application.

Implant Electronics
The rest of the implant was implemented using standard electronic components. A microcontroller was programmed to control the implant; communication as well as the different treatment and monitoring modes. The software was written in C.
An amplifier was designed to amplify the signal from the photodiodes. The bandwidth of this amplifier is 50 kHz. This is enough for a continuous wave reflection measurement but not fast enough for a time resolved fluorescent measurement. A/D conversion is done by the onboard AD conversion of the microcontroller.
The circuit was designed in such a way that one photodiode can also be used as temperature sensor. The temperature sensor has a resolution of 0.7K.
The communication was implemented using a transponder chip, a custom designed coil and a communication protocol programmed in the microcontroller. The communication is high level, making it possible to adjust every treatment parameter, such as intensity and treatment time.
The implant is powered by an inductive power link. The powering circuit was implemented with a coil, a super capacitor and a voltage regulator. The coil was designed for low losses in the coil to prevent heating of the tissue. The super capacitor is used as a buffer to ensure operation when the rat moves out of the plane. The implant can be provided with power anywhere within the primary coil.
A flexible circuit board was designed and manufactured. All the components and optode were mounted on a flexible substrate and tested extensively. Unfortunately the vias of the substrate were not very reliable, short-term solution was to make extra connection with wires. The circuit is flexible, which allows the laboratory rat to move without destroying the electronics.

External Electronics
The primary side of the communication electronics is implemented with a custom made 15 cm radius coil. The primary coil is controlled with a standard RFID control board from ATMEL. The software to control this board, and with it the implant, was made with Java. The user interface is a simple menu in which all treatment and monitoring options can be selected and parameters of treatment can be adjusted. It is also possible to change the excitation frequency, both by software and hardware. This allows custom tuning for different implants.

The primary side of the inductive power link is implemented with a custom made coil and is driven with a Class-E driver. The class-E driver can be adjusted for several frequencies around 1 MHz, allowing custom tuning for different implants.

A specially made supporting plate on which treatment can be done supports both the powering and the communication coils

Functionality
The LEDs controlled by the microcontroller make treatment possible. Different intensities and illumination times can be selected.

The monitoring of PDT is partly achieved; the fluence rate and temperature can be monitored by the system. This allows feedback on whether treatment is being done and the temperature response of the chip during treatment.

The time resolved fluorescence measurement is implemented in the software of the microcontroller but the amplifier implementation has a bandwidth of only 50 kHz, which is too slow for a time resolved fluorescence measurement. Another option for the fluorescence is an implementation with filters in front of the photo detectors. This would be possible on the basis of the current implementation of the optode but further development is needed. As a consequence no indication on photosensitizer concentration can be measured with this system.

The oxygen measurement is not implemented. Just like the fluorescence measurement it is possible to implement this on the current design of the optode. At this moment the system is not capable of measuring oxygen concentrations in the tissue.

The whole implant can be fitted in the laboratory rat, although the first prototype is bigger than expected due to the bigger coils and due to the fact that encapsulation was done manually with no molds or specially developed tooling or machines. This allows an experiment within the laboratory rat.

The implant is fully controllable within the two primary coils with a radius of 15 cm. The measurement data can be read out anywhere within the area of the two coils. This allows the rat to move freely within the 15 cm radius confined circle during a treatment.

The implant is provided with power with an inductive power link. The device needs 10 minutes in the field to charge. After this, the device can monitor without the powering field on. This is important because the field influences measurement results significantly.

The implant has been made biocompatible by encapsulating it with biocompatible epoxy and biocompatible silicone. The implant can thus be used in a laboratory rat without causing unintended damage, or biological response of the rat.

Outlook

This project was a pilot project for the development of system for treating cancer with metronomic photodynamic therapy. Although a system has been made which is useful in this phase, this thesis is only the beginning of a large project. In this perspective one can imagine that a lot of recommendations for future work are presented.

In the near future the present system can be tweaked to perform a lot better. First of all the bandwidth of the amplifier must be increased in such a way that time resolved fluorescent measurements are possible or change to a dedicated topology for fluorescence measurements.

To understand the measurement result better both LED and the photodiode have to be characterized. The illumination pattern and intensity of the LED and the quantum efficiency and spectral response of the photodiodes are essential for good interpretation.

The implant can also be made smaller in the near future by making a mold for the silicone encapsulation, resorting to external encapsulation services and/or by decreasing the size of the secondary coils.

The interface to the user can be improved by developing a graphical interface for the control software.

To add functionality to the current setup filters can be applied on top of the photodiode allowing fluorescent measurements. An oxygen measurement technique must also be implemented like the fluorescent technique implemented in the pO2 sensor of TNO or the Differential Pathlength Spectroscopy developed by Amelink et al.

The next step would be to implement the electronics on chip. The readout electronics: amplification, sample and hold, A/D conversion and LED drive on chip.

The external electronics can be improved by developing a dedicated communications board for the RFID and an auto tuning circuit for the powering coil.

The final step for developing the system would be to implement multiple optodes with one power and communications chip. This will make the system adaptable for use in bigger animals and humans.

The ultimate goal of the project would be to get the system approved for human treatment of cancer.

References

[1]   Robert L.P. van Veen, *In vivo optical measurements for Diagnostics and Monitoring of Treatment*, PhD Thesis, Erasmus University Rotterdam, Rotterdam, 2006.

[2]   "Photodynamic Therapy (PDT)", May 26, 2008. [Online]. Available: http://photochembgsu.com/applications/therapy.html. [Accessed: May 26, 2008].

[3]   N.R. Finsen. *Phototherapy*. London: Arnold, 1901.

[4]   R.R. Allison, H.C. Mota, C.H. Sibata, "Clinical PD/PDT in North America: An historical review", *Photodiagnosis and Photodynamic Therapy*, vol., no. 4, pp. 263-277, December 2004.

[5]   H. Von Tappeiner, Jodlbauer A. *Die Sensibilisierende Wirkung fluorieszierender Substanzer. In: Gesammte untersuchungen uber die photodynamische (The sensitizing action of fluorescent substances. An overall account of investigations on photodynamic phenomena).* Leipzig: F.C.W. Vogel, 1907.

[6]   R. Lipson, E. Baldes and A. Olsen, "The use of a derivative of hematoporhyrin in tumor detection.", *J Natl Cancer Inst,* vol. 26, pp.1-11, 1961.

[7]   D.J. Robinson, "Implantable photonics", *Erasmus University*,2007. [Online]. Available: http://www.erasmusmc.nl/radiotherapie/research/pdthome/research_grants/5190 59/ [Accessed: September 24, 2008].

[8]   P.K. Sneed et al., "Patterns of recurrence of glioblastoma multiforme after external irradiation followed by implant boost"., *Int J Radiat Oncol Biol Phys*, vol. 29, no4, pp. 719-727, 1994.

[9]   Ian J MacDonald, Thomas J. Dougherty, "Basic principles of photodynamic therapy", *Journal of Porphyrins and Phthalocyanines*, vol. 5, no. 2, pp 105-129, 2001.

[10]   Thomas H. Foster, Richards S. Murant, Robert G. Bryant et al. "Oxygen consumption and diffusion effects in photodynamic therapy." *Radiation Research*, Vol. 126, No. 3, pp. 296-303, June 1991.

[11]   Tuan Vo-Dinh, Ed., *Biomedical Photonics Handbook*, Boca Raton, FL: CRC Press LLC, 2003.

[12] Dominic J. Robinson, Henriëtte S. de Bruijn, Nynke van der Veen, Mark R. Stringer, Stanley B. Brown, Willem M. Star "Fluorescence Photobleaching of ALA-induced Protoporphyrin IX during Photodynamic Therapy of Normal Hairless Mouse Skin: The Effect of Light Dose and Irradiance and the Resulting Biological Effect", *Photochemistry and Photobiology*, vol.67, no.1, pp. 140-149, jan. 1998.

[13] D. G. Boyle, W. R. Potter, *"Photobleaching Photofrin II as a means of eliminating skin photosensitivity"*. *Photochemistry and Photobiology*, vol. 46, no. 6, pp. 997–1001, 1987.

[14] E. Margallo-Balbás, P. J. French, "Shape based Monte Carlo code for light transport in complex heterogeneous Tissues," *Optical Express*, vol. 15 no. 21, pp. 14086-14098, 2007.

[15] L. Wang, S. L. Jacques, and L. Zheng, ''MCML—Monte Carlo modelling of light transport in multi-layered tissues,'' *Computer Methods & Programs in Biomedicine*, vol. *47*, pp. 131-46, 1995.

[16] Donald A Neamen, *Semiconductor Physics and Devices 3rd Edition*, New York: McGraw-Hill, 2003

[17] Jerald G. Graeme, *"Photodiode Amplifiers. Op Amp Solutions"* Gain Technology., New York: McGraw-Hill, 1996.

[18] C.J.M. Verhoeven, *Structured Electronic Design, negative-feedback amplifiers*. Boston: Kluwer Acadamic Publishers, 2003.

[19] Atmel Corporation., "Datasheet ATTiny 861V", [Online]. Available: http://www.atmel.com. [Accessed: Sep. 20, 2007].

[20] Atmel Corporation, "U3280M Transponder Interface for Microcontroller Datasheet," [Online] Available: http://www.atmel.com. [Accessed: Dec. 11, 2007]

[21] F.E. Terman, *Radio engineers' handbook*, New York: McGraw-Hill, 1943.

[22] Kendir, G.A.; Wentai Liu; Guoxing Wang; Sivaprakasam, M.; Bashirullah, R.; Humayun, M.S.; Weiland, J.D., "An optimal design methodology for inductive power link with class-E amplifier," *Circuits and Systems I: Regular Papers, IEEE Transactions on* , vol.52, no.5, pp. 857-866, May 2005.

[23] Sokal, N.O.; Sokal, A.D., "Class E-A new class of high-efficiency tuned single-ended switching power amplifiers," *Solid-State Circuits, IEEE Journal of* , vol.10, no.3, pp. 168-176, Jun 1975.

[24] Kazimierczuk, M.; Puczko, K., "Exact analysis of class E tuned power amplifier at any Q and switch duty cycle," *Circuits and Systems, IEEE Transactions on* , vol.34, no.2, pp. 149-159, Feb 1987

[25] Robert A. Freitas Jr., *Nanomedicine, Volume IIA: Biocompatibility*, Georgetown, TX: Landes Bioscience, 2003.

[26] Jonathan Black, *Biological Performance of Materials 3rd edition*, New York: Marcel Dekker inc., 1999.

[27] D.F. Williams, *The Williams Dictionary of Biomaterials*, Liverpool: Liverpool University Press, 1999.

[28] M. Nagl, T. Lechleitner, "Barrier coatings for medical electronic implants." *Vakuum in Forschung und Praxis,* vol. 17, no. S1, pp. 47-50, 2005.

[29] Applied Silicone Corporation, "Implant grade liquid silicone rubber (LSR) 10:1 Systems datasheet", [Online] Available: http://www.appliedsilicone.com/products/ps40029.html, [Accessed: Jun. 11, 2008].

[30] J. W. Swanson, J. E. Lebeau, "The effect of implantation on the physical properties of silicone rubber", *Journal of Biomedical Materials Research,* vol. 8, no. 6, pp. 357-367, 1974.

[31] Tyntek Corporation, "Datasheets LEDs", [Online] Available: http://www.tyntek.com.tw/, [Accessed: Jun. 3, 2007].

[32] Roman Dedic, Alexander Molnár, Miloslav Korínek,et al. "Spectroscopic study of singlet oxygen photogeneration in meso-tetra-sulphonatophenyl-porphin", *Journal of Luminescence*, vol. 108, no. 1-4, pp. 117-119, 2004

[33] Phycomp, "datasheet general purpose chip resistors, RC0402" [Online] Available: www.Yageo.com, [Accessed Sep. 12, 2007].

[34] Arjen Amelink, "In vivo measurement of the local optical properties of tissue by use of differential path-length spectroscopy", *Optics Letters*, vol. 29, no. 10, pp. 1087-1089, May 2004.

[35] D. Tanase, N. Komen, A. Draaijer, G.J. Kleinrensink, J. F. Lange, J. Jeekel, P. J. French, "Animal studies using an oxygen-tension sensor for tissue viability monitoring", *Proceedings of the International Conference on Biomedical Electronics and Devices*, pp. 50-55, Madeira, Portugal, 2008.

[36] A. Pauchard, P. -A. Besse, M. Bartek, R. F. Wolffenbuttel, R. S. Popovic, "Ultraviolet-selective avalanche photodiode", *Sensors and Actuators A: Physical,* vol. 82, no. 1-3, pp. 128-134, May 2000.

[37] Daniel Golden, Wireless Retrieval of a Mouse's Vital Signs via RFID, Cornell University, 2004 [Online] Available: http://instruct1.cit.cornell.edu/courses/eceprojectsland/STUDENTPROJ/2004to2005/dig4/Wireless_Retrieval_of_Mouse_Vital_Signs_via_RFID-dig4.pdf [Accessed May. 21, 2007].

[38] Rousche, P.J.; Pellinen, D.S.; Pivin, D.P., Jr.; Williams, J.C.; Vetter, R.J.; Kirke, D.R., "Flexible polyimide-based intracortical electrode arrays with bioactive capability," *Biomedical Engineering, IEEE Transactions on*, vol.48, no.3, pp.361-371, March 2001

Acknowledgement

Over the last 18 months I have been developing a system that can treat and monitor metronomic photodynamic treatment. This project was done to finish my Master of Science education in the field of Electrical Engineering at the Delft University of Technology. Although it was sometimes pretty frustrating I am happy with the final result, a working implant that can be implanted in a laboratory rat.

APPENDIX A: Flowchart

Fabrication Process for The optode for demonstrating PDT
Based on DIMES02

STARTING MATERIAL

Use processwafers, with the following specifications:

Wafer specifications:	type:	p-type, boron
	orientation:	1-0-0, 0 deg off orientation
	resistivity:	2-5 Ωcm
	thickness:	525 ± 15 μm
	diameter:	100.0 ± 0.2 mm

If the wafers are taken out of an unopened wafer box, no cleaning will be necessary.
Wafers taken from an already opened box must be cleaned following the standard procedure.

6 wafers

1. MARKER OXIDATION 1

Furnace no: C1   Program name: MARKOXB
Total time: 198.5 min   Program no: N9

Process	temperature [°C]	gasses & flows [liter/min]		time [min]	remarks
boat in	800	nitrogen:	3.0	5	
		oxygen:	0.3		
stabilize	800	nitrogen:	3.0	10	
		oxygen:	0.3		
heat up	+10 °C/min	nitrogen:	3.0	30	
		oxygen:	0.3		
stabilize	1100	nitrogen:	3.0	10	
		oxygen:	0.3		
oxidation	1100	oxygen:	2.25	38.5	
		hydrogen:	3.85		
cool down	-5 °C/min	nitrogen:	3.0	100	wait for operator
boat out	600	nitrogen:	3.0	5	

Note: - The total process time can be slightly reduced in the "cool down" step: the "boat out" step can be started after ± 60 minutes, when the actual temperature of the furnace will be about 800 °C.
- When this furnace is already in use, it is also possible to use program MARKOXB-N7 in furnace D1.

2. MEASUREMENT: OXIDE THICKNESS

Use the Leitz MPV-SP measurement system to measure the oxide thickness:
Program: Th. SiO2 on Si, >50nm auto5pts
Oxide thickness: 500 - 530 nm on the processwafers

3. COATING AND BAKING

Processing will be performed on the CONVAC wafertrack automatically:
this includes a HMDS (hexa methyl disilazane) treatment with nitrogen carrier gas , the coating with
Shipley SPR 3012 resist (spin velocity 3430 rpm ; spin time 30 s) , and prebaking for 1 minute at 95 °C.
Follow the instructions specified for this equipment, and always check the temperature of the hotplate first.

Use coating **program 2** (resist thickness: 1.400 µm at 48% RV).

4. ALIGNMENT AND EXPOSURE

Processing will be performed on the ASM PAS 5000/50 automatic waferstepper.
Follow the operating instructions from the manual when using this machine.

Use **mask COMURK** , job Litho/EPI2.0 and the correct exposure energy (check energy list).
This procedure will result in alignment markers necessary for further processing with a 2.8 µm thick epilayer.

5.   DEVELOPMENT

After exposure a post-exposure bake at 115 °C for 1 minute is performed on the CONVAC wafertrack, followed by
a development step using Shipley MF322 developer (single puddle process) and a postbake at 100 °C for 1 minute.
Follow the instructions specified for this equipment, and always check the temperature of the hotplates first.

Use development **program 2** and temperature program 2.

6.   INSPECTION: LINEWIDTH AND OVERLAY

Visually inspect the wafers through a microscope, and check linewidth and overlay.

7.   WINDOW ETCHING

Rinse   Use wetbench "H_2O/TRITON X-100" and the special carrier with the blue dot;
               added to the tank: 1 ml Triton X-100 per 5000 ml demi water. Rinse for 1 minute.

Etchant   Use wetbench "SiO_2-ets (1:7)"; use the carrier with the blue dot.
               Buffered HF solution (Merck LSI selectipur, SiO_2 1:7)

Etch time   Depends on the oxide thickness and composition.
               Etch until the backside is **hydrophobic**, plus an extra 30 seconds.
               The etchrate of thermally grown oxide is 1.3 ± 0.2 nm/s at 20 °C.

QDR   Rinse in the Quick Dump Rinser with the standard program until the resistivity is 5 MΩ.

Drying   Use the Semitool "Rinser/dryer" with the standard program. Always use the special orange carrier.

Inspection   Visually, through a microscope. All the windows must be open.
               The hydrophobic test may be applied.

8.   CLEANING PROCEDURE

Acetone   Use wetbench "aceton" and the carrier with the two red dots.
               Dissolve the photoresist in acetone (temp. 40 °C). Time = ± 1 minute.

Cleaning   Use wetbench "HNO_3 (100%)" and the carrier with the red dot.
               10 minutes in fuming nitric acid (Merck: HNO_3 (100%), selectipur; ambient temperature).

QDR   Rinse in the Quick Dump Rinser with the standard program until the resistivity is 5 MΩ.

Cleaning   10 minutes in concentrated nitric acid (Merck: HNO_3 (65%), selectipur; temp. 110 °C).

QDR   Rinse in the Quick Dump Rinser with the standard program until the resistivity is 5 MΩ.

Drying   Use the Semitool "Rinser/dryer" with the standard program. Always use the special orange carrier.

27.   EPITAXY

Use program **DIMES02** on the ASM-Epsilon reactor to grow the following epitaxial layer:

Process conditions: Layer characteristics:
arsenic doping: 1 x 10^{16} (1E16) atoms/cm^3 thickness: 2.8 ± 0.1 µm
temperature: 1050 °C   sheet resistance: 1600 - 2000 ohm/sq
pressure: 60 Torr   resistivity: 0.5 ± 0.1 ohmcm

Note: Immediately after the epitaxial process the weight measurement and the "Wet oxidation: masking oxide 1"
steps must be performed.

28.   MEASUREMENT : WAFER WEIGHT WITH EPI LAYER

Use the Mettler Toledo AT20 measurement system to measure the weight of the new **p-type
process wafer** (with DIMES02 EPI layer). Store the weight in the measurement computer
for layer thickness calculations.

Use the CDE ResMap measurement system to measure the sheet resistance of the epitaxial layer: 1600 - 2000
ohm/sq

Note: The maximum allowed weight on this system is only 20 grams, and therefore it is strictly
prohibited to use it for other purposes than measuring the weight of one single wafer !!

29.   WET OXIDATION: MASKING OXIDE 1

Furnace no: C1   Program name: DPMASOX
Total time: 175 min   Program no: N10

Process	temperature [°C]	gasses & flows [liter/min]		time [min]	remarks
boat in	800	nitrogen:	3.0	5	
		oxygen:	0.3		
stabilize	800	nitrogen:	3.0	10	
		oxygen:	0.3		
heat up	+10 °C/min	nitrogen:	3.0	30	
		oxygen:	0.3		
stabilize	1100	nitrogen:	3.0	10	
		oxygen:	0.3		
oxidation	1100	oxygen:	2.25	55	
		hydrogen:	3.85		
cool down	-5 °C/min	nitrogen:	3.0	60	
boat out	800	nitrogen:	3.0	5	

Note: When this furnace is already in use, it is also possible to use program DPMASOX-N9 in furnace D1.

30.   MEASUREMENT: OXIDE THICKNESS

Use the Leitz MPV-SP measurement system to measure the oxide thickness:
    Program: Th. SiO2 on Si, >50nm auto5pts
    Oxide thickness: 615 - 625 nm

31. COATING AND BAKING

Processing will be performed on the CONVAC wafertrack automatically:
this includes a HMDS (hexa methyl disilazane) treatment with nitrogen carrier gas , the coating with
Shipley SPR 3012 resist (spin velocity 3430 rpm ; spin time 30 s) , and prebaking for 1 minute at 95 °C.
Follow the instructions specified for this equipment, and always check the temperature of the hotplate first.

Use coating **program 2** (resist thickness: 1.400 µm at 48% RV).

32. ALIGNMENT AND EXPOSURE

Processing will be performed on the ASM PAS 5000/50 automatic waferstepper.
Follow the operating instructions from the manual when using this machine.

Use **mask DP** , the correct litho job and the correct exposure energy (check energy list).

33. DEVELOPMENT

After exposure a post-exposure bake at 115 °C for 1 minute is performed on the CONVAC wafertrack, followed by
a development step using Shipley MF322 developer (single puddle process) and a postbake at 100 °C for 1 minute.
Follow the instructions specified for this equipment, and always check the temperature of the hotplates first.

Use development **program 2** and temperature program 2.

34. INSPECTION: LINEWIDTH AND OVERLAY

Visually inspect the wafers through a microscope, and check linewidth and overlay.

35. WINDOW ETCHING

Rinse	Use wetbench "H$_2$O/TRITON X-100" and the special carrier with the blue dot; added to the tank: 1 ml Triton X-100 per 5000 ml demi water. Rinse for 1 minute.
Etchant	Use wetbench "SiO$_2$-ets (1:7)"; use the carrier with the blue dot. Buffered HF solution (Merck LSI selectipur, SiO$_2$ 1:7)
Etch time	Depends on the oxide thickness and composition. Etch until the backside is **hydrophobic**, plus an extra 30 seconds. The etchrate of thermally grown oxide is 1.3 ± 0.2 nm/s at 20 °C.
QDR	Rinse in the Quick Dump Rinser with the standard program until the resistivity is 5 MΩ.
Drying	Use the Semitool "Rinser/dryer" with the standard program. Always use the special orange carrier.
Inspection	Visually, through a microscope. All the windows must be open. The hydrophobic test may be applied.

36.   CLEANING PROCEDURE

Acetone   Use wetbench "aceton" and the carrier with the two red dots.
               Dissolve the photoresist in acetone (temp. 40 °C). Time = ± 1 minute.

Cleaning   Use wetbench "HNO$_3$ (100%)" and the carrier with the red dot.
               10 minutes in fuming nitric acid (Merck: HNO$_3$ (100%), selectipur; ambient temperature).

QDR   Rinse in the Quick Dump Rinser with the standard program until the resistivity is 5 MΩ.

Cleaning   10 minutes in concentrated nitric acid (Merck: HNO$_3$ (65%), selectipur; temp. 110 °C).

QDR   Rinse in the Quick Dump Rinser with the standard program until the resistivity is 5 MΩ.

Drying   Use the Semitool "Rinser/dryer" with the standard program. Always use the special orange carrier.

37.   BORON DEPOSITION

Furnace no: B3   Program name: DEPOSBN2
Total time: 157 min   Program no: N10

Process	temperature [°C]	gasses & flows [liter/min]		time [min]	remarks
Heat up	600	nitrogen:	6.0	20	
boat out	700	nitrogen:	6.0	10	Wait for operator
boat in	700	nitrogen:	6.0	15	
Heat up	+10 °C/min	nitrogen:	3.0	10	
		Oxygen:	3.0		
stabilize	800	hydrogen:	0.1	5	
sourcing	800	nitrogen:	3.0	10	
H2 injection	800	nitrogen:	3.0	2	
		oxygen:	3.0		
		hydrogen:	0.1		
heat up	+10 °C/min	nitrogen:	6.0	35	
soaking	975	nitrogen:	6.0	55	
cool down	-5 °C/min	nitrogen:	6.0	50	
boat out	400	nitrogen:	6.0	15	

Notes: The front side of each processwafer must face a boron nitride wafer.

As soon as the boat is out, immediately put the processwafers into the drive-in furnace.

Process **two n-type process wafers**: one for measurement of oxide thickness and sheet resistance directly after the deposition, and the other one for processing in the subsequent boron drive-in step.

Before processing a test run can be performed to check the boron deposition process.

38. MEASUREMENT: OXIDE THICKNESS AND SHEET RESISTANCE

Immediately rinse one of the testwafers after the "boron deposition" step in demi water for 1 minute. After drying measure the oxide thickness and sheet resistance.

Use the Sagax measurement system to measure the oxide thickness:
    Oxide thickness: 60 - 160 nm

Use the CDE measurement system to measure the sheet resistance:
    Sheet resistance: 28 ohm/sq

39. BORON DRIVE-IN: ISOLATION DIFFUSION

Furnace no: B1   Program name: DPDRIVE3
Total time: 215 min   Program no: N10

Process	temperature [°C]	gasses & flows [liter/min]		time [min]	remarks
boat in	800	nitrogen:	3.0	5	
		oxygen:	0.1		
heat up	+10 °C/min	nitrogen:	3.0	25	
		oxygen:	0.1		
stabilize	1050	nitrogen:	3.0	10	
		oxygen:	0.1		
drive in	1050	nitrogen:	3.0	100	
		oxygen:	0.1		
oxidation	1050	oxygen:	2.25	10	
		hydrogen:	3.85		
cool down	-5 °C/min	nitrogen:	3.0	60	
boat out	800	nitrogen:	3.0	5	

Process the **second testwafer** from the "Boron deposition" step for measurement purposes.

40. MEASUREMENT: OXIDE THICKNESS AND SHEET RESISTANCE

Use the second testwafer from the "Boron deposition" step to perform the following measurements:

Use the Sagax measurement system to measure the oxide thickness:
    Oxide thickness: 330 - 400 nm   Note: these values are old and may have changed slightly.

Use the CDE measurement system to measure the sheet resistance:
    Sheet resistance: 9.5 - 11.5 ohm/sq   Note: these values are old and may have changed slightly.

Clean the testwafer after the measurements and use it in the "Wet oxidation (DPDRIVEW3)" step.

41. OXIDE STRIPPING

Etchant	Use wet bench "HF (40%)"; use the carrier with the two black dots. Concentrated HF (Merck selectipur), ambient temperature.
Etch time	Depends on the oxide thickness and composition. Etch until the whole wafer is **hydrophobic**. The etchrate of thermally grown oxide is about 13 nm/s.
QDR	Rinse in the Quick Dump Rinser with the standard program until the resistivity is 5 MΩ.
Drying	Use the Semitool "Rinser/dryer" with the standard program. Always use the special orange carrier.
Inspection	Visually, in floodlight.

42. CLEANING PROCEDURE

Cleaning	Use wetbench "HNO_3 (100%)" and the carrier with the red dot. 10 minutes in fuming nitric acid (Merck: HNO_3 (100%), selectipur; ambient temperature).
QDR	Rinse in the Quick Dump Rinser with the standard program until the resistivity is 5 MΩ.
Cleaning	10 minutes in concentrated nitric acid (Merck: HNO_3 (65%), selectipur; temp. 110 °C).
QDR	Rinse in the Quick Dump Rinser with the standard program until the resistivity is 5 MΩ.
Drying	Use the Semitool "Rinser/dryer" with the standard program. Always use the special orange carrier.

43. **WET OXIDATION (DPDRIVEW3)**

Furnace no:	B1		Program name:	DPDRIVEW3
Total time:	225 min		Program no:	N13

Process	temperature [°C]	gasses & flows		time [liter/min]	remarks [min]
boat in	800	nitrogen:	3.0	5	
		oxygen:	0.3		
stabilize	800	nitrogen:	3.0	15	
		oxygen:	0.3		
heat up	+10 °C/min	nitrogen:	3.0	25	
		oxygen:	0.3		
stabilize	1050	nitrogen:	3.0	15	
		oxygen:	0.3		
oxidation	1050	oxygen:	2.25	100	
		hydrogen:	3.85		
cool down	-5 °C/min	nitrogen:	3.0	60	
boat out	800	nitrogen:	3.0	5	

Process the **second testwafer** from the "Boron deposition" step for measurement purposes.

---

44. **MEASUREMENT: OXIDE THICKNESS, SHEET RESISTANCE AND JUNCTION DEPTH**

Use the second testwafer from the "Boron deposition" step to perform the following measurements:

Use the Leitz MPV-SP measurement system to measure the oxide thickness:
Program: Th. SiO2 on Si, >50nm auto5pts
Oxide thickness: 650 - 700 nm   Note: these values are old and may have changed slightly.

Use the CDE measurement system to measure the sheet resistance:
Sheet resistance: 17 - 19 ohm/sq   Note: these values are old and may have changed slightly.

Use the bevel measurement equipment to measure the junction depth:
Junction depth: 3.0 - 3.4 µm   Note: these values are old and may have changed slightly.

45 **OXIDE STRIPPING**

Etchant   Use wet bench "HF (40%)"; use the carrier with the two black dots.
Concentrated HF (Merck selectipur), ambient temperature.

Etch time   Depends on the oxide thickness and composition. Etch until the whole wafer is **hydrophobic**.
The etchrate of thermally grown oxide is about 13 nm/s.

QDR   Rinse in the Quick Dump Rinser with the standard program until the resistivity is 5 MΩ.

Drying   Use the Semitool "Rinser/dryer" with the standard program. Always use the special orange carrier.

Inspection   Visually, in floodlight.

C46 DRY OXIDATION: DIRT BARRIER

Furnace no: A1
Total time: 115 min

Program name: DIBAR
Program no: N10

Process	temperature [°C]	gasses & flows [liter/min]		time [min]	remarks
boat in	800	nitrogen:	8.0	5	Temperature goes to 800°C after selecting the program !
stabilize	800	nitrogen:	3.0	10	
heat up	+10 °C/min	nitrogen:	3.0	15	
stabilize	950	nitrogen:	3.0	10	
oxidation	950	oxygen:	3.0	35	
cool down	-5 °C/min	nitrogen:	3.0	35	
boat out	800	nitrogen:	3.0	5	

Process a testwafer for oxide thickness measurements and continue processing this wafer in the next process steps until the "Antimony drive-in buried layer" step. Then this wafer will be used for measurements again.

C47. MEASUREMENT: OXIDE THICKNESS

Use the Leitz MPV-SP measurement system to measure the oxide thickness:
Program: Th. SiO2 on Si, <50nm auto5pts
Oxide thickness: 20 - 21 nm

C48. COATING AND BAKING

Processing will be performed on the CONVAC wafertrack automatically:
this includes a HMDS (hexa methyl disilazane) treatment with nitrogen carrier gas , the coating with Shipley SPR 3012 resist (spin velocity 3430 rpm ; spin time 30 s) , and prebaking for 1 minute at 95 °C. Follow the instructions specified for this equipment, and always check the temperature of the hotplate first.

Use coating **program 2** (resist thickness: 1.400 µm at 48% RV).

C49. ALIGNMENT AND EXPOSURE

Processing will be performed on the ASM PAS 5000/50 automatic waferstepper.
Follow the operating instructions from the manual when using this machine.

Use **mask DP** , the correct litho job and the correct exposure energy (check energy list).

C50. **DEVELOPMENT**

After exposure a post-exposure bake at 115 °C for 1 minute is performed on the CONVAC wafertrack, followed by
a development step using Shipley MF322 developer (single puddle process) and a postbake at 100 °C for 1 minute.
Follow the instructions specified for this equipment, and always check the temperature of the hotplates first.

Use development **program 2** and temperature program 2.

C51. **INSPECTION: LINEWIDTH AND OVERLAY**

Visually inspect the wafers through a microscope, and check linewidth and overlay.

C52. **BORON IMPLANTATION: DP+**

Ion	B^+
Energy	40 keV
Dose	5×10^{15} (5E15) ions/cm^2
Remarks	The angle of implant is standard 7 deg.
	The flat side of the wafer must be turned 22 deg north east; this is only possible in end station no 1.

C53. **CLEANING PROCEDURE**

Plasma strip	Use the Tepla plasma system to remove the photoresist in an oxygen plasma.
	Follow the instructions specified for the Tepla stripper, and use the quartz carrier.
	Use **program 1**: 1000 watts power and automatic endpoint detection + 2 minutes overetching.
Cleaning	Use wetbench "HNO$_3$ (100%)" and the carrier with the red dot.
	10 minutes in fuming nitric acid (Merck: HNO$_3$ (100%), selectipur; ambient temperature).
QDR	Rinse in the Quick Dump Rinser with the standard program until the resistivity is 5 MΩ.
Cleaning	10 minutes in concentrated nitric acid (Merck: HNO$_3$ (65%), selectipur; temp. 110 °C).
QDR	Rinse in the Quick Dump Rinser with the standard program until the resistivity is 5 MΩ.
Drying	Use the Semitool "Rinser/dryer" with the standard program. Always use the special orange carrier.

C54. **COATING AND BAKING**

Processing will be performed on the CONVAC wafertrack automatically:
this includes a HMDS (hexa methyl disilazane) treatment with nitrogen carrier gas , the coating with
Shipley SPR 3012 resist (spin velocity 3430 rpm ; spin time 30 s) , and prebaking for 1 minute at 95 °C.
Follow the instructions specified for this equipment, and always check the temperature of the hotplate first.

Use coating **program 2** (resist thickness: 1.400 µm at 48% RV).

C55. **ALIGNMENT AND EXPOSURE**

Processing will be performed on the ASM PAS 5000/50 automatic waferstepper.
Follow the operating instructions from the manual when using this machine.

Use **mask WN** , the correct litho job and the correct exposure energy (check energy list).

C56. DEVELOPMENT

Sep 1998

After exposure a post-exposure bake at 115 °C for 1 minute is performed on the CONVAC wafertrack, followed by
a development step using Shipley MF322 developer (single puddle process) and a postbake at 100 °C for 1 minute.
Follow the instructions specified for this equipment, and always check the temperature of the hotplates first.

Use development **program 2** and temperature program 2.

C57. INSPECTION: LINEWIDTH AND OVERLAY

Feb 1996

Visually inspect the wafers through a microscope, and check linewidth and overlay.

C58. ARSENIC IMPLANTATION: WN

Jan 1995

Ion	As^+
Energy	100 keV
Dose	5.0×10^{15} (5.0E15) ions/cm^2
Remarks	The angle of implant is standard 7 deg
	The flat side of the wafer must be turned 22 deg north east; this is only possible in end station no 1.

C59. CLEANING PROCEDURE

Sep 1998

Plasma clean	Use the Tepla plasma system for wafer cleaning.
	Follow the instructions specified for the Tepla stripper, and use the quartz carrier.
	Use **program 2**: etch for 1 minute at 600 watts.
Cleaning	Use wetbench "HNO$_3$ (100%)" and the carrier with the red dot.
	10 minutes in fuming nitric acid (Merck: HNO$_3$ (100%), selectipur; ambient temperature).
QDR	Rinse in the Quick Dump Rinser with the standard program until the resistivity is 5 MΩ.
Cleaning	10 minutes in concentrated nitric acid (Merck: HNO$_3$ (65%), selectipur; temp. 110 °C).
QDR	Rinse in the Quick Dump Rinser with the standard program until the resistivity is 5 MΩ.
Drying	Use the Semitool "Rinser/dryer" with the standard program. Always use the special orange carrier.

****HOLE ETCHING****

C60. DEPOSITION OF LPCVD TEOS (380 nm)

Furnace no: E1   Program name: LO300
Total time: 152 min   Program no: N2

Deposition temperature: 700 °C / pressure: 250 mTorr / gasses: TEOS bubbler (40 °C).

Follow the instructions for the LPCVD furnace; after backfill, loading, and pumpdown cycles the deposition will start. The final thickness of the TEOS layer depends on the total deposition time (variable command). It can be necessary that a test deposition must be done in advance. Ask the responsible process technician for the condition of the furnace tube.

A testwafer can be deposited together with the processwafers to check the etch process in the Drytek plasma etcher.
The deposition time for a 300 nm layer will be about 40 minutes.

Depositon time 50:40 minutes for a 380 nm layer

C61. MEASUREMENT: TEOS OXIDE THICKNESS

Use the Leitz MPV-SP measurement system to measure the TEOS oxide thickness:
    Program: Th. SiO2 on Si, >50nm auto5pts
    TEOS thickness: 380 ± 10 nm on a bare testwafer

C62. COATING AND BAKING

Use Program 4

C63. ALIGNMENT AND EXPOSURE

Use mask **TMAH** with energy E= 105 mJ

C64. DEVELOPMENT

Use program 4

C65. INSPECTION: LINEWIDTH AND OVERLAY

C66. WINDOW ETCH

Use program **OX3300A** on the Drytek 384T plasma etcher.
Follow the operating instructions from the manual when using this machine.
The process conditions of the etch program may not be changed !

Program description:
1. bulk step (RIE): C_2F_6/CHF_3 = 36/144 sccm   180 mTorr   300 Watt RF   12 Torr He   time   =   0'**41**"

C67. TMAH ETCHING

265 um deep.

C68. PLASMA ETCH TEOS OXIDE

Use program **C3DMTEOS** on the Drytek 384T plasma etcher.
Follow the operating instructions from the manual when using this machine.
The process conditions of the etch program may not be changed !

Program description:
1. bulk step (RIE): C_2F_6/CHF_3 = 12/108 sccm   130 mTorr   300 Watt RF   12 Torr He   time   =   0'36"

C69. CLEANING PROCEDURE: HNO₃ 100% AND 65%

Cleaning   10 minutes in fuming nitric acid (Merck: HNO$_3$ 100% selectipur) at ambient temperature.
             Use wet bench "HNO$_3$ (100%)" and the carrier with the red dot.

QDR   Rinse in the Quick Dump Rinser with the standard program until the resistivity is 5 MΩ.

Cleaning   10 minutes in concentrated nitric acid (Merck: HNO$_3$ 65% selectipur) at 110 °C.
             Use wet bench "HNO$_3$ (65%)" and the carrier with the red dot.

QDR   Rinse in the Quick Dump Rinser with the standard program until the resistivity is 5 MΩ.

Drying   Use the Semitool "rinser/dryer" with the standard program, and the white carrier with a red dot.

112. ANNEAL ARGON GAS

Jan 1995

Furnace no: C2   Program name: ANNEALN1
Total time: 165 min   Program no: N5

Process	temperature [°C]	gasses & flows [liter/min]		time [min]	remarks
boat in	600	argon:	6.0	5	argon shower
stabilize	600	argon:	6.0	10	
anneal	600	argon:	6 .0	20	
heat up	+10 °C/min	argon:	3.0	40	
stabilize	1000	argon:	3.0	10	
anneal	1000	argon:	3.0	35	
cool down	-5 °C/min	argon:	3.0	40	
boat out	800	argon:	3.0	5	argon shower

Note: - Each processwafer must be placed between two dummy wafers!
          - In **all** cases this step must be performed before metallization!
          - TCA-cleaning before processing is very important!

C70. DEPOSITION OF LPCVD TEOS (300 nm)

Jul 1995

Furnace no: E1   Program name: LO300
Total time: 152 min   Program no: N2

Deposition temperature: 700 °C / pressure: 250 mTorr / gasses: TEOS bubbler (40 °C).

Follow the instructions for the LPCVD furnace; after backfill, loading, and pumpdown cycles the deposition will start. The final thickness of the TEOS layer depends on the total deposition time (variable command). It can be necessary that a test deposition must be done in advance. Ask the responsible process technician for the condition of the furnace tube.

A testwafer can be deposited together with the processwafers to check the etch process in the Drytek plasma etcher.
The deposition time for a 300 nm layer will be about 40 minutes.

Depositon time 50:40 minutes for a 380 nm layer

C71. MEASUREMENT: TEOS OXIDE THICKNESS

Use the Leitz MPV-SP measurement system to measure the TEOS oxide thickness:
    Program: Th. SiO2 on Si, >50nm auto5pts
    TEOS thickness: 380 ± 10 nm on a bare testwafer

113. COATING AND BAKING

Processing will be performed on the CONVAC wafertrack automatically:
this includes a HMDS (hexa methyl disilazane) treatment with nitrogen carrier gas , the coating with
Shipley SPR 3012 resist (spin velocity 3630 rpm ; spin time 30 s) , and prebaking for 1 minute at 95 °C.
Follow the instructions specified for this equipment, and always check the temperature of the hotplate first.

Use coating **program 3** (resist thickness: 1.358 µm at 48% RV).

114. ALIGNMENT AND EXPOSURE

Processing will be performed on the ASM PAS 5000/50 automatic waferstepper.
Follow the operating instructions from the manual when using this machine.

Use **mask CO** , the correct litho job and the correct exposure energy (check energy list).

115. DEVELOPMENT

After exposure a post-exposure bake at 115 °C for 1 minute is performed on the CONVAC wafertrack, followed by
a development step using Shipley MF322 developer (single puddle process) and a postbake at 100 °C for 1 minute.
Follow the instructions specified for this equipment, and always check the temperature of the hotplates first.

Use development **program 2** and temperature program 2.

116. INSPECTION: LINEWIDTH AND OVERLAY

Visually inspect the wafers through a microscope, and check linewidth and overlay.

117. WINDOW ETCHING (constant time)

Rinse	Use wetbench "H_2O/TRITON X-100" and the special carrier with the blue dot; added to the tank: 1 ml Triton X-100 per 5000 ml demi water. Rinse for 1 minute.
Etchant	Use wetbench "SiO_2-ets (1:7)"; use the carrier with the blue dot. Buffered HF solution (Merck LSI selectipur, SiO_2 1:7).
Etch time	Etch the same time as in the previous window etching step (for WN). **NOTE: The DP and DN areas must be hydrophobic !**
QDR	Rinse in the Quick Dump Rinser with the standard program until the resistivity is 5 MΩ.
Drying	Use the Semitool "Rinser/dryer" with the standard program. Always use the special orange carrier.
Inspection	Visually, through a microscope. All the windows must be open. The hydrophobic test may be applied. Especially check the DP and DN windows!

118. CLEANING PROCEDURE

Acetone   Use wetbench "aceton" and the carrier with the two red dots.
Dissolve the photoresist in acetone (temp. 40 °C). Time = ± 1 minute.

Cleaning   Use wetbench "HNO_3 (100%)" and the carrier with the red dot.
15 minutes in fuming nitric acid (Merck: HNO_3 (100%), selectipur; ambient temperature).

QDR   Rinse in the Quick Dump Rinser with the standard program until the resistivity is 5 MΩ.

Drying   Use the Semitool "Rinser/dryer" with the standard program. Always use the special orange carrier.

Note: No 65% HNO_3 cleaning step!

119. DIP ETCHING

Etchant   Use wetbench "SiO_2-ets (1:7)"; use the carrier with the blue dot.
Buffered HF solution (Merck LSI-selectipur, SiO_2 1:7).

Etch time   30 seconds. The etch rate of thermally grown oxide is 1.3 ± 0.2 nm/s at 20 °C.

QDR   Rinse in the Quick Dump Rinser with the standard program until the resistivity is 5 MΩ.

Drying   Use the Semitool "Rinser/dryer" with the standard program. Always use the special orange carrier.

Note: Immediately after drying, metallization must be performed.
Don't use the rinse module with Triton X-100.

120. FIRST METALLIZATION: SPUTTERING OF Al/Si

Use the TRIKON SIGMA sputter coater for the deposition of the 1st metal layer on the processwafers.
The target must exist of 99% Al and 1% Si; deposition must be done at 350 °C and with a 100 sccm Ar flow.
Follow the operating instructions from the manual when using this machine.

- If **no anodisation** step is needed:
   Use recipe **#0.6mu Al @350C** to obtain a 0.6 ± 0.1 µm thick layer.
   In this case the optional process steps on the next pages can be skipped, and processing can
   be continued with coating of the wafers and exposing the IC mask.

131. COATING AND BAKING

Processing will be performed on the CONVAC wafertrack automatically:
this includes a HMDS (hexa methyl disilazane) treatment with nitrogen carrier gas , the coating with
Shipley SPR 3012 resist (spin velocity 3430 rpm ; spin time 30 s) , and prebaking for 1 minute at 95 °C.
Follow the instructions specified for this equipment, and always check the temperature of the hotplate first.

Use coating **program 2** (resist thickness: 1.400 µm at 48% RV).

132. ALIGNMENT AND EXPOSURE

Processing will be performed on the ASM PAS 5000/50 automatic waferstepper.
Follow the operating instructions from the manual when using this machine.

Use **mask IC** , the correct litho job and the correct exposure energy (check energy list).

133. DEVELOPMENT

After exposure a post-exposure bake at 115 °C for 1 minute is performed on the CONVAC wafertrack, followed by
a development step using Shipley MF322 developer (single puddle process) and a postbake at 100 °C for 1 minute.
Follow the instructions specified for this equipment, and always check the temperature of the hotplates first.

Use development **program 2** and temperature program 2.

Note: etch as soon as possible if <u>wet</u> aluminium etching must be performed !!

134. INSPECTION: LINEWIDTH AND OVERLAY

Visually inspect the wafers through a microscope, and check linewidth and overlay.

NOTE: Always check for sufficient Aluminium overlap at the contacts holes. If there is not enough overlap then dry etching may be necessary. Contact Liz Nanver for instructions.

135. ALUMINIUM ETCHING: 1ST METAL

Rinse	Use the special container filled with demi-water, to which Triton X-100 is added. Rinse for 1 minute.
Etchant	Use wetbench "Aluminium-ets" (35 ± 1 °C); use the carrier with the yellow dot. 1 liter buffered etch fluid (Merck selectipur) contains: 770 ml concentrated phosphorus acid ($H3PO4$, 85%), 14 ml concentrated nitric acid (HNO_3, 65 %), 140 ml concentrated acetic acid ($CH3COOH$, 100%) and 76 ml deionized water
Etch time	Depends on the aluminium thickness and composition. Etch until the pattern is **clearly visible** over the whole wafer. The etchrate is ± 150 nm/min at 35 °C. Etch time 4:30 min
QDR	Rinse in the Quick Dump Rinser with the standard program until the resistivity is 5 MΩ.
Drying	Use the Semitool "Rinser/dryer" with the standard program. Always use the special <u>black</u> carrier with the red dot.
Inspection	Visually, through a microscope. Cross-links between patterns are not allowed.
Note:	If the time between development and wet aluminium etching is more than 4 hours, an extra oven bake of 1 hour at 120 °C must be performed !!

136. POLY SILICON DIP ETCHING

Etchant	Use wetbench "HNO_3/HF (poly-ets)" (ambient temperature); use the carrier with the green dot. 1 liter poly etch fluid (Merck selectipur) contains: 705 ml concentrated nitric acid (HNO_3, 65 %), 15 ml concentrated hydrogen fluoride acid (HF, 50%) and 280 ml deionized water.
Etch time	30 seconds.
QDR	Rinse in the Quick Dump Rinser with the standard program until the resistivity is 5 MΩ.
Drying	Use the Semitool "Rinser/dryer" with the standard program. Always use the special <u>black</u> carrier with the red dot.
Inspection	Visually, through a microscope.

139.   **CLEANING PROCEDURE**

Cleaning   Use wetbench "HNO$_3$ (100%) metaal" and the carrier with the yellow and red dots.
10 minutes in fuming nitric acid (Merck: HNO$_3$ (100%), selectipur; ambient temperature).

QDR   Rinse in the Quick Dump Rinser with the standard program until the resistivity is 5 MΩ.

Drying   Use the Semitool "Rinser/dryer" with the standard program.
Always use the special <u>black</u> carrier with the red dot.

145.   **INSPECTION: LINEWIDTH AND OVERLAY**

Visually inspect the wafers through a microscope, and check linewidth and overlay.

146.   **PLASMA-OXIDE WINDOW ETCHING**

Use program **PLASMOX** on the Drytek 384T plasma etcher.
Follow the operating instructions from the manual when using this machine.
The process conditions of the etch program may not be changed !

<u>Program description:</u>
1. bulk step: C$_2$F$_6$/CHF$_3$ = 36/144 sccm   180 mTorr   300 Watt RF   12 Torr He   time   =
1'03"
2. landing step: C$_2$F$_6$/CHF$_3$ = 36/144 sccm   180 mTorr   100 Watt RF   12 Torr He   time   =
1'30"

147.   **CLEANING PROCEDURE**

Plasma strip   Use the Tepla plasma system to remove the photoresist in an oxygen plasma.
Follow the instructions specified for the Tepla stripper, and use the quartz carrier.
Use **program 1**: 1000 watts power and automatic endpoint detection + 2 minutes overetching.

Cleaning   Use wetbench "HNO$_3$ (100%) metaal" and the carrier with the yellow and red dots.
15 minutes in fuming nitric acid (Merck: HNO$_3$ (100%), selectipur; ambient temperature).

QDR   Rinse in the Quick Dump Rinser with the standard program until the resistivity is 5 MΩ.

Drying   Use the Semitool "Rinser/dryer" with the standard program.
Always use the special <u>black</u> carrier with the red dot.

<u>Note:</u>   No 65% HNO$_3$ cleaning step!

SECOND METAL LIFT OFF

LO1 COATING AND BAKING (AZ 5214 E)

<div align="right">Sep 1998</div>

* Evaporate HMDS on the substrates
* Start with AZ 5214 E
Spin it with the following parameters:
RPM: 3000
Accel.:   750rpm/min
Time: 30s5
* Pre-bake at 90C, 2min

LO2 ALIGNMENT AND EXPOSURE

<div align="right">Sep 1998</div>

Processing will be performed on the ASM PAS 5000/50 automatic waferstepper.
Follow the operating instructions from the manual when using this machine.

Use **mask IN** , the correct litho job and the correct exposure energy (check energy list).

LO3 DEVELOPMENT

<div align="right">Sep 1998</div>

*   Expose,   3.5secs   in   the   new   contact   aligner
* Bake for Image Reversal: 120C, 42sec
* Flood expose, 8s
*   Develop   in   2min   in   MF321   pure
* Rinse in water and spin dry

LO4 INSPECTION: LINEWIDTH AND OVERLAY

<div align="right">Nov 2000</div>

Visually inspect the wafers through a microscope, and check linewidth and overlay.

NOTE: Always check for sufficient Aluminium overlap at the contacts holes. If there is not enough
overlap then dry etching may be necessary. Contact Liz Nanver for instructions.

LO5 SECOND METALLIZATION: EVAPORATION OF Al

<div align="right">Jan 2000</div>

Use the Temerscal the deposition of the 2nd metal layer on the processwafers.
Standard recipe for 200nm thick layer

LO7 CLEANING PROCEDURE

<div align="right">Jan 1995</div>

Acetone   Use wetbench "aceton" and the carrier with the two red dots.
              Dissolve the photoresist in acetone (temp. 40 °C). Time = ± 1 minute.

Cleaning   Use wetbench "HNO_3 (100%) metaal" and the carrier with the yellow and red dots.
              15 minutes in fuming nitric acid (Merck: HNO_3 (100%), selectipur; ambient temperature).

Rinse   Rinse in demiwater

Drying   Use the spindryer in MEMSlab with the standard program.
              Always use the special <u>black</u> carrier with the red dot.

<u>Note:</u>   No 65% HNO_3 cleaning step!